NASA CONTRACTOR REPORT

NASA CR-448

NASA CR-448

THE STUDY OF MULTIPACTOR BREAKDOWN IN SPACE ELECTRONIC SYSTEMS

Prepared by
HUGHES AIRCRAFT COMPANY
Culver City, Calif.
for Goddard Space Flight Center

NATIONAL AERONAUTICS AND SPACE ADMINISTRATION • WASHINGTON, D. C. • JULY 1966

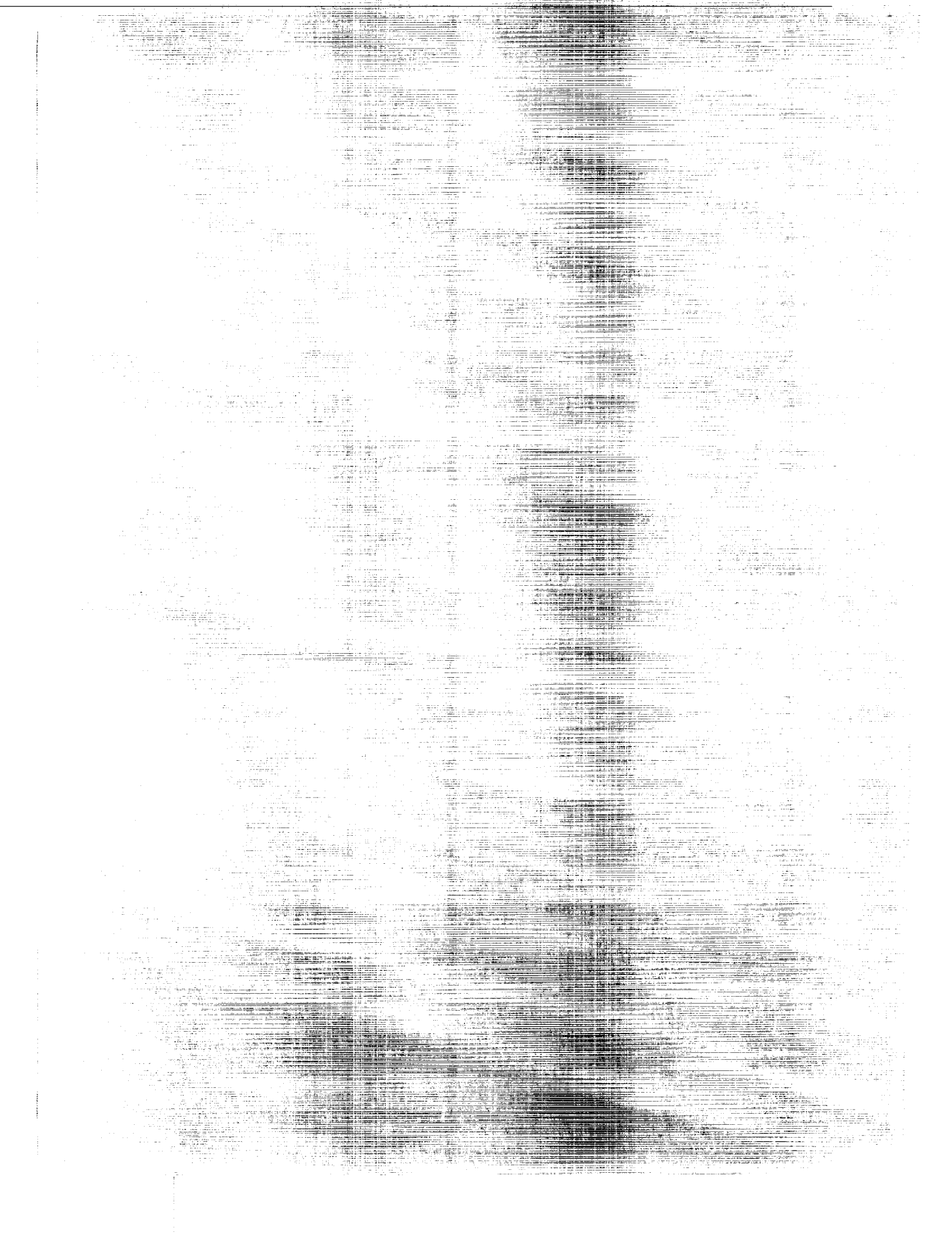

NASA CR-448

THE STUDY OF MULTIPACTOR BREAKDOWN IN SPACE ELECTRONIC SYSTEMS

Prepared under Contract No. NAS 5-3916 by
HUGHES AIRCRAFT COMPANY
Culver City, Calif.

for Goddard Space Flight Center

NATIONAL AERONAUTICS AND SPACE ADMINISTRATION

For sale by the Clearinghouse for Federal Scientific and Technical Information
Springfield, Virginia 22151 – Price $4.00

SUMMARY

In this final report on contract NAS 53916, we have incorporated the theoretical and experimental findings of a study to determine the conditions and causes of multipactor breakdown, the deleterious effects of the discharge, and methods of preventing its occurrence. The study is intended to provide information for the design of space electronic systems and equipment which would be used by the National Aeronautics and Space Administration; no work has been directed toward the problems of multipactor T-R switches or klystron or linear accelerator components, for example.

Our results have substantiated the theoretical and experimental work found in the literature, which describes the conditions under which a multipactor discharge may be initiated. We have, however, found some new and pertinent problems during our observations of discharges which are sustained under test conditions in vacuum chambers; since spacecraft equipment is qualified for use under such conditions, it is important to understand the extent to which the vacuum chamber test results are or are not a true indication of the effects of multipactor.

A detailed discussion of the investigations on each of the tasks defined in the contract is included.

CONTENTS

CONTENTS (Continued)

ILLUSTRATIONS

ILLUSTRATIONS (Continued)

TABLES

INTRODUCTION

GENERAL

Several years ago, work on two NASA projects was affected by discovery of failures in radio frequency transmitter equipment which were found to be due to the so-called multipactor effect, a secondary emission electron resonance phenomenon.* The failures occurred in a cavity resonator of a 10-watt, 400 mHz transmitter, and in a type N connector which carried a power level of 60 watts at a frequency of 960 mHz. Although the difficulties were cured in an acceptable manner, the evaluation of the causes indicated that there was a significant possibility that future problems might occur in space electronic systems where medium or high power radio frequencies were in use. Since knowledge of the multipactor effect was not adequately disseminated among circuit engineers and since the potential deleterious results of the discharge were not fully understood, this study program was initiated under the technical supervision of the Goddard Space Flight Center, NASA. The scope of the program included both experimental and theoretical investigations on the following tasks:

I. Investigate the Multipactor Effect
II. Deleterious Effects of Multipactor
III. Methods of Eliminating Multipactor

In addition to these three tasks, it was required to prepare, as part of the final report, a collection of data which would be useful, as a handbook, to designers.** Another significant task which was implicit in the effort was to devise methods of generating and sustaining a multipactor discharge, as well as methods of sensing its existence and measuring the magnitude of effects; in fact, the early portion of our efforts was

---

*"Investigation of Failures of Wideband OAO Transmitter," Hughes Aircraft Company Report TM-756, July 1963, by H. H. Baller and E. V. Phillips.
"Space Programs Summary Report," No. 37-21, Volume I, Jet Propulsion Laboratory, May 1963, pp. 29-32.

**"The Study of Multipactor Breakdown in Space Electronic Systems," Volume II, NASA CR-71999.

mainly devoted to the development of adequate experimental facilities and techniques, which turned out to be much more difficult than anticipated.

THE MULTIPACTOR EFFECT

A concise qualitative description of secondary electron resonance breakdown is given by S. C. Brown* as follows:

> "Many studies have been made of high-frequency breakdown in regions outside that controlled by diffusion. If the pressure is low, the mean free path becomes long compared with the containing vessel, and ionization in the gas becomes highly unlikely. A number of workers have studied this case and have shown that the secondary emission of electrons by direct bombardment of the walls can cause a breakdown. Not only is the magnitude of the electric field important, but the phase of the electron motion with respect to the field has a governing effect.
>
> Under optimum conditions, the electron motion must be in phase with the field. Thus an electron starting across the gap between the walls should collide with the walls and release secondary electrons just as the electric field passes through zero. The reversed electric field accelerates the secondary electrons back across the gap. The electric field must be of such a value that the transit time across the gap be equal to one half cycle of the a-c field. In this way the secondary electrons formed by the initial electron become primary electrons for the next cycle to form another group of secondary electrons, with the optimum conditions again requiring that the secondaries be formed just as the field reverses its direction.
>
> It is obvious that a breakdown does not require the optimum conditions to occur, and there is a fairly broad region of fields and frequencies over which a phenomenon may be observed. It should be apparent that, for any one frequency, breakdown should be possible in a bounded region between two values of the field corresponding to too little or too much acceleration of the electrons to maintain the proper phase relations.
>
> Because this type of breakdown relies for its electron multiplication on the secondary emission of electrons from the walls, the breakdown field is shown to be independent of the type of gas and very dependent on the nature of the walls of the vessel in which the discharge takes place."

---

*Brown, S. C., "Basic Data on Plasma Physics," Technology Press, MIT, Cambridge, Mass., 1959.

Furthermore, one can deduce from Brown' s qualitative description that the multipactor effect will exhibit the following properties:

1. The multipactor discharge may be expected to disappear under given conditions of frequency and electrode configuration if the applied voltage is raised or lowered beyond the point at which the electron velocity becomes either too slow or too fast to maintain a condition of resonance.
2. The multipactor discharge may be expected to disappear under fixed conditions of applied voltage and electrode configuration, if the applied frequency is raised or lowered beyond the values which are resonant with the electron movement.
3. The multipactor discharge may be expected to disappear under fixed conditions of applied voltage and frequency when the electrode separation is increased or decreased beyond the values which are resonant with the electron movement.

Most of the studies reported in the literature available to us at the start of our program were directed toward the investigation of conditions which were necessary and sufficient to initiate a discharge. Some of our theoretical and experimental efforts have been used to confirm and to extend this knowledge. In general, we have found the published information to be valid. However, almost none of the data in the literature could be used to answer questions about the characteristics of a multipactor discharge <u>in being</u>, including questions such as:

1. What is the effect of the discharge on the surface of a <u>real</u> (non-ideal) secondary emitter under conditions of a real (non-zero pressure) vacuum environment?
2. What is the effect of the current flow in the multipactor discharge on a typical power source which causes the discharge; for example, what happens to the circuit impedance of capacitor plates when the discharge is present?
3. What is the noise content of the discharge current, and what is the waveform?

4. What non-linear effects may be present which would be of significance as potential modulation elements in a spacecraft transponder which is affected by a discharge?
5. What is the effect of residual gas ions on the time history of the discharge?

Although the scope of our study has not been adequate to answer all of these questions in an exhaustive manner, we have found interesting and pertinent facts of some importance as a result of the investigation; this information is described in detail in the body of this report. In brief, we have found the following behavior:

1. The multipactor discharge causes a change in the surface condition of electrodes which, in time, may extinguish an established discharge. The characteristic history of a discharge is fundamentally different when tested in a vacuum chamber with ambient pressure of 10^{-5} mm from the behavior in an environment of 10^{-7} mm pressure, the discharge being more stable and less dissipative in the lower pressure.
2. The current flow in the discharge has real and reactive components at the fundamental frequency. Under certain circumstances, these may be sufficient to load or detune an element by a substantial amount.*
3. There is a measurable and significant noise content in the multipactor discharge.
4. Non-linear effects, including harmonics, are present. If these occur in sensitive portions of a system, such as a diplexer or in the antenna connections, there is a possibility of modulation of transmitted signals by received signals, and an opportunity for electromagnetic harmonic interference.

---

*This effect has long been known as a nuisance in klystrons, which sometimes cannot achieve their ultimate power output because of a multipactor discharge which occurs during power build-up, but could not exist at full power.

5. Residual gas can be liberated by a multipactor discharge and ionized; in some cases a gas ionization breakdown of destructive effect may occur.

In addition to the questions and answers cited above, we have included descriptions of our experimental techniques, some theory and experiment on single surface multipactor, and some of the results of an investigation of multipactor in high power microwave slot antenna arrays. Tests of a government furnished transmitter equipment were performed. Due to the low power and low voltage levels existing in this equipment, no multipactor effects were observed.

THE DELETERIOUS EFFECTS OF MULTIPACTOR

The second major task of our study has been to determine effects of the multipactor discharge. Among the problems which have been studied are the electrical effects, such as noise, harmonic generation, intermodulation, impedance loading, loss of power output, and also the physical damage to components.

The noise resulting from the multipactor discharge appears to result from space charge effects and from the collision of rapidly moving electrons with residual gas ions. The qualitative physics of the discharge is not fully understood; however it appears that the electrons travel back and forth across the gap between parallel plates in a flat sheet. The glow which is observed is diffuse and appears to indicate that ionized gas molecules are present throughout the region. The sheet of electrons which strikes the surface contains individual electrons from a wide range of angles to the normal. The secondary electrons are emitted also with a wide angular distribution. As a result, many of the electrons as well as some of the gas ions escape beyond the region of the discharge; some of the experiments reported herewith show evidence of this behavior since a current collecting plate located near the discharge receives current with both positive and negative voltages applied to it. Because of our lack of exact knowledge of the charge distributions, it has not been possible to attempt analysis of the electrical parameters of the discharge, and

therefore the experimental approach has been used. The data which is reported in detail is believed to be representative and typical of the magnitudes which would be encountered in spacecraft systems.

Our investigation of the physical effects of multipactor has revealed that it has produced surface emission changes in the electrodes, which are transient in the sense that continued exposure to the discharge or temporary change of the ambient pressure will alter or reverse the initial effects. For instance, a surface on which a multipactor discharge is initiated may gradually become inactive under moderate high vacuum pressure (10^{-5}mm), but may again become active (i.e., produce a multipactor discharge) if it is exposed to atmospheric p essure momentarily or if the environmental pressure is temporarily reduced, by pumping, to 10^{-7} or 10^{-8} mm.

Physical destruction of components has only appeared as a result of gas ionization breakdown, which is induced by the liberation of gas due to heating from a prior multipactor discharge. Although this problem may appear to be unimportant at first sight, it is of considerable significance in the inner regions of connector plugs, coaxial tuning capacitors, cavity resonators, or volumes sealed by foam.

Even if the component is not physically damaged by the gas ionization breakdown, a power loss may occur which will reduce the level of performance in the communication system. An example of this effect is indicated in HAC Report TM-756 as indicated in Figure 1, showing the power drop due to a failure in a 400 mHz transmitter under test for the OAO spacecraft. This report states:

> "When the transmitter was turned on, it would operate at normal power (P_O) for a period of time (T_F) usually lasting from 5 to 150 seconds until there was a sudden drop of power in a short time to a significantly lower level (P_F). Ordinarily the power output would recover partially to an ultimate value (P_U) over a period of time (T_E) lasting for a number of minutes. All of the parameters (T_F, P_F, P_U, P_O, T_E) would vary widely in an unrepeatable manner from one test to the next; some observations showed several consecutive failure cycles, and others no failure with the same test conditions. The theory of gas ionization breakdown in the RFI filter tuning capacitors was tested, and confirmed, by measurements on the transmitter and filter unit

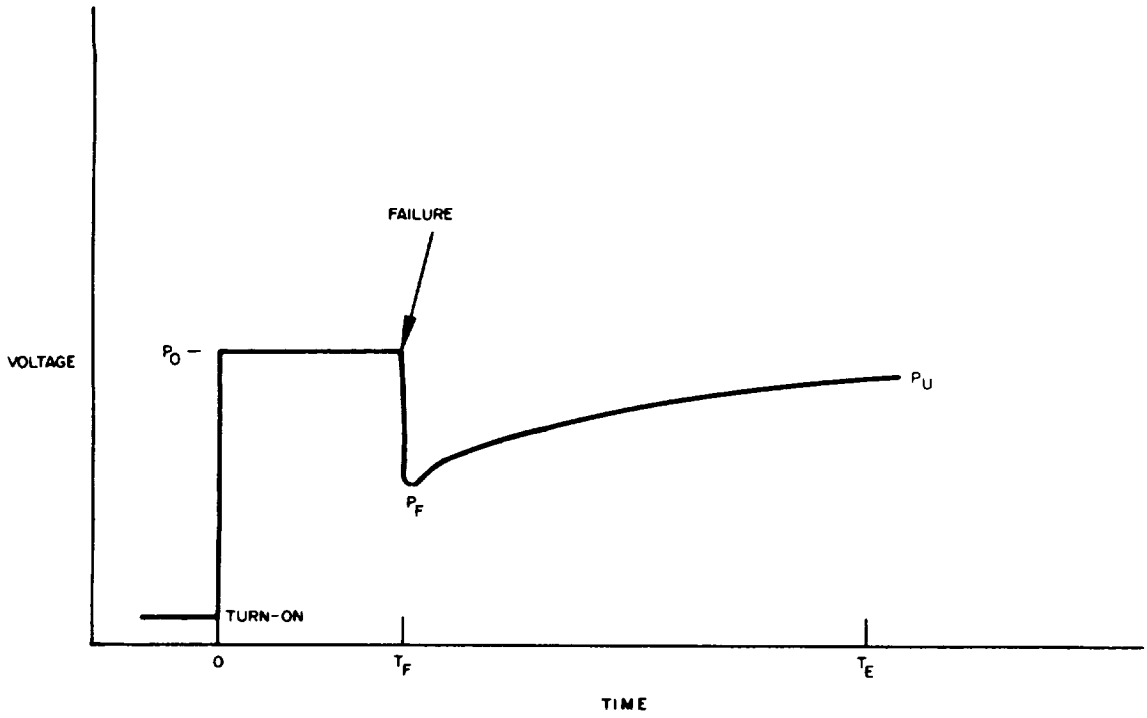

Figure 1. Typical recording of power drop in OAO wideband transmitter test due to gas ionization discharge.

separately in and outside of the vacuum, and by measurements of filter, transmitter, and capacitors under varying pressure conditions. During the variable pressure test, the filter operated satisfactorily starting at room pressure, failed in the range of 10^{-3} to 10^{-4}mm, and recovered at 10^{-5} mm."

A further example of transient failures induced by multipactor is also shown in report TM-756; after the gross failure due to gas ionization was eliminated by venting the tuning capacitors, the phenomenon illustrated in Figure 2(b) was observed. The input, output and reflected power in the RFI filter was measured as a function of time using the test setup shown in Figure 2(a).

"Features of the record, which are significant, include (1) the starting transient in P_{ref}, (2) the transient failures at t = 260, with simultaneous increase in reflected power and decrease in transmitted power, (3) the repetitive spikes in P_{ref}, starting at t = 260, and appearing with some regularity

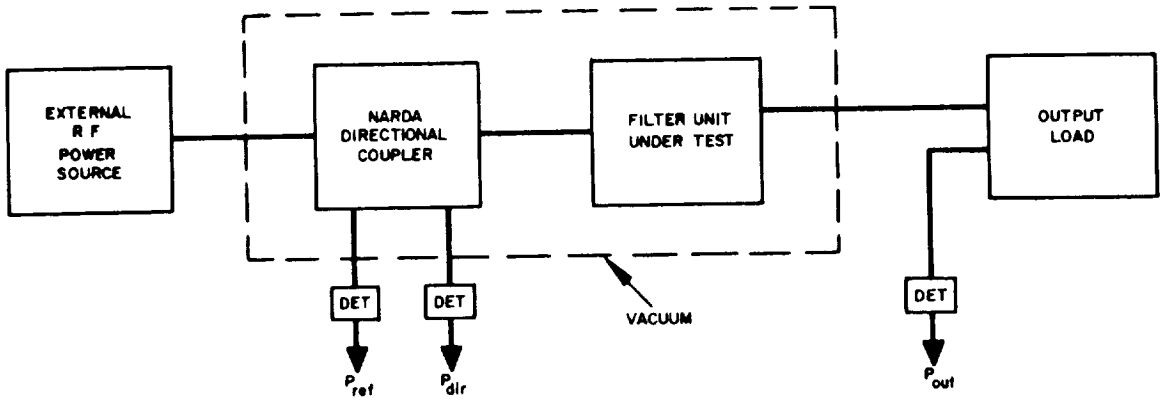

(a) Test setup - filter power measurements.

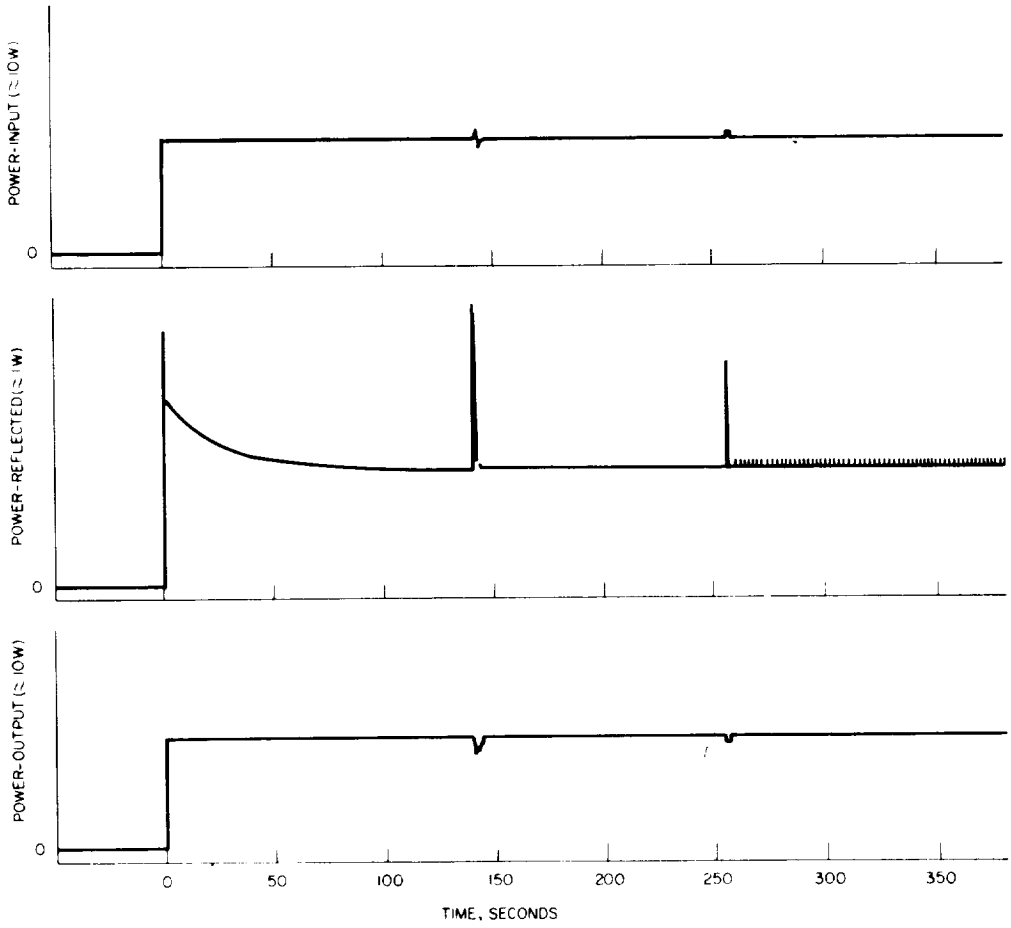

(b) Power; input, output and reflected.

Figure 2. Filter power tests.

at three second intervals, (4) gradual change in P_{ref}, apparently due to heating and slight retuning of the resonator, and (5) the absence of any gross long term effect on power output. After a series of experiments which yielded baffling results, we began to suspect that our instrumentation setup might contain some of these failures, rather than the filter itself. The coaxial fittings were checked and eventually the directional coupler unit was found to be responsible for the spikes and for some of the transient failures. A brief investigation of the directional coupler indicated that it was partially sealed, and was, in fact, producing the results shown in Figure 2(b). Apparently, a multipactor discharge inside it would liberate enough gas to "snuff out" the multipactor by raising the internal pressure. The voltage level was not large enough to produce gas ionization failure. When the directional coupler was removed from the test setup in the vacuum chamber, the transient failures were eliminated."

In general, it appears to be essential to avoid the possibility of a multipactor breakdown where undesirable electrical effects may occur, and it is also essential to prevent the establishment of a multipactor-initiated gas ionization failure where the magnitude of power available is sufficient to cause permanent physical damage to the component by heating. Photographs of such damage are shown in detail in this report, including components such as coaxial resonators, small capacitors, and a diplexer section.

METHODS OF ELIMINATING MULTIPACTOR

Since the necessary and sufficient conditions for the multipactor discharge are well understood, it is possible to eliminate it in many instances. In order to establish a multipactor discharge, all of the following conditions must exist.

1. The mean free path of electrons must be long enough to permit the electron to be accelerated between the emitting surfaces with low probability of collison with ambient atoms or molecules. As described in our Technical Proposal, TP-412, November 1963,

"The velocity of gas molecules in equilibrium is distributed in a Maxwellian distribution about a most probable value

$$V_m = \left(\frac{2\,k\,T}{m}\right)^{1/2}$$

where

m is mass of molecule – grams

k is Boltzmann's constant 1.4×10^{-16} ergs/°K

T is temperature °Kelvin

V_m is velocity cm/sec.

For nitrogen at room temperature, V_m is roughly comparable to the speed of sound (420 meters/sec.). The molecules travel in straight lines until there is a collision; the distance traveled between collision is called the free path. The classical analysis for λ, the mean free path, shows that there is an exponential decrease with distance in the number of molecules which have not suffered collisions after traveling out from an origin; the value, λ, is the distance at which 37 percent (1/e) of the molecules will have had no collisions. At a distance of 4λ, only 2 percent of the original molecules will have had no collisions. The mean free path of an electron, λ_e, is calculated to be $4\sqrt{2}\,\lambda$ when it is present in a gas filled volume, the mean free path of the electron being longer because of its smaller cross section. In general, the mean free path of molecules and electrons is inversely proportional to pressure. The mean free path of representative gas molecules and electrons is given below in Table I.

Pressure, mmHg	Gas Molecule	Molecule Mean Free Path λcm	Electron Mean Free Path λ_e cm
10^{-3}	He	17	96
10^{-3}	Ne	12	68
10^{-3}	A	8	45
10^{-3}	N_2	6.7	38
10^{-3}	K_r	6.6	37
10^{-3}	C_s	0.14	8

Table I. Molecular and electron mean free path at 0°C.

Typical gap dimensions in radio frequency devices may be as small as one millimeter, and consequently λ_e will be long enough to permit multipactor at pressures as high as 10^{-1} or 10^{-2} mm Hg, since λ_e for the gases listed above would range up to 1 to 10 cm. The multipactor discharge can exist at the low pressure end of the range of typical gas ionization discharge, and, in fact, the multipactor effect is sometimes made visible by the ionization of gas molecules by the electrons. Typical resonance ionization potentials for electron collisions with gas molecules exist for H_2 at 11.2 eV, for O_2 at 5 eV, for N_2 at 6.1 eV, and for Ne at 16.7 eV. The transitions of these ionized states back to the ground state usually result in emission of light in the ultraviolet and blue spectrum. The appearance of a multipactor discharge in our vacuum test chamber is a pale blue green with slight pink color. Its brightness appears to be a function of the power level and the gas pressure; it seems probable that the visible effects would be smaller at very low pressures due to the smaller numbers of gas molecules."

The typical blue glow of a multipactor discharge in a coaxial region is illustrated in the cover illustration of this report.

2. The arrival energy of the incident electrons must produce a net secondary emission ratio greater than one. As indicated in Report TP-412,

"For a typical material, the value of δ is a function of the energy and angle of incidence of the primary electron as shown in Figure 3(a) and (b). The shape of the curve of Figure 3(a) is commonly explained as an indication that at low incident energy the primary electron does not have enough energy to liberate many secondaries, and at very high incident energy the primary electron penetrates so deeply into the surface that the secondaries which might be produced are trapped in the substance and do not reach the surface. Table II summarizes the values of δ for typical materials.

Reliable measurements of δ have been made for pure substances. However, the measurement is difficult to perform,

particularly at low incident energy, and there are large variations in δ caused by compounds or surface impurities, such as oil or oxides or chlorides. Most contaminants increase the maximum value of δ and lower the threshold incident energy. As a result, measures to control multipactor by surface treatment will often fail because it is not practical to achieve or maintain the required surface purity."

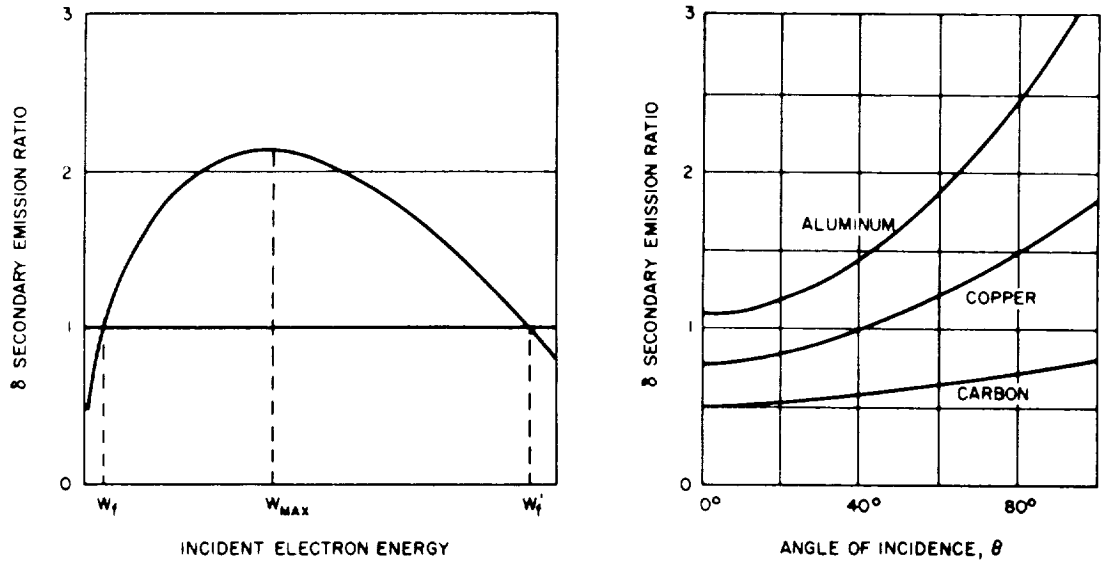

(a) δ vs. W (b) δ vs. θ

Figure 3. Secondary emission parameters.

Material	$W_{\delta = \delta max}$ (eV)	δ_{max}	W_f (eV)
Copper	600	1.3	75-175
Mica	380	2.4	30
Quartz	400	2.1	30
NaCl	600	6.8	15
Al_2O_3	350	2.5	20
Fe	350	1.3	125

Table II. Secondary emission ratio as a function of electron energy.

5. The electron transit time must be in resonance with the applied frequency. As shown in our Technical Proposal,

"The equation of motion of electrons in secondary emission resonance can be calculated approximately, neglecting the effects of the electron bunch which rapidly accumulates, and by the use of empirically determined constants for the velocity and angular distribution of secondary electrons. Using this theoretical-plus-experimental technique, Brown has derived equations for the voltage required to create resonance conditions for a single electron oscillating between parallel plates. The equation for resonance is

$$V = \frac{\omega^2 d^2}{\left(\frac{e}{m}\right)\Phi} \quad \text{or} \quad d = \frac{1}{\omega}\sqrt{V\Phi\left(\frac{e}{m}\right)} \tag{1}$$

$$\Phi = \left(\frac{K+1}{K-1}\right)\pi \cos\phi + 2\sin\phi \tag{2}$$

where

V = the voltage for secondary emission electron resonance, one half cycle mode

ω = angular frequency

d = plate spacing

$\frac{e}{m}$ = a well known physical constant of the electron

K = ratio of electron arrival velocity to component of emission velocity in the direction of the electronic field

ϕ = phase angle (with respect to RF field) at which secondary electron is emitted

Φ is a function of both K and ϕ, neither of which may be predicted theoretically. Limiting values of Φ are determined empirically by fitting of experimental observations. Typically, K is of the order of 4, and $-60° < \phi < 18°$. For these limits Φ varies between 0.77 and 5.44. Since the permissible values of Φ have a minimum and maximum for fixed frequency and spacing, there is a discrete range of voltage

which permits multipactor; for voltages outside this range it will not occur.* Similarly, if the voltage and frequency are constant, there is a discrete range of spacings which permit the discharge; smaller and larger spacings eliminate it."

"In addition to the half cycle resonance mode, Hatch and Williams* have studied higher order modes resulting from high voltages which cause transit periods of an odd number of half cycles."

The occurrence of multipactor for the half wave mode is illustrated in Figure 4.

4. It is also implicit in the foregoing conditions that the applied voltage, ambient pressure, and emitting surface are maintained constant throughout the duration of the discharge. Our experiments have shown that the multipactor discharge causes change in the surface, as evidenced by the appearance of a brownish irridescent film on the metal electrode. In addition, the ambient pressure may be increased because of the finite value of pumping speed in the test setup. The applied voltage may also be altered because of detuning and load effects, i. e., because the RF generator is not a constant voltage source.

The methods of eliminating multipactor which were investigated and described in this report represent the opposite, or negation, of conditions 1, 2, and 3 listed above. The mean free path of electrons may be reduced by pressurization, or by filling the empty spaces of the discharge region with foam or solid dielectric. The secondary emission ratio of the surfaces may be "spoiled" by use of dielectric coatings or by choice of materials of low emission ratio. The electron transit time may be made non-resonant by proper choice of the physical dimensions or the amplitude of the radio frequency voltage. A d. c. bias voltage may be applied

*His equations and graphs are stated in terms of electric field strength. Since the fundamental parameter is voltage, which determines electron energy, we have converted the equations slightly. The graphs may be interpreted in terms of voltage, since in the parallel plate field example the voltage is proportional to E.

*Hatch, A. J. and Williams, H. B., Physical Review No. 112, p.681; 1958, "Multipacting Modes of High Frequency Gaseous Breakdown."

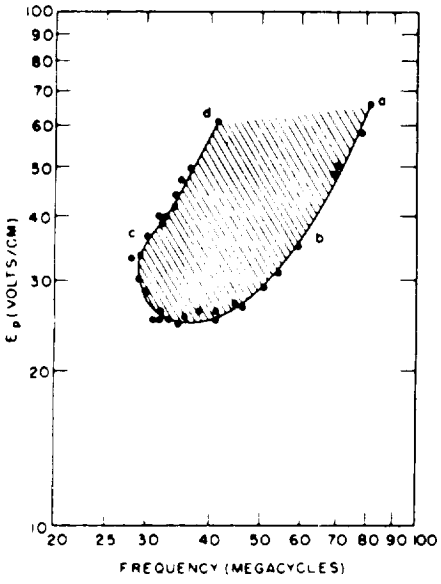

(a) Breakdown in hydrogen at a pressure less than 0.1 μ Hg.

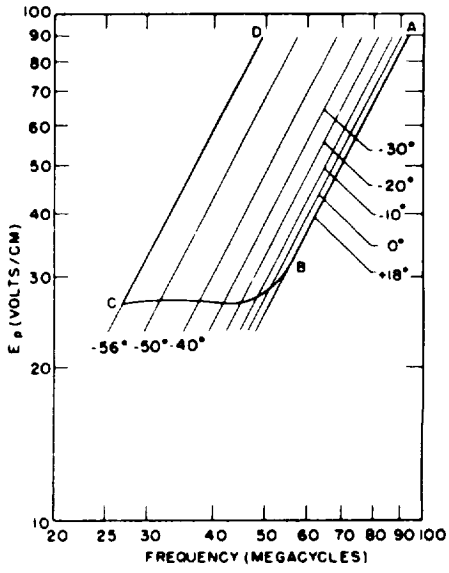

(b) Theoretical calculation of breakdown for 3-cm electrode separation, minimum electron arrival energy of 60 ev, and k = 3. Various lines represent condition for half-cycle electron transit times at indicated phase angles.

Figure 4. From Brown.

to one of the electrodes to alter the electron resonance equation. All of these techniques have been exploited in our study; detailed description of the results is included.*

*Magnetic fields can be used to deflect the electron trajectories. Because of the special complications of this method, it has not been investigated.

INVESTIGATIONS OF MULTIPACTOR EFFECT – TASK I

INTRODUCTION

The original proposed definition of Task I was:

a. Study necessary and sufficient conditions for existence of multipactor discharge, including (1) geometrical configurations which have not been analyzed; (2) effect of pressure on appearance, stability, and impedance of discharge; (3) devise and test methods of detecting the discharge and measuring its parameters, the scattered electron current, and the ion potential well; (4) existence and characteristics of multiple modes, single surface modes, and bias modes.

b. Study linear and non-linear electrical parameters of two surface half-cycle multipactor as a function of voltage input, gas pressure, and surface conditions, including measurement of resistance and reactance components at the applied frequency, harmonic currents, modulation characteristic, and noise generation.

c. Study secondary emission properties of typical surface materials of electronic components, and evaluate new surface treatments which have been proposed.

All of the goals of Task I have been completed with the exception of the effort to study the ion potential well. However, although the difficulty of measurement was greater than expected, we have devised sensitive, non-visual methods of detecting the discharge and measuring its parameters. Among the important accomplishments are the improvement and thorough development of the collector plate technique for sensing electron and ion currents, the use of a sampling oscilloscope to measure the electrode current due to multipactor (which has not been done previously, to the best of our knowledge), and the successful solution, by a method of successive approximation, of the non-linear partial differential equation for coaxial half-wave multipactor modes. The effect of pressure has been observed carefully; the relationship between the

vacuum test chamber pressure history and the stability of the discharge has been partly clarified. It is obvious that a clear understanding of pressure effects will be beneficial in interpretation of the results of environmental tests for multipactor. Linear and non-linear properties of the discharge have been measured, as planned, and the secondary emission properties of typical surface materials of electronic components have been observed.

During pre-contract negotiations, the NASA Project Technical Director recommended a greater emphasis on the goals of Task II and Task III. The measurement of common electrode materials originally planned as part of Task I was therefore extended to cover additional surfaces, such as epoxy coated copper, glass laminate, teflon, and vacuum grease, in an effort to discover methods of eliminating multipactor, which is the goal of Task III.

The individual experiments and analyses which report our work on Task I are described below.

STABILITY AND DURATION OF MULTIPACTOR DISCHARGE

The goal of this experiment was to establish a suitable test setup to generate multipactor discharges and to observe the effects of time and ambient pressure.

The equipment which was used is illustrated in Figure 5. A pair of 1" square brass plates was mounted on insulators and provision was made to vary the spacing between the plates by means of a motor drive. A coaxial line was connected to the plates to provide power, and an additional 1" square collector plate was mounted behind a hole in the grounded plate. Several pieces of phosphor coated tape were placed on and near the electrodes to detect the presence of electrons, and the chamber was evacuated. Test frequencies of 100 mHz and 400mHz were used. Whenever a discharge occurred the phosphor strips fluoresced, the typical blue glow was observed in the region between the plates, and current could be detected flowing to the collector plate.

Although one of the additional objectives of this experiment was to obtain quantitative data from which to calculate power loss as a function

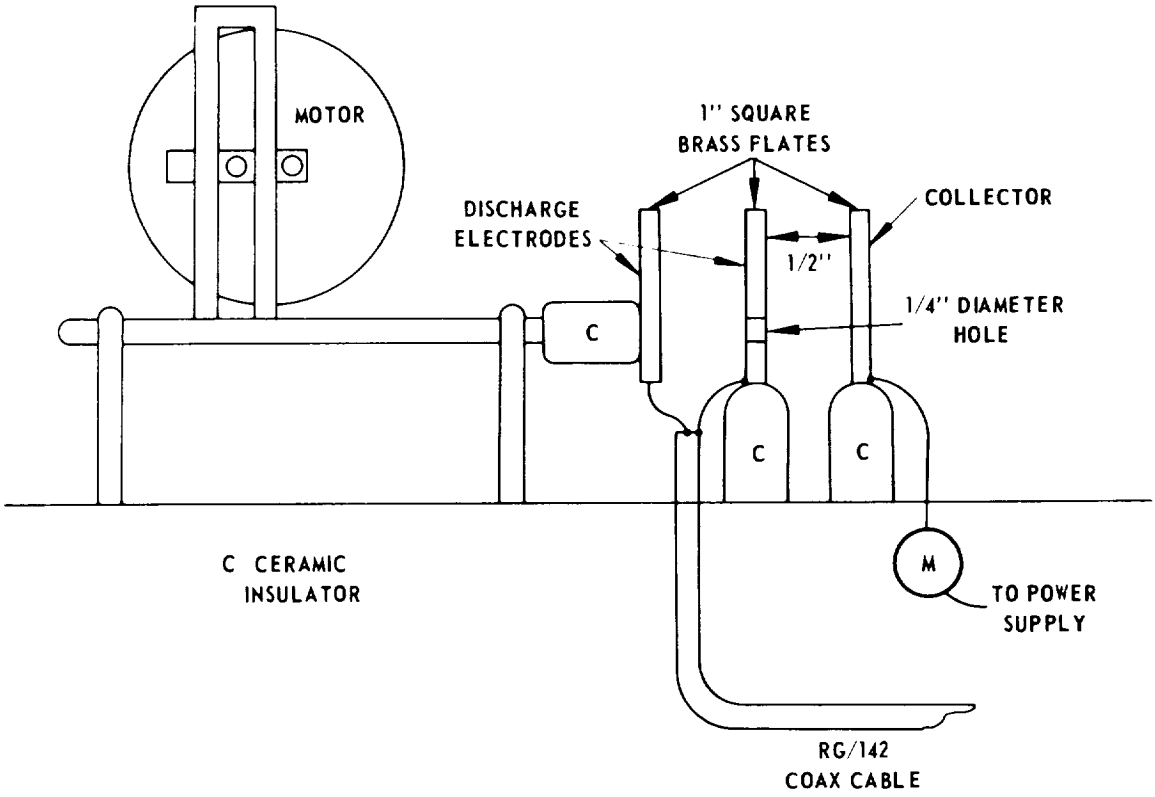

Figure 5. Variable electrode spacing fixture.

of electrode spacing and voltage, it was immediately apparent that this would not be easy. After a few hours of operation with any set of electrodes, it became impossible to obtain a significant discharge, and only dismounting the equipment and cleaning the electrodes could restore operation. The same results were noted for brass, silver-plated brass, gold-plated brass, aluminum, and anodized aluminum electrodes, and in general there was as much difference in behavior between different electrodes of the same material as there was between electrodes made of different materials. In each case, after a few hours of operation all multipactor operation ceased and examination of the plates would reveal the extensive discoloration which has been observed by most experimenters. In these experiments, the deposit seemed to be a combination of organic contamination from the vacuum pumps and sputtered metal from the electrodes. Since most of this series of experiments were conducted

at relatively high pressures (between 10^{-6} and 10^{-5} mm Hg), the gas probably had a significant effect on contamination of the electrodes and perhaps also on the electrical characteristics of the discharge. As the gas pressure was raised, the same general electrical behavior was noted, but the plates deteriorated much more rapidly.

Because of the necessity of obtaining much longer effective life of the electrodes for the long term exposure experiments, another series of experiments was set up, using a much cleaner vacuum pump and capable of operation at much lower pressures (to 10^{-10} mm). From the experience reported by other experimenters* it was hoped that lower pressure vacuum operation would result in more repeatable experiments and in longer life for the discharge, but preliminary experimental results did not prove this. In the first experiment, using brass plates, the RF power was first applied at a pressure of 2.5×10^{-8} mm, but as power was applied the pressure rose quickly to about 5×10^{-7} mm, and then stabilized. Since the pump had a pumping speed of 125 liters per second, the amount of gas liberated must have been very large. After about 3 hours of operation the discharge had died down to a very low level, and after the RF power was removed the discharge could not be restarted. The equipment was left in the chamber and pumped for 48 hours more, and then energized at a pressure of about 10^{-7} mm and a discharge was noted; after 45 minutes of operation the discharge again failed. An experiment with silver-plated electrodes produced similar results. An interesting result of these lower pressure experiments was that the blue glow in the discharge region was still visible at 10^{-8} mm, indicating that there was appreciable ionization of the residual gas by the electron cloud.

In view of the difficulty of obtaining a sustained discharge, the experimental setup was revised to achieve substantially lower pressures. In an actual unpressurized spacecraft environment the local pressures may have any value from a few millimeters down to perhaps 10^{-12} mm, depending on the external pressure, local outgassing, and the extent of venting to the exterior of the spacecraft. While any multipactor activity

*Secondary Electron Multiplication in Microwave Field, Frank Fu Fang, 15 May 1959, ASTIA Document No. AD 217035.

would probably cease after a few hours of operation at the higher pressures, sustained discharges are to be expected when the pressure is below about 10^{-9} mm. In order to permit operation of the discharge in this pressure range, it was necessary to bake the vacuum chamber and the experimental apparatus at a temperature of 250°C for 24 hours or more. In light of this rather extreme treatment, there is considerable doubt that pressures as low as 10^{-9} mm will ever be reached in the interior regions of spacecraft, even if they are fairly freely vented.

The vacuum chamber used in these tests is about 6" in diameter and 12" long, and is pumped through a 6" port in the long side by a 125 liter per second pump, which is equivalent to a 1.5" diameter orifice opening into a perfect vacuum. Although both the equipment and the chamber were carefully cleaned before evacuation, the ultimate pressure of this system at room temperature was about 2×10^{-8} mm.

In a typical spacecraft installation the equipment may be installed in a bay with a comparable volume, but with a much smaller opening to the external pressure. Furthermore, the surface area inside the bay may be quite large (particularly if multi-layer aluminized mylar heat shields are used), and there may be considerable contamination by relatively high vapor pressure materials.

For the first high vacuum tests the electrodes used were copper which had been treated with an organic magnesium salt. (This material was chosen because it had been found to be a stable secondary emitter when used in a controlled atmosphere at considerably higher pressure.) After extended bakeout the pressure was reduced to 8×10^{-10} mm and RF voltage was applied. In order to provide a purely electrical indication of the existence of the discharge, a hole was drilled in one of the electrodes, as shown in Figure 5, and an electrically isolated collector plate was placed behind the electrode in a position to intercept electrons from the multipactor which might pass through the hole. A d.c. collector current was found to be a good indication of the multipactor discharge. As voltage was varied through the optimum value for multipactor a momentary fluorescence of the detector phosphor was occasionally noted, together with a slight current to the collector plate. However, no

sustained discharge could be obtained and no experimental data was obtained. The electrodes were exposed to air and then the system was pumped down to 10^{-6} mm and RF power applied. Under these conditions a strong discharge was obtained. No further experiments were run with this electrode material since it had become evident that beryllium copper would probably make more useful electrodes.

A pair of bright dipped beryllium copper electrodes were installed, and the chamber was again evacuated. When the pressure reached 4×10^{-6} mm, RF voltage was applied and a strong discharge occurred, with a collector current of 80 microamperes. Power was removed and the assembly was then baked out and pumped until a room temperature pressure of 6×10^{-9} mm was reached. RF power was again applied and a strong discharge was obtained, as indicated by fluorescence of the detector phosphor and flow of collector current. Initial collector current was 80 microamperes, the same value noted at 4×10^{-6} mm. During 2 hours of operation at the same power level the current increased and then stabilized at 180 microamperes (see Figure 6). At this time the power input was reduced until the collector current was 160 microamperes, and the test was then continued for 15 hours at this same power

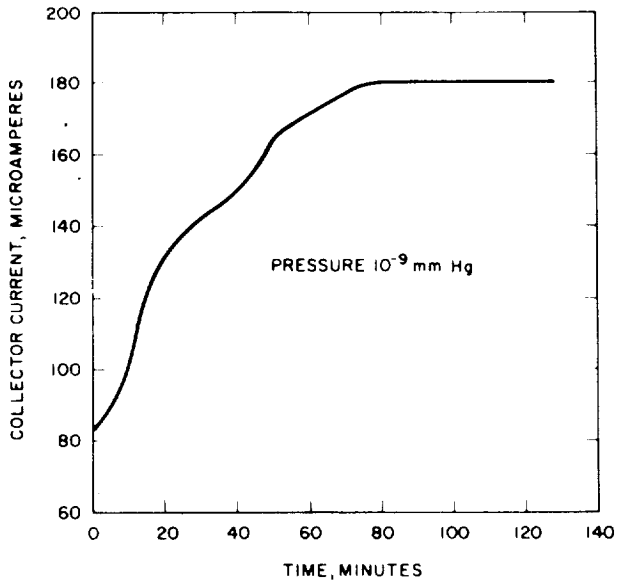

Figure 6. Beryllium copper - current in hard vacuum.

level. At the end of the test, the chamber pressure had dropped to 1.8×10^{-10} mm and the collector current was 158 microamperes, indicating that within the stability of the measuring equipment, no change in multipactor level had occurred.

In order to verify the previous observations of electrode-deterioration at high pressure, a leak was introduced into the vacuum system, the pressure was increased to 10^{-6} mm, and RF power was applied. The initial collector current was 220 microamperes, and it dropped to 168 microamperes at the end of 3-1/2 hours of operation, as shown in Figure 7. While the current decreased steadily during the run, the rate of decay was not as great as that which is usually observed, probably because the residual gas was air without any organic contamination.

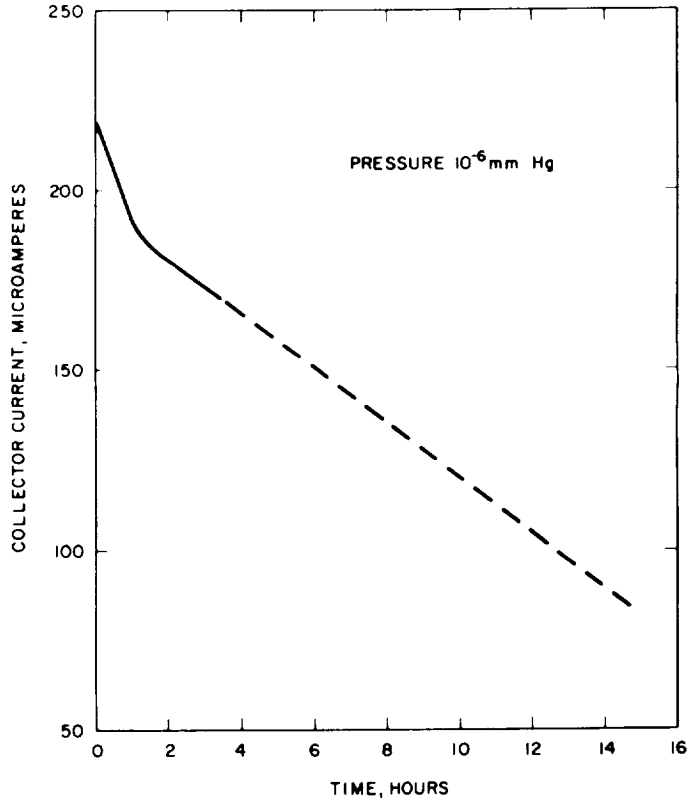

Figure 7. Beryllium copper - current in average vacuum.

The equipment was left operating for an additional 16 hours. At the end of this time the chamber pressure had dropped to 4×10^{-9} mm, the collector current was 135 microamperes, and the detector phosphor (which had ceased to glow at the end of the 3-1/2 hour run) again glowed brightly. This confirmed previous observations that exposure to high vacuum would arrest the deterioration of the electrodes, and probably restore their activity.

The conclusion which can be reached from these results is that tests of spacecraft equipment should be conducted over the full range of pressures at which it will actually be operated, at least insofar as multipactor behavior is to be evaluated.

Many system vacuum tests are run in the 10^{-6} mm range, a pressure range where a discharge may last for only a few minutes and perhaps escape observation. If, in subsequent operation, the pressure were to drop to the 10^{-9} mm range or below, multipactor activity could return and remain permanently, although the equipment had apparently passed a "vacuum" test.

THEORY AND EXPERIMENTS ON MULTIPACTOR ELECTRON RESONANCE

a. Analysis of Multipactor Effect between Plane Parallel Electrodes

The configuration to be analyzed contains a pair of plane parallel electrodes, the length of whose sides is sufficiently large compared to the spacing to provide a uniform field in the intervening volume.

Let the parameters be as follows:

V_p = peak sine voltage between the plates
ω, ϕ = frequency and phase angle of the applied sine wave
d = spacing between plates; x-distance from one electrode
e, m = charge and mass of the electron
u = velocity
t = time
f = frequency

K = ratio of electron velocity as it strikes electrode to the normal component of the velocity of the secondary electrons

i = current flowing in the connection to an electrode

If we neglect the effect of the free charges in the volume, the electric field is constant and produces an accelerating force on an electron given by

$$\text{force} = m\frac{du}{dt} = -eV_p \sin(\omega t + \phi) \tag{3}$$

Integration of this equation twice and the application of the boundary conditions $x = 0$ at $t = 0$, and u_o = initial velocity results in the following solutions for:

arrival velocity
$$u_f = u_o + \frac{2eV_P \cos\phi}{\omega dm} \tag{4}$$

distance
$$x = u_o t + \frac{eV_P}{\omega^2 dm}\left|\omega t \cos\phi + \sin\phi - \sin(\omega t + \phi)\right| \tag{5}$$

and by applying the principle of conservation of energy to the motion of charges in the external circuit and in the discharge volume, we may calculate that the current is

$$i = \frac{eu}{d} = \frac{eu_o}{d} + \frac{e^2 V_P}{\omega d^2 m}\left|\cos\phi - \cos(\omega t + \phi)\right| \tag{6}$$

Equations (4), (5), and (6) apply to the first trip of a primary electron across the gap. By assuming symmetry, we can analyze the travel of the secondary electrons in the same manner with due allowance for the reversed direction of travel. Due to these assumptions the primary electron is replaced by the secondary instantly, and with a discontinuous change in velocity; therefore, it is clear that the current flow in the external circuit will not be sinusoidal and should be expected to have harmonic content.

The power input to the electrodes may be calculated from the average value of the product of applied voltage and current per electron.

$$\text{Power input per electron} = \frac{2eu_o V_P}{\pi d} \cos \phi + \frac{2e^2 V_P^2}{\omega m \pi d^2} \cos^2 \phi \qquad (7)$$

The electron resonance conditions for the stable discharge may be obtained by substitution of the condition that the electron will arrive at the electrode an odd number of half-cycles after it starts. Higher modes are discussed in the appendix of this report, but for this particular analysis we will only study the half-wave mode, i.e., electron transit time of one half-cycle, or $\omega t = \pi$ when $x = d$. Substituting these values in equations (4) and (6), we obtain

$$u_f - u_o = \frac{2eV_P}{\omega md} \cos \phi = u_f \left(\frac{K-1}{K}\right) \qquad (8)$$

and

$$d = \frac{u_o \pi}{\omega} + \frac{eV_P}{\omega^2 md} (\pi \cos \phi + 2 \sin \phi) \qquad (9)$$

which may be expressed in a more convenient form for experimental verification by use of a little algebra, including the substitution of (8) in (9), we can obtain

$$V_P = \frac{\omega^2 md^2}{e} \frac{1}{\frac{K-1}{K+1} \pi \cos \phi + 2 \sin \phi} \qquad (10)$$

Equation (10) contains the essential features of the resonance conditions. The peak voltage necessary for a discharge is seen to depend on the square of quantity, ωd, indicating the transit time resonance to be a function of the initial phase of electron emission and the parameter, K, the ratio of arrival to emission velocity. A phase focusing characteristic is also clearly indicated, since for $K \cong 1$, the

value of V_p is nearly inversely proportional to $\sin \phi$, while for large values of $K \gg 1$, much smaller values of V_p will satisfy the equation. Consequently, the resonance condition does not result in an eigenvalue but instead permits a range of phase angles and V_p combinations to exist. In fact, since the value of K for individual secondary emission events is undoubtedly distributed in a statistical range of magnitudes, the analysis is seen to be based on reasonable, but inexact, assumptions. In fact, the usual procedure found in past literature is to determine K by experiment and to utilize the result in the analysis herein quoted.

As shown in the appendix, for each assumed value of K, there is an associated value of ϕ which will result in a minimum initial breakdown voltage V_p. Since such information is of great importance in design of equipment, a family of curves has been plotted in Figure 8, summarizing the data. Levels of arrival energy are indicated by dotted lines; these values were shown because they represent the minimum range of magnitudes which are likely to produce a sufficient secondary emission ratio to sustain a discharge on the surface of ordinary materials.

Typical points on the curve may be cited to show the dimensions which are of interest in design of equipment. For example,

$f = 100$ mHz, $V_p = 100$, $d = 0.9$ to 2.6 cm

$f = 400$ mHz, $V_p = 50$, $d = 0.15$ to 0.76 cm

Voltages, such as these, are frequently present in medium power transmitters or even in low power transmitters at high impedance junctions; spacings, such as these, are also commonplace. Consequently, the multipactor effect is not unlikely to appear in typical equipment.

b. Analysis of Electron Trajectory across the Gap

Under conditions defined in equations (2) through (10), the position of the electron as a function of time may be computed from (5). The magnitude of initial velocity is important in determining what combinations

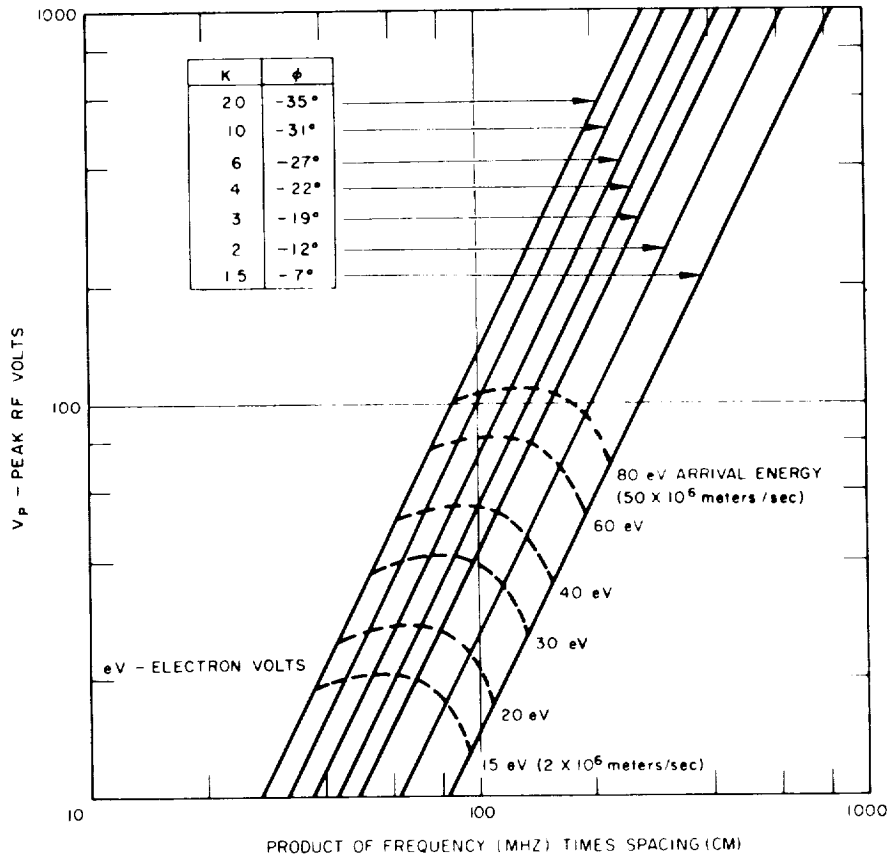

Figure 8. Multipactor breakdown resonance conditions (minimum voltage versus product, F x D).

of phase and initial velocity are compatible. The curve also may be used as a rough quantitative indication of the thickness of the sheet of electrons which oscillates back and forth.

Figure 9 is an electron trajectory plot for a particular spacing (1 cm) and frequency (100 Mc). The electron is assumed to have zero initial velocity ($v_o = 0$) and in order for the electron to meet the requirements of a multipactor discharge, it must initially experience no negative force that would drive it back into the electrode; this includes negative values of phase angle ϕ. The electron must arrive at $d = 1 \times 10^{-2}$ m when $t = 0.5 \times 10^{-8}$ sec. with sufficient velocity to produce secondary electron emission. Final velocity reaches zero at $\phi = +90°$ so that the value of ϕ is limited between 0 and less than 90°.

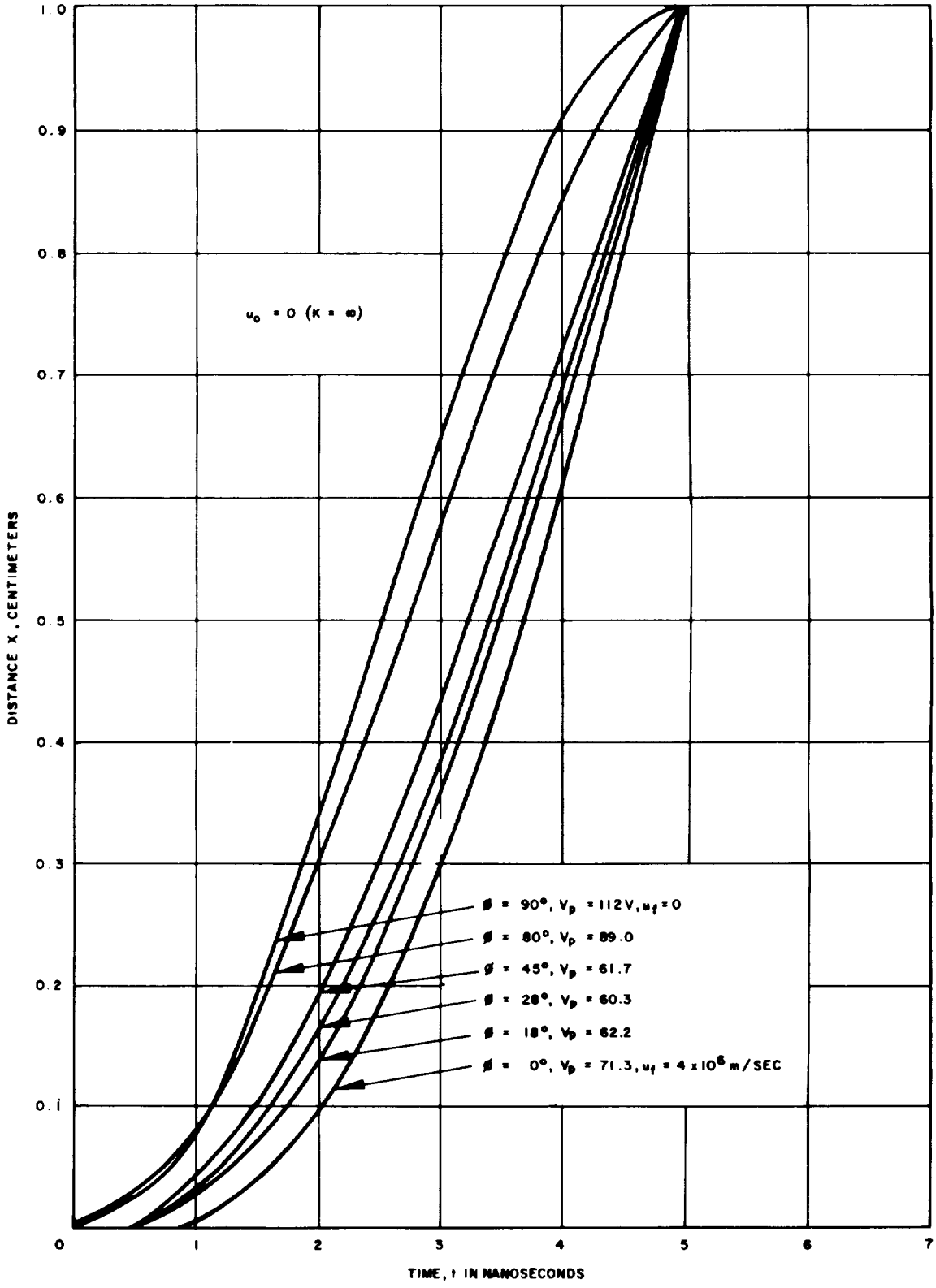

Figure 9. Electron trajectory.

Figure 10 shows the same type of electron trajectory plot for another initial velocity (v_o = 1 x 10^6 m/sec.). Here negative values of ϕ are permissible. With large values of k and negative phase angles the electron can be directed back toward the emitting electrode. It is lost in this way for k = 42, ϕ = -20°; k = 10, ϕ = -40°; k = 3.7, ϕ = -60°.*

For values of K = 4 or less the limiting value of ϕ is -57.5°, where an infinite value of V_P electrode volts is required. In the positive ϕ range, at ϕ = +90°, the arrival velocity equals the emission velocity which is not a plausible condition. The range of values of ϕ then falls between -57.5° and +90°.

For starting conditions, it is of importance to determine the minimum peak voltage, V_P, needed to produce a given arrival velocity. A range of initial velocities is possible and for each value an optimum ϕ can be determined. In addition, the value of fd (frequency x spacing) must be calculated to satisfy the voltage, phase and velocity conditions.

c. Experimental Verification of Resonance Equation and Minimum Value of W_f for Common Materials

As a test of the theory described above, and in order to establish the empirical behavior of materials and surfaces found in spacecraft transmitters, the test setup illustrated in Figure 11 was used.

A pair of 5" diameter plates, spaced 1/2" apart, was used for the discharge electrodes, which also served to tune a resonant transmission line used to couple energy into the plates. Figure 11 is a side view of the electrode structure used in the impedance and detector experiments to be described below.

Both plates were mounted so that the spacing could be varied, although in general the "hot" plate was the one which was moved to adjust the line tuning. As shown in Figure 11, several holes were drilled in the grounded plate, and behind one of them a collector plate was mounted to the ground plane in such a manner as to bypass it to ground for radio frequencies. This plate served as a detector for electrons produced by

*Gill and Von Engel, Royal Society of London, Proceedings, Ser. A 192, 1947, p. 446.

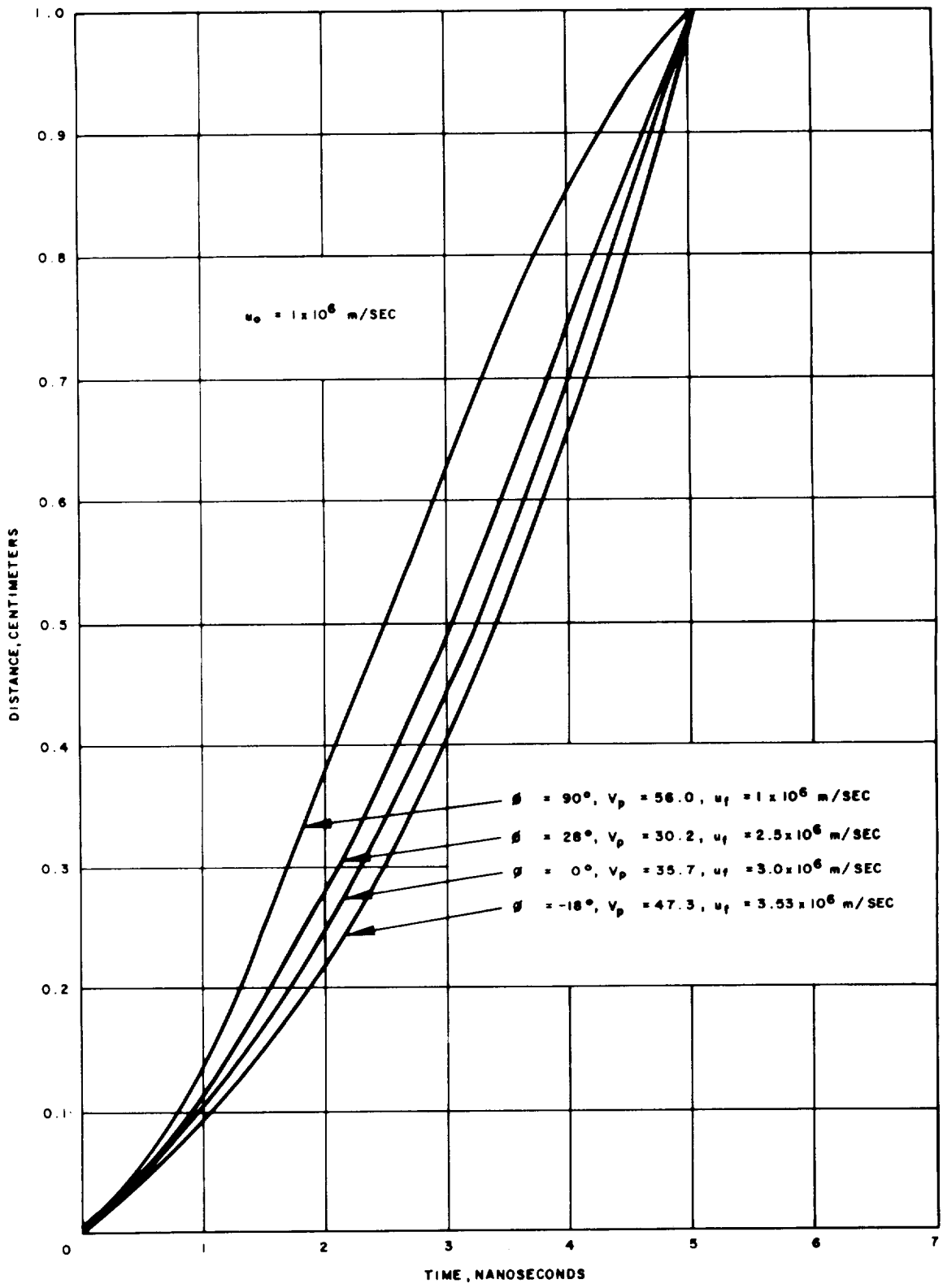

Figure 10. Electronic trajectory.

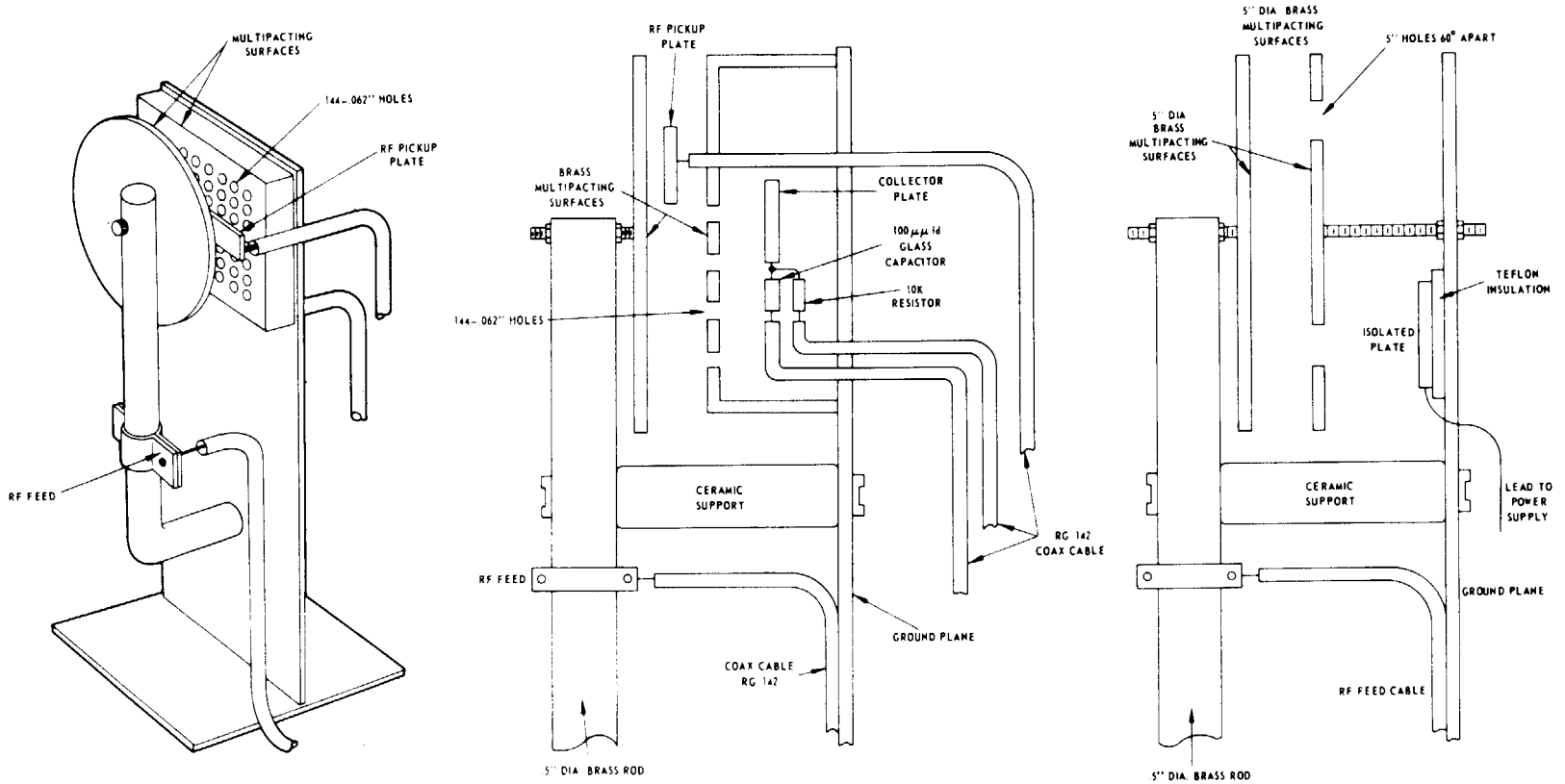

(a) "STANDARD" 100mc EXPERIMENT DETAILS

(b) ELECTRODE DETAILS HARMONIC EXPERIMENT

(c) ELECTRODE DETAILS, FOR IMPEDANCE MEASUREMENTS

Figure 11. Test fixtures.

a multipactor discharge. Input power was coupled to the tuned line from a coaxial cable which could be tapped up or down for impedance matching purposes. Although not shown in the figures, a high frequency rectifier diode was also connected to the plates to measure the RF voltage between them.

The procedure for obtaining the data was as follows: with a given electrode spacing, the RF voltage would be slowly increased until current was indicated on a 0 to 60 microampere meter measuring the collector plate current, showing multipacting had started. The voltage would be increased through the value at which discharge started and beyond the point at which the discharge ceased.

Table III shows these minimum and maximum voltages for the various spacings. At the wider spacings, the multipactor discharge would load the RF resonant assembly to the extent that it was not possible to deliver enough voltage to extinguish the discharge. However, the purpose of the experiment was to determine minimum spacing and voltage, and this was accomplished.

A thin coating of epoxy was applied to a pair of copper electrodes. Multipacting could not be obtained with a spacing of less than 7/16" (1.11 cm) and a minimum voltage of 73 volts. The multipacting also appeared weak and erratic. A sheet of 1/32" glass laminate board was attached to each of a pair of beryllium copper electrodes. Multipacting began at a spacing of 3/8" (0.953 cm) and at a potential of 72 volts. The blue glow from the multipactor discharge appeared to be as strong as that observed from metallic surfaces.

Thin sheets of teflon were attached to the beryllium copper electrodes. The minimum spacing and voltage was 1.1 cm and 70 volts. A pair of beryllium copper electrodes were rubbed with a silicon oil consisting of Dow Corning No. 200 fluid. Multipacting was very weak and erratic. No multipacting was obtained at 5/16" (0.793 cm) spacing as shown in Table III.

A 0.1-percent salt solution consisting of salt and distilled water was applied to gold-flashed aluminum electrodes and also to silver-plated aluminum electrodes. The water was permitted to evaporate.

Material	Discharge at Various Spacings (electron volts)						
	0.716 cm	0.793 cm	0.953 cm	1.11 cm	1.27 cm	1.9 cm	2.22 cm
Tin-plated Beryllium Copper	24-76	24-90	28-116	28-168	40-	126-	186-
Aluminum	26-110	28-137	34-166	44-190	52-	145-	187-
Copper	28-	26-114	28-148	38-178	40-197	132-	185
Copper (3.5" dia.)	24-68	24-105	33-150	40-170	50-185	125-	---
Beryllium Copper	35-100	29-116	35-132	46-165	66-	152-	---
Beryllium Copper (3.5" dia.)	36-105	---	33-125	41-160	52-	148-	190-
Gold-flashed Aluminum	48-86	34-117	32-150	35-175	45-	124-	182-
Silver-plated Aluminum	55-	31-102	35-130	51-180	55-	150-	200
Brass	None	36-128	32-175	40-	51-	147-	215
Thin Epoxy on Copper	None	None	None	73-170	78-	137-	187-
Glass Laminate on Beryllium Copper	None	None	72-95	89-185	98-205	160-	---
Teflon on Beryllium Copper	None	None	None	70-170	89-	154-	195-
Dow Corning 200 Fluid on Beryllium Copper	None	None	27-130	None	40-	121-	200-
0.1-percent Salt Solution on Gold-flashed Aluminum	---	35-100	33-133	41-	48-	132	---
0.1-percent Salt Solution on Silver-plated Aluminum	38-68	34-105	31-137	38-	52-	138-	---

Table III. Spacing and voltage to multipactor, f = 100 mHz.

(Weak salt solutions could be deposited on electronic components during assembly due to perspiration from the assembler's hands.) Salt requires only 15 electron volts of incident energy to produce a secondary emission ratio of one. Copper requires from 75 to 175 electron volts. The weak salt solutions decreased the tendency to multipactor slightly, contrary to expectations. In an attempt to verify the nature of this result, we treated copper with a strong salt solution and salt crystals, but once again found greater resistance to multipactor breakdown than before salt treatment.

Two pairs of 3.5" diameter electrodes consisting of copper and beryllium copper which were half the area of 5" diameter electrodes were also tested. It will be noted from the tabulated data that there was no significant difference in minimum or maximum voltage breakdowns for the smaller electrodes.

The voltage versus spacing tests were also performed at a frequency of 430 mHz. In general, the results of the first nine materials so tested were completely consistent with the electron resonance equation, since the minimum spacings observed were compatible with a constant value of the product, f x d. Table IV summarizes the data. The only anomaly in the 430-mHz test is the result for epoxy-coated material; this is believed to be due to a lack of uniformity between the material used in this test and in the 100-mHz measurement.

All of the voltage breakdown data is plotted in Figure 12, indicating the envelope of conditions under which breakdown may occur. In addition, the curve of Figure 13 is included to demonstrate the degree of conformity between theory and experiment. It is noteworthy that spacing and breakdown voltages occur very frequently which corresponds to low voltage amplitudes, in the range of 20 to 40 peak volts, and low electron arrival energies, in the range of 15 to 30 electron volts. The surface-coated materials appear to require higher arrival energy and are therefore to be considered as definitely beneficial in inhibiting multipactor discharges.

Material	Discharge at Various Spacings (electron volts)				
	0.175 cm	0.190 cm	0.254 cm	0.304 cm	0.545 cm
Tin-plated Beryllium Copper	34-72	30-115	42-178	53-	190-
Aluminum	27-110	42-150	48-	60-	190-
Copper	26-80	32-110	45-	57-206	195-
Beryllium Copper	36-120	29-120	42-	60-	210
Gold-flashed Aluminum	26-110	36-130	30-	40-	190-
Silver-plated Aluminum	38-	35-112	46-	57-	225-
Brass	28-80	38-	44-200	72-	198-
Thin Epoxy on Copper	None	85-152	50-	50-	210-
Teflon on Beryllium Copper	None	None	None	85-	210-

Table IV. Spacing and voltage to multipactor, F = 430 mHz.

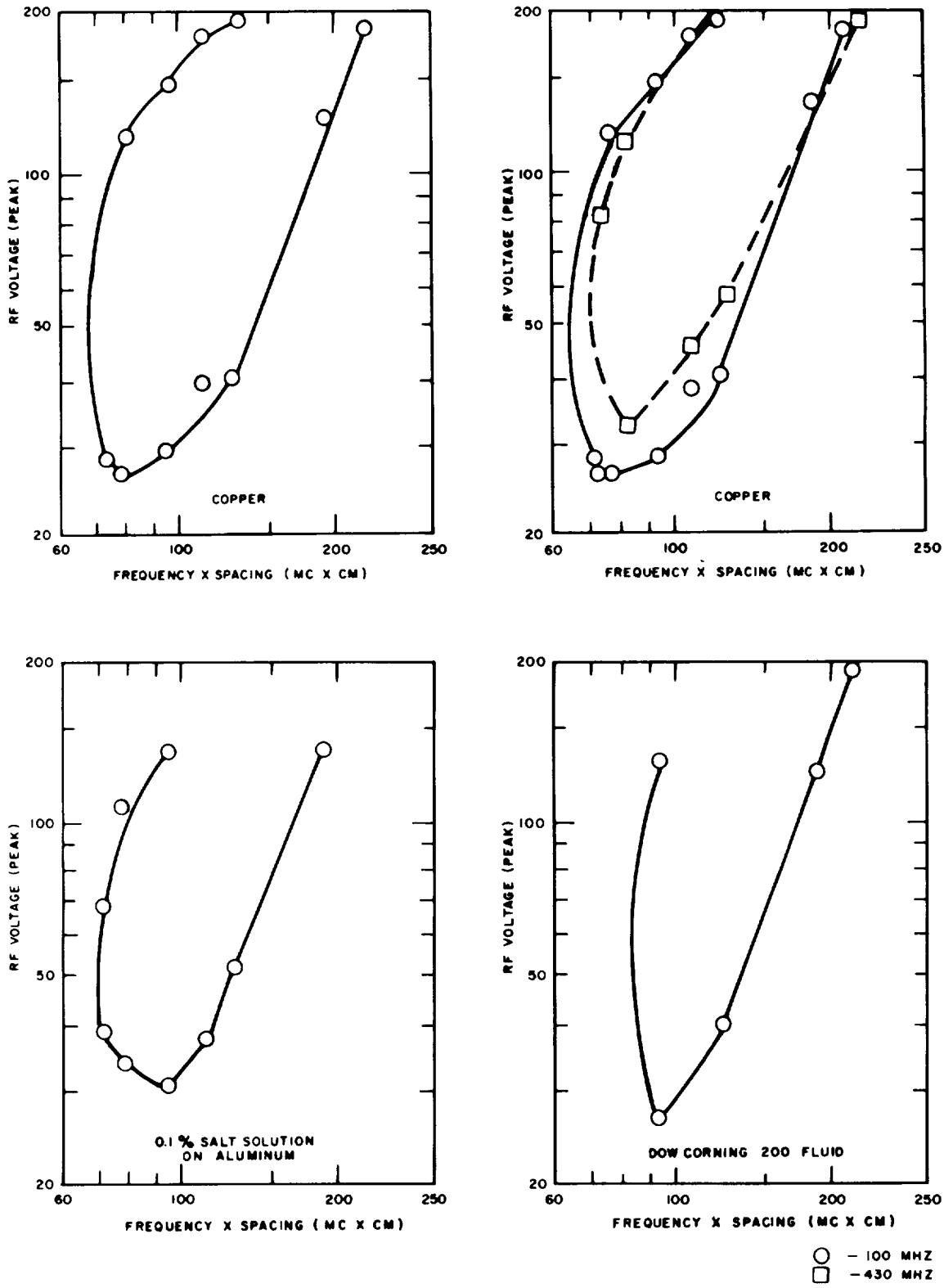

Figure 12. RF breakdown voltage for common materials.

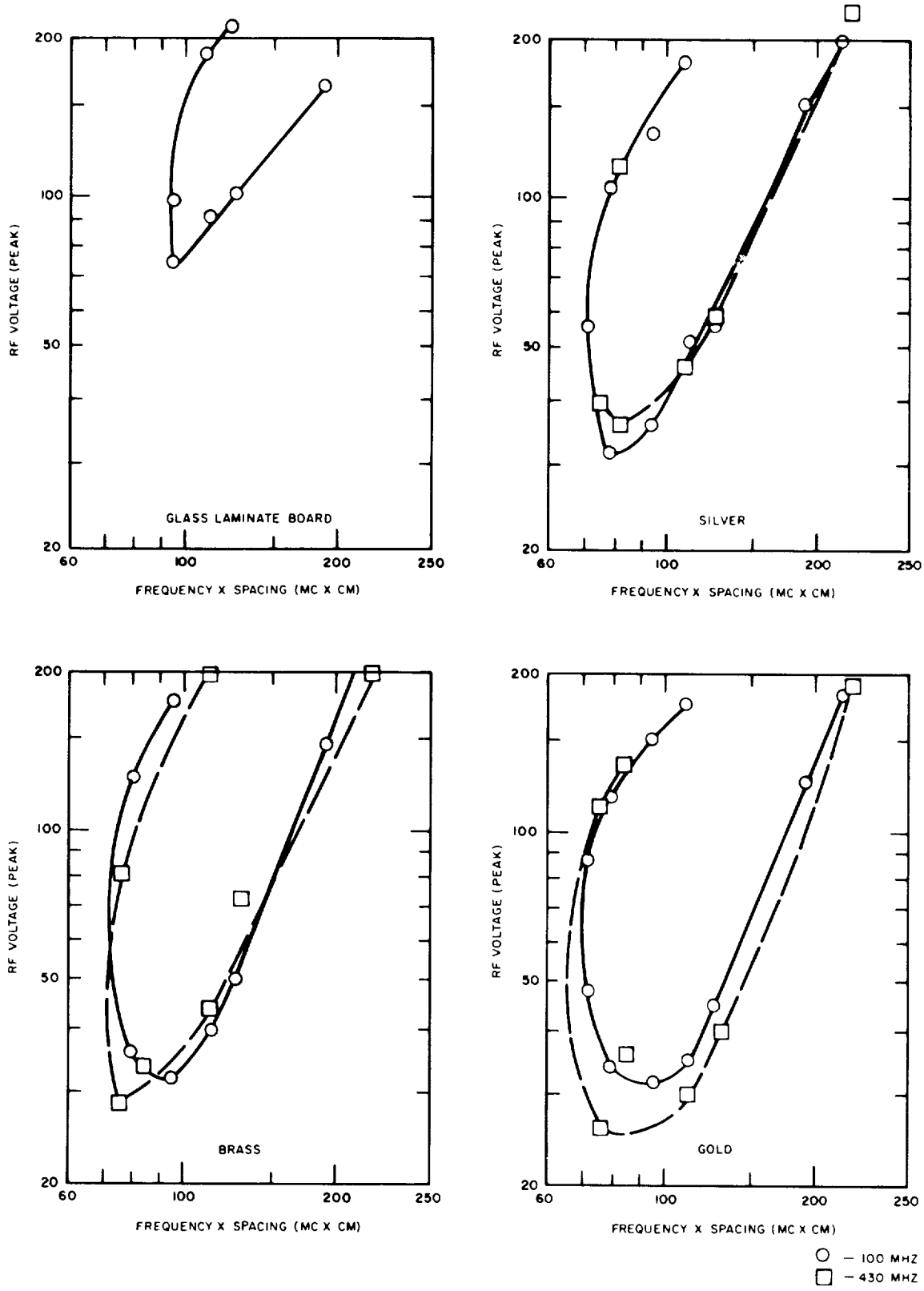

Figure 12. (continued)

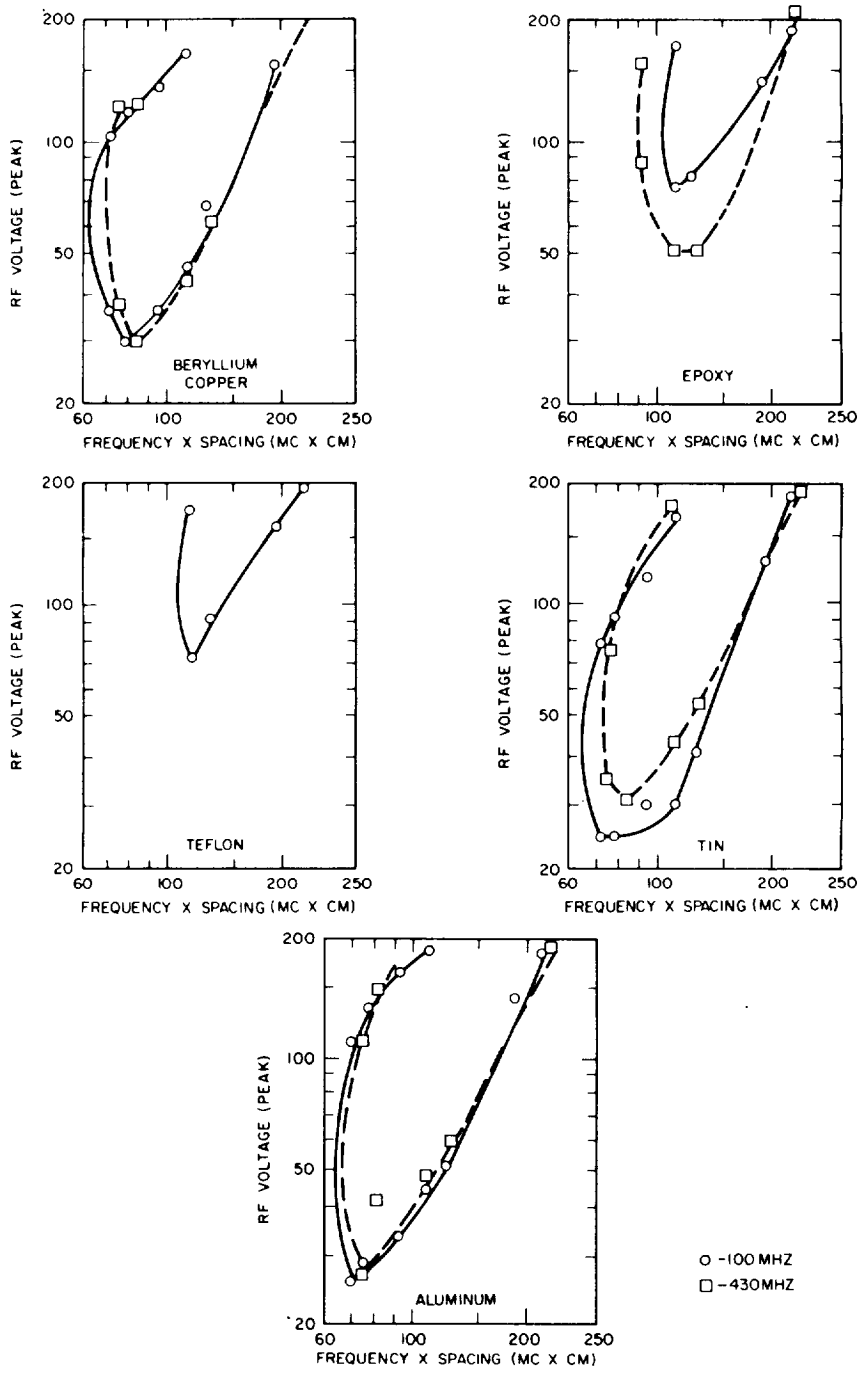

Figure 12. (continued)

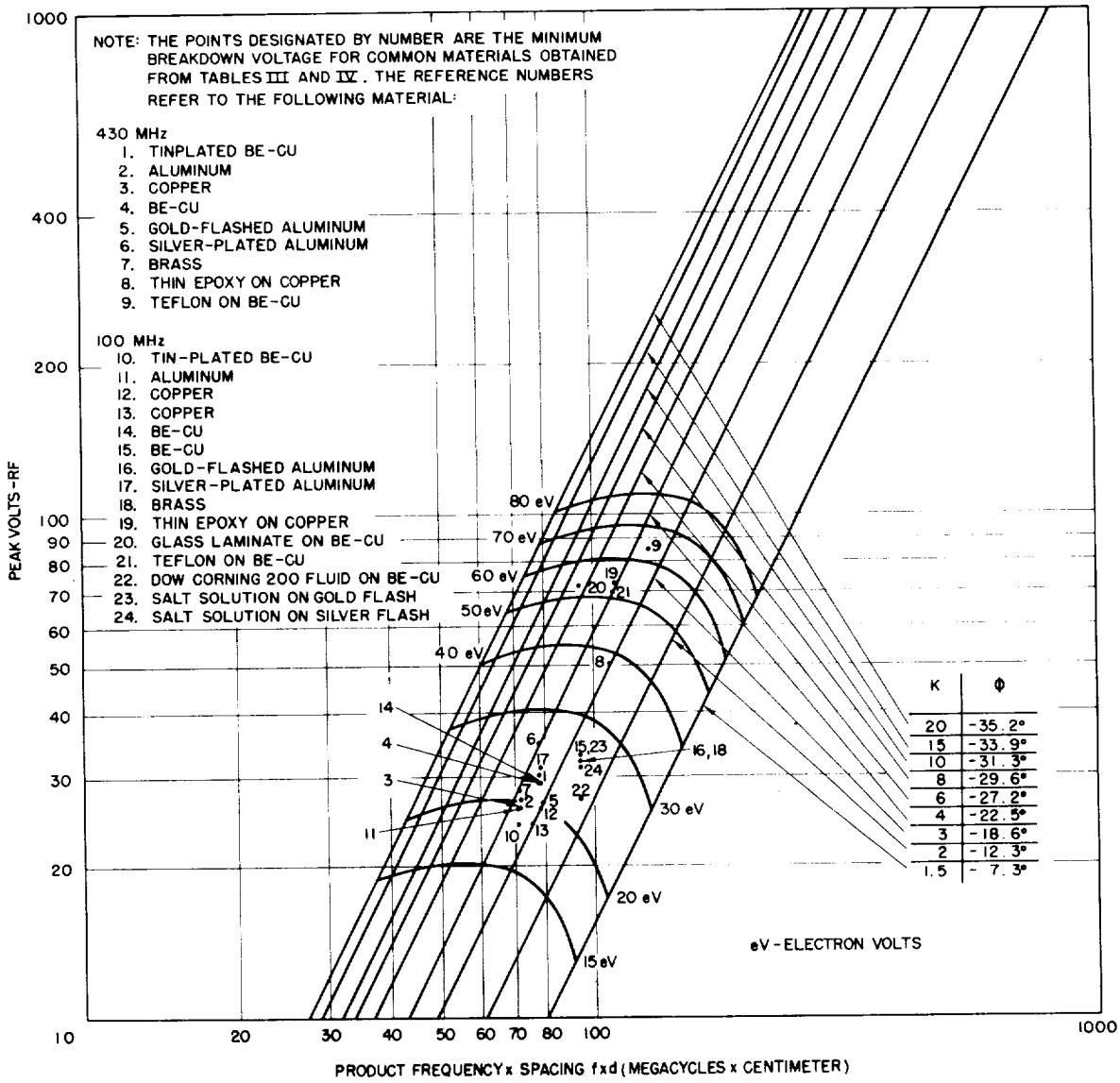

Figure 13. Minimum observed breakdown voltage for common materials.

d. Analysis of Multipactor Discharge between Concentric Cylinders

Since coaxial geometry is frequently utilized in space electronic equipment, it is worthwhile to analyze and test the properties of voltage breakdown. If we assume concentric cylinders of radius r_o and r_i, neglect the effect of free charges in the volume between the cylinders, and assume that the cylinders are very long compared to their radii, then the electric field will be in a radial direction and the electrostatic force acting on an electron will be given by equation (11):

$$m\ddot{r} = - \frac{eV_P \sin(\omega t + \phi)}{r \ln\left(\frac{r_o}{r_i}\right)} \tag{11}$$

in which r is the radius to the electron, and $\ddot{r}$ indicates a second derivative with respect to time. The initial conditions of emission of an electron may be assumed: at $t = 0$, we will take $r = r_i$, $\dot{r} = u_o$, and $\ddot{r} = \frac{e}{m} \frac{V_P \sin \phi}{\ln\left(\frac{r_o}{r_i}\right)}$.

In order to simplify computation, let us choose a constant,

$$\alpha = \frac{1}{r_i \omega_o^2} \frac{e}{m} \frac{V_P}{\ln\left(\frac{r_o}{r_i}\right)}$$

and, using the method of successive approximations, as outlined in "Partial Differential Equations," by H. Bateman, we will attempt a solution in the form of a summation of functions of the form

$$r = \Sigma \alpha^n C_n(t) \tag{12}$$

where $n = 0, 1, 2, 3 \cdots$, and C_n is a function of time. By substituting the assumed solution into the original equation for the force on the electron, i.e., equation (11), we obtain:

$$\left|C_o + \alpha C_1 + \alpha^2 C_2 + \cdots\right| \cdot \omega^2 \cdot \left|C_o + \alpha C_1 + \alpha^2 C_2 + \cdots\right| = \alpha r_i \omega^2 \sin(\quad t + \phi) \tag{13}$$

Using the initial condition, r_i may be taken as C_o, which is the only constant not dependent on time, and by equating the coefficients of like powers of α on both sides of (13), we obtain a family of differential equations:

$$C_o \ddot{C}_o = 0 \tag{14}$$

$$\ddot{C}_o C_1 + C_o \ddot{C}_1 = r_i \sin(\omega t + \phi) \tag{15}$$

$$\ddot{C}_o C_2 + C_1 \ddot{C}_1 + C_o \ddot{C}_2 = 0 \tag{16}$$

From these equations, we can obtain the following results by integration of equations (14), (15), (16), etc., starting with the equations of lowest order. Thus,

$$\ddot{C}_o = 0$$

$$C_o \ddot{C}_1 = r_i \sin(\omega t + \phi); \qquad C_1 = -\frac{\sin(\omega t + \phi)}{\omega^2} + m_1 t + m_2$$

$$r_1 \ddot{C}_2 + (m_1 t + m_2) \sin(\omega t + \phi) - \frac{1}{\omega^2} \sin^2(\omega t + \phi) = 0$$

$$C_2 = \frac{\cos 2(\omega t + \phi)}{8\omega^4 r_i} + \frac{2m_1 \cos(\omega t + \phi)}{r_i \omega^3} + \frac{(m_1 t + m_2) \sin(\omega t + \phi)}{\omega^2 r_i} + \frac{t^2}{4\omega^2 r_i} + m_3 t + m_4$$

Because the higher order solutions including C_3, C_4, etc., are multiplied by α^3, α^4, etc., and since α is a very small number, the solution is quite exact with only the first two terms. By applying boundary conditions to evaluate constants of integration and by dropping terms of negligible sizes, one can ultimately obtain the solution

$$r = r_o - \alpha\left[\left(\omega \cos \phi + \frac{u_o}{\alpha}\right)t - \sin(\omega t + \phi) - \sin \phi\right] \qquad (17)$$

which describes the motion of the electron from the inner cylinder outward. The multipactor cycle of oscillation is computed by using the same technique, making due allowance for the reversal of the field direction, for the inward motion. Unlike the parallel plate theory, the two half-cycles are unsymmetrical, and so a second solution of the non-linear equation must be fitted to the first. The boundary values are given by the equations:

$$t_2 = \frac{2\pi}{\omega} - t_1$$

and

$$\phi_2 = \omega t_1 + \phi_1 - \pi$$

and

$$\alpha_o = \frac{r_o}{r_i}\alpha$$

where t_1, t_2 are the electron transit times outward and inward; ϕ_1, ϕ_2 are the emission phases for the two portions of the cycle; and α_o is the constant used for the second part of the cycle.

The ultimate results of the calculation is an equation for resonance, in which

$$V_P = 2\frac{m}{e}\frac{\omega^2 r_i \ell n \frac{r_o}{r_i}\left(r_o - r_i - \frac{\pi u_o}{\omega}\right)}{\left[\frac{r_o}{r_i}(\omega t_1 - 2\pi)\cos(\omega t_1 + \phi_1) - \omega t_1 \cos\phi_1 - \frac{r_o + r_i}{r_o}\sin\phi_1 - \frac{r_o + r_i}{r_o}\sin(\omega t_1 + \phi_1)\right]} \qquad (18)$$

Equation (18) is similar in form to equation (10) and may be studied for maximum and minimum values of V_p or spacing as a function of the phase of the applied voltage.

As a check on the solution, it was also programmed for a digital computer. The computer study of the concentric cylinder case consisted of a numerical integration of the equation of motion, including a term for analysis of d. c. bias.

$$\ddot{r} = \frac{\left(\frac{e}{m}\right) V_{RF} \sin(\omega t + \phi)}{r \ln\left(\frac{r_o}{r_i}\right)} + \frac{\left(\frac{e}{m}\right) V_{dc}}{r \ln\left(\frac{r_o}{r_i}\right)} \qquad (19)$$

where

V_{RF} = RF voltage amplitude
V_{dc} = d. c. voltage amplitude

In each case the computed range of the variables was:

V_{dc} = ±50 volts and zero volts.
ϕ = -75° to +75° including zero.,

Values of V_{RF} were based on the experimental range found for 100 mHz frequency and the following three cylinders.

In all three cases the experimental data and the computed multipactor region data agreed completely. The initial velocity assumed was 1.3×10^6 meters/sec which is the optimum or most probable* secondary electron emission velocity. The impact velocities computed were of high enough energy to cause secondary emission.

The results of the computer study and the experimental data coincide to such an extent that the equation of motion and resultant theory must be valid. The approximate analytical solution was also compared to the computer results, and it is accurate to within 10 percent. The equation (18) above can be used to predict a multipactor region. However,

*See H. Bruning, Physics and Applications of Secondary Electron Emission, Pergamon Press, Ltd. (London, 1954).

the dependence of t_1 on ϕ_1 and V is not really known. This leads to some inaccuracy in the prediction since values for t_1 and ϕ_1 must be assumed. For the computed cases it was seen that a definite relationship exists between the voltage and ϕ_1. The time, t_1, is also related to the voltage and/or ϕ_1. Table V below gives the relations found for the three computed cases. For each voltage there is only one phase angle.

Case	Dimensions (inches)		Applied Voltage Range	Computed (Critical Voltages)
	r_o	r_i		
1	0.817	0.394	15-265	39, 190
2	0.500	0.220	20-100	40, 60
3	0.500	0.142	20-180	20, 120

Table V. Dimensions of coaxial electrodes and computed critical voltages.

Although it was not practicable to perform experimental verification of the theory in all cases, the cylinders of Case 1 were tested in the laboratory. Measured values of critical voltages were found to be 39 and 190, an exact confirmation. The results for Cases 2 and 3 are in good agreement with test results, although the precise dimensions entered into the computer could not be made available for test (see Table VI).

The correlated phase (ϕ_1) data versus applied voltage obtained from computer calculation is shown in Figure 14.

e. Laboratory Investigation of Coaxial Multipactor Effect

The object of this test was to determine the critical voltages which would initiate or extinguish a multipactor discharge between concentric cylindrical surfaces. The measurements were performed only with metallic surfaces, since there appeared to be no reason to suspect that

Case	ϕ_1 (degrees)	V_{RF} (volts)	$t_1 \times 10^8$ sec
1	+18	40	0.46
	-18	64	0.47
	-28.8	90	0.48
	-32.4	115	0.49
	-39.6	140	0.49
	-39.6	165	0.47
	-32.4	190	0.42
2	-64.8	40	0.60
	-47.5	60	0.48
3	-7.2	20	0.476
	-36	40	0.516
	-47.5	60	0.54
	-47.5	80	0.512
	-36	100	0.43
	-10	120	0.308

Table VI. Computed relationship between phase, transit time, and voltage in coaxial multipactor.

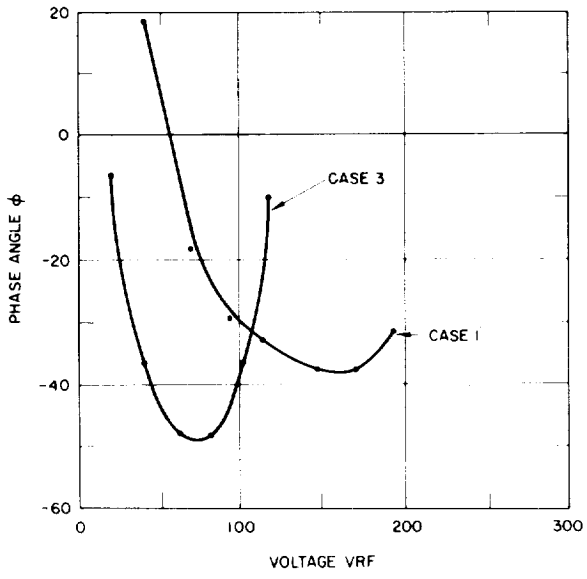

Figure 14. Coaxial multipactor phase-voltage computed dependence.

change of surface material would not result in different effects than those already recorded in parallel plate tests.

The procedure which we followed was to use a fixed diameter outer cylinder, approximately 2" long, and to vary the diameter of an inner cylinder and the applied radio frequency voltage.

Figure 15 is a sketch of the configuration. The coaxial cylinders were part of a resonant line. The trombone line was adjusted for maximum voltage buildup at the end of the line. The transmitter

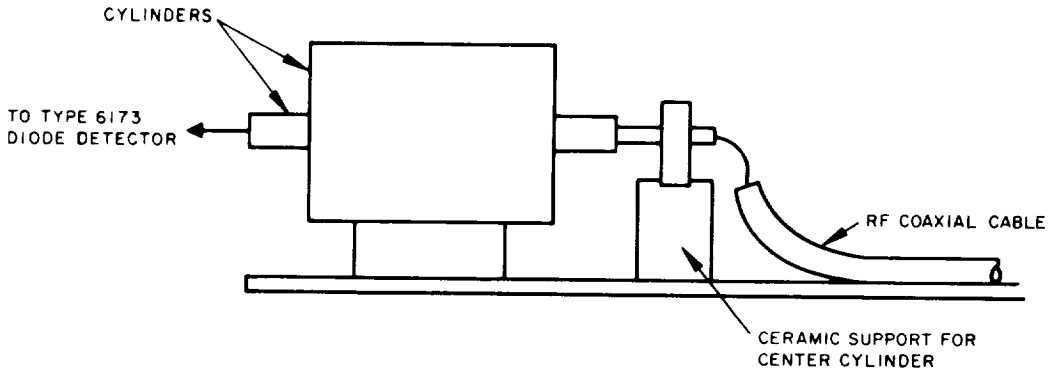

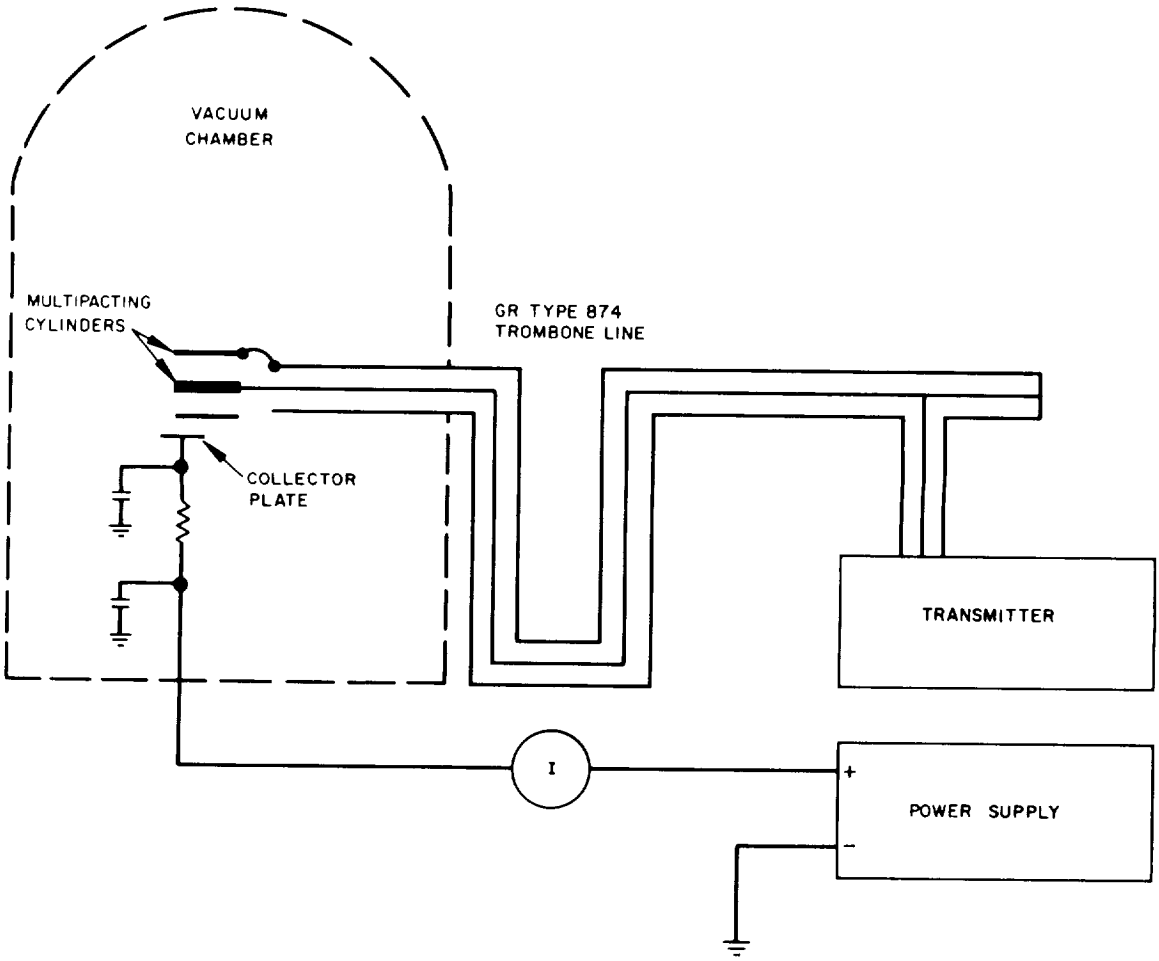

Figure 15. Test apparatus for coaxial multipactor.

output impedance was matched to the line at the proper distance from the shorted end of the resonant line. A 6173 RCA diode was used as the detector to measure RF voltage between the inner and outer cylinders. Multipacting was determined by visual observations of the usual blue glow and by current flow to a collector plate placed approximately 1" from the outer cylinder and parallel to it. Electrons emitted from the surfaces near the open end of the cylinder occur in angular directions which carry them out of the intra-cylindrical volume, and can be attracted to the collector plate by a bias voltage.

The collector plate was the most sensitive detector of the start of multipactor, and could be used under external conditions with greater ease than direct observation or the phosphorescent zinc sulfide tape. A potential of +50 volts was used to provide bias for the collector plate, and current was measured with a microammeter.

Figure 16 contains the data of tests of three cylinders at 100 mHz frequency. The fundamental behavior is seen to be similar to that observed with parallel plates; an enclosed region of the graph contains parameters suitable for multipactor breakdown, and the breakdown can be initiated and then extinguished by steady increase of applied voltage, or, with fixed voltage, by a change in the spacing between cylinders. It is to be expected that the conditions for multipactor in a pair of cylinders for which the spacing is much smaller than the average radius would be quite similar to conditions found in parallel plates. Such dimensions tend to make the electric field constant in magnitude.

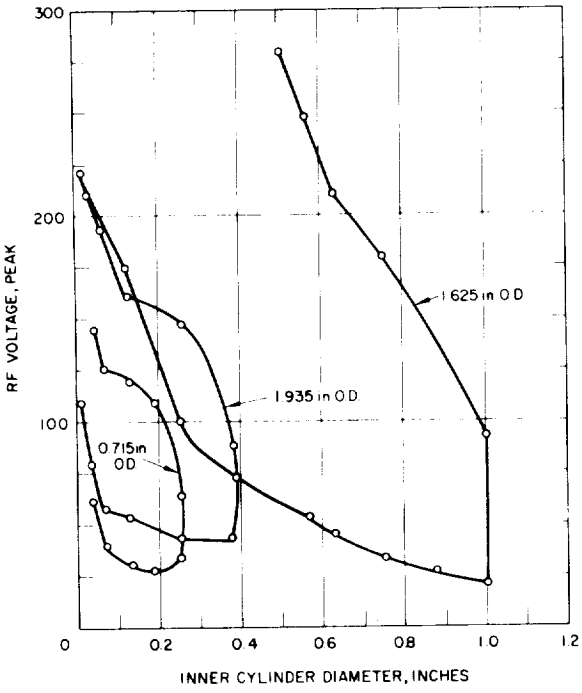

Figure 16. Breakdown voltage versus dimensions coaxial multipactor, F = 100 Mc.

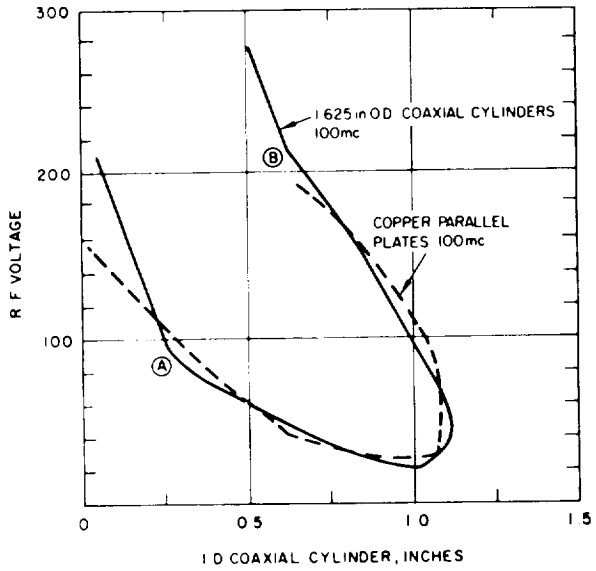

Figure 17. Comparison of flat plate and cylindrical breakdown.

As an exercise the curve of Figure 17 was constructed, using data obtained from parallel plate tests for comparison. The results were as anticipated. The portions of the curve showing close cylindrical spacing do, indeed, fit very well on a parallel plate curve. At points marked A and B, there is a kink in the curve; for these points, the inner diameter is less than half the outer diameter, and non-linear electrical fields mentioned in previous analysis would cause a difference in behavior.

Figure 18 is a record of a breakdown voltage test performed with 430 mHz applied frequency, using three different outer cylinders. All curves have the characteristic "kink".* The data plotted in Figure 19 is intended for reference use, since it demonstrates the critical voltages for multipactor effect inside air insulated 50-ohm transmission lines. The minimum breakdown voltage is found for small cable, approximately 0.3" in diameter; the power level through the line to a matched load under the circumstances is approximately 25 watts. Most flexible coax line now used in spacecraft does not have air insulation. In particular, if a solid dielectric is everywhere present to raise the breakdown voltage there may be little danger. It is clear, however, that the proper design of an RF transmission system to handle a 25-watt power level will require deliberate design practices to avoid breakdown.

*It has been proposed by a member of our staff that the kink is due to the drop in the percentage of electrons which strike the inner conductor. As the radius of the inner conductor is decreased, electrons will tend to miss it, and be accelerated outward by the field reversal.

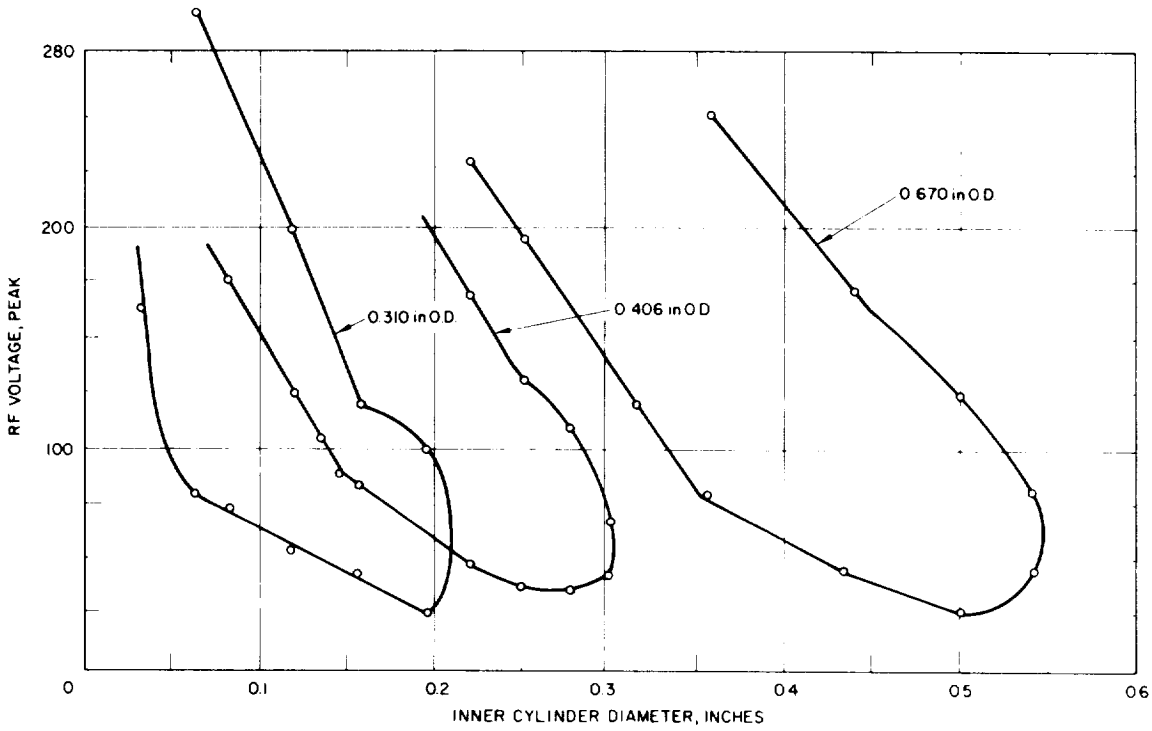

Figure 18. Breakdown voltage for multipactor coaxial cylinders, F = 430 Mc.

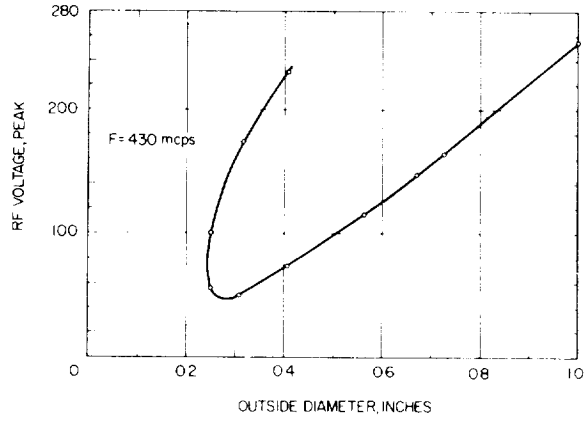

Figure 19. Multipactor breakdown voltage for 50-ohm cable, F = 430 Mc.

ANALYSIS AND EXPERIMENTAL INVESTIGATION OF POWER IN MULTIPACTOR DISCHARGE

An equation for power delivered to an electron by a multipactor discharge is given in the analysis of parallel plate characteristics earlier in this report. This equation is

$$\text{Power input per electron} = \frac{2eu_o V_P}{\pi d} \cos \phi + \frac{2e^2 V_P^2}{\omega m \pi d^2} \cos^2 \phi \qquad (7)$$

A limitation on the use of this equation is due to the idealized assumptions made in its derivation, including absence of spacecharge effects and no treatment of the energy expended in producing wasted electrons, and in electron collisions with heavy ions producing the familiar visible glow. For these reasons, any quantitative estimate based on the equation cited above is likely to be of questionable accuracy. With this in mind, we can attempt to interpret the meaning of the laboratory measurements.

Since the electron resonance condition which is essential to the very existence of a discharge is a sensitive function of the applied voltage, we should not look for a simple relationship between power and voltage to apply in any specific test. Therefore, we have made a test setup to measure the total power input to the discharge to obtain basic data.

The experimental setup for measurements of power is indicated in Figure 20. The input power to the discharge was calculated by subtracting the input power to the plates under atmospheric conditions from the values observed with a discharge. Our first measurements of this type indicated that the gross input power increased steadily with applied voltage after the discharge was initiated; however, the influence of the resonance equation eventually caused further increases in voltage to decrease the power input. As noted in an early status report, no "catastrophic" multipactor events have been observed in any tests. The maximum power loss observed has been only 135 milliwatts per square inch of electrode area, with more typical values being 60 mw/in^2 or less.

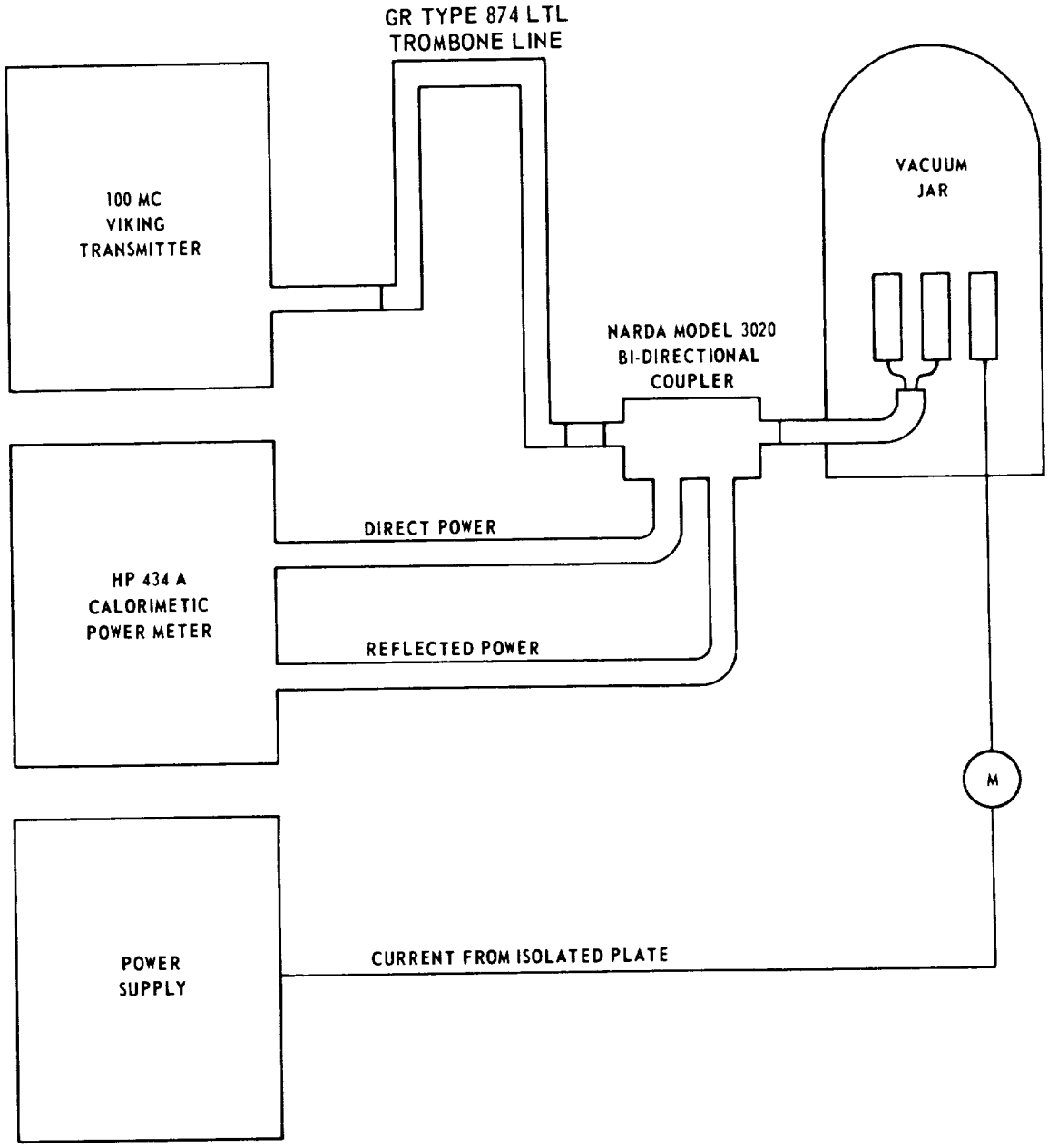

Figure 20. Schematic of power and impedance measurement setup.

Furthermore, these measurements were taken under conditions which are not likely to be encountered in actual equipment – plane parallel electrodes and spacing optimized for the frequency and voltage (180 volts, 5/8" plate spacing, 100-Mc frequency). At higher frequencies and voltages the power will be higher, but it seems unlikely that any of

the so-called "catastrophic" failures (400-Mc OAO filter at Hughes, 960-Mc coaxial structure at JPL and RCA) in which severe burning or pitting were observed could have been the result of multipactor alone. A more reasonable explanation is that they were the result of an arc initiated by a gas discharge which resulted from high gas pressure due to local outgassing caused by multipactor induced heating. It is significant that such effects have been observed only in tightly confined volumes.

The curve of Figure 21 indicates the type of data which has been obtained. For a well established discharge, i.e., at a voltage toward the peak of the curve of Figure 21, the multipactor glow is reasonably well contained in the volume between the electrodes and the power input is near the maximum achievable. The data collected in several hundred typical observations has been summarized in Figures 22 and 23. The conclusions which can be drawn from careful study of the data are as follows.

1. The multipactor power per unit area is not critically dependent on material.
2. In general, multipactor power is not directly related to the parameter, f x d, which controls the existence of the discharge.
3. Within limits between initiation and extinction, the multipactor power input may be increased by increasing applied voltage.
4. We have not observed power density greater than 22 milliwatts per square centimeter. Although this magnitude is not sufficient to cause direct physical damage in a well designed equipment, it does appear to be capable of liberating gases.
5. The equivalent ohmic resistance per square centimeter, treated as a lossy element in parallel with the electrodes, has had observed values in the range from 80,000 ohms up to very high values.
6. Our data does not prove any conclusive dependence of power on total area of plates or separation of plates.

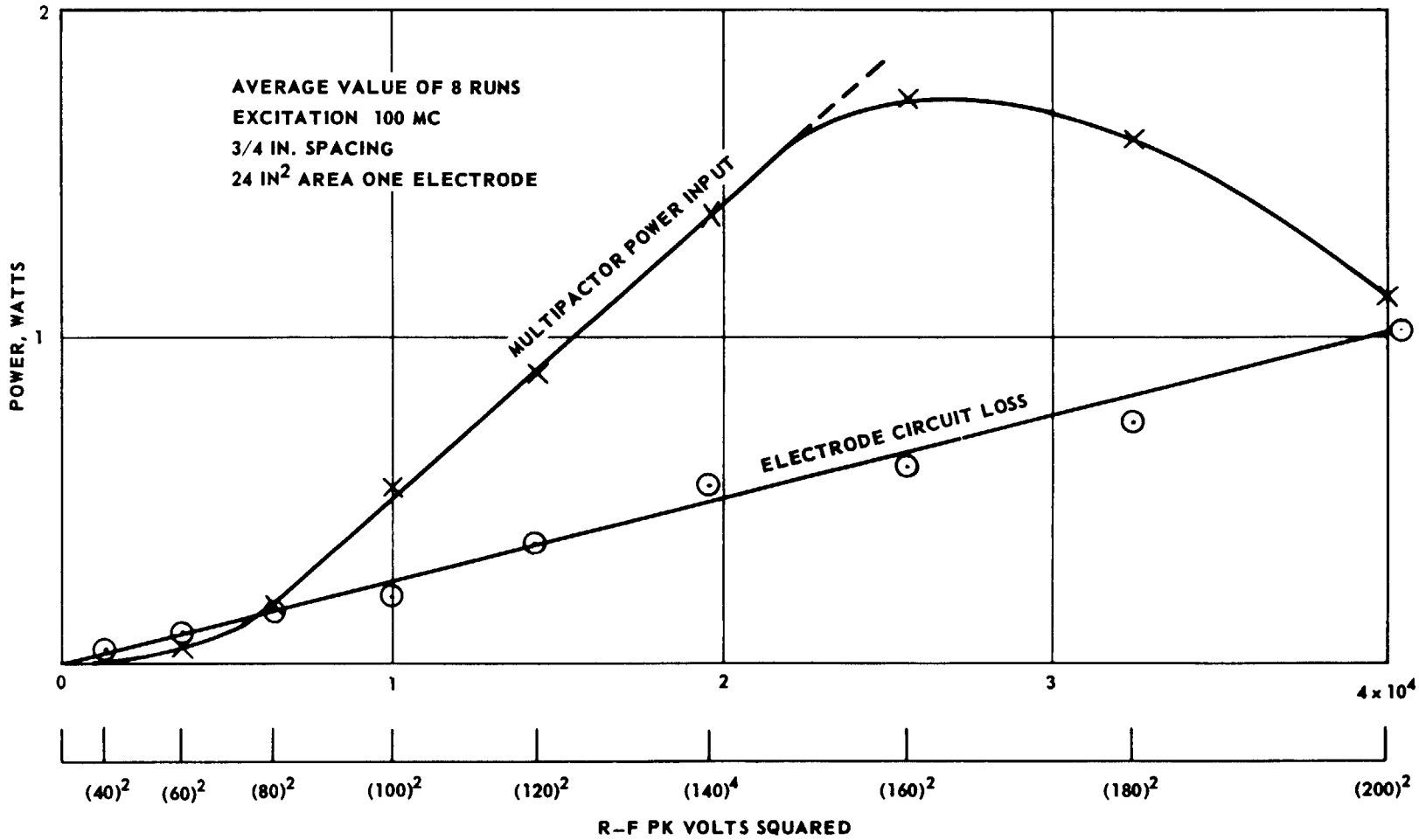

21. Power versus volts squared.

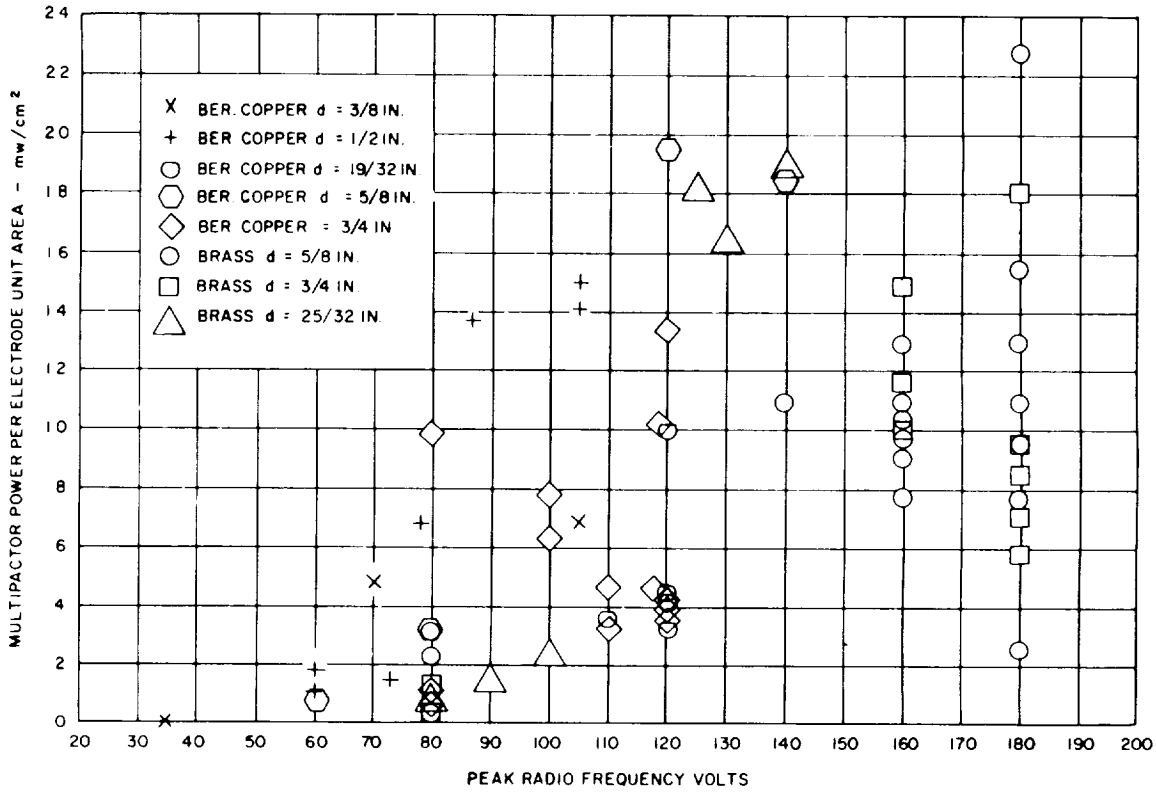

Figure 22. Multipactor power versus peak volts.

Using the equation for power per electron and the known power per square centimeter, one can calculate a nominal estimate of the total number of effective electrons. Such calculations indicate numbers like 1 to 2 x 10^6 electrons per square centimeter, or more than 10^8 in the entire discharge. Since much of the power is not effective in the discharge but is dissipated in collisions and light emission, and since large numbers of electrons escape the electrodes, no engineering reliance can be placed in the figures.

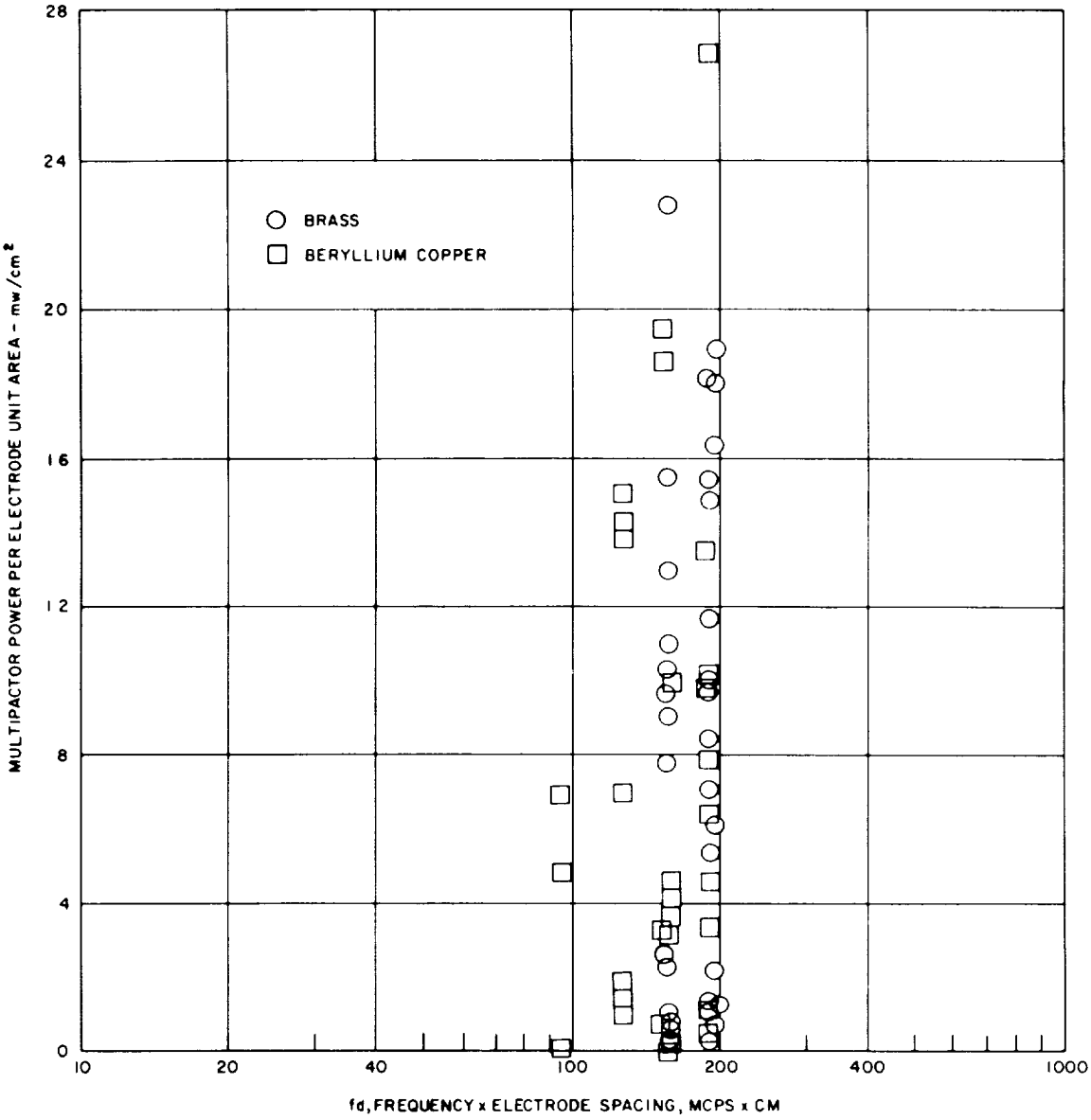

Figure 23. Multipactor power versus parameter f x d.

SCREEN ELECTRODE EXPERIMENT

In many of the experiments described in this report, the multipactor current is sampled by collections of electrons which fly through openings drilled in one of the electrodes. In at least one of the tests performed to study single surface multipactor modes, we have also used a perforated electrode. The screen electrode experiment, described

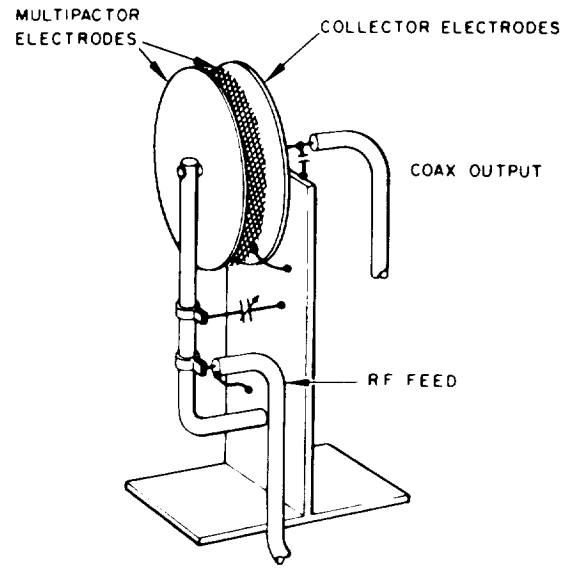

(a) EXPERIMENTS

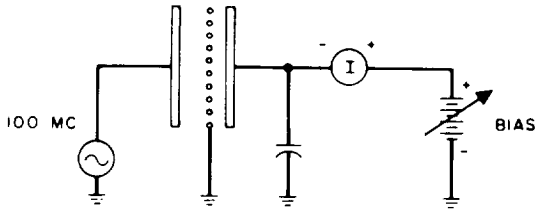

(b) CIRCUIT

Figure 24. Screen electrode.

below, was performed to study the behavior of a multipactor discharge on such a screen. A large collector plate was employed, as illustrated in Figure 24. The electrodes were all 5" in diameter with a spacing of 3/4" between the multipacting electrodes and a spacing of 1/2" between the screen and collector electrode. It is estimated that the screen grid intercepted 20 percent of the electrons.

The experiment was run with a pressure of 3×10^{-5} mm of Hg. The characteristic blue glow was observed between the multipacting electrodes. The parameters measured were peak RF volts between discharge electrodes, input RF power, and collector electrode bias and d. c. current. The minimum value of multipacting breakdown voltage was found to increase as the bias voltage was made more positive. The bias could be set to a value such that the multipacting would intermittently start and stop for a particular peak RF input voltage, as illustrated in Figure 25. The multipactor input power was also controlled by the bias voltage; a maximum was found at +25 volts. This characteristic is shown in in Figure 26 with a plot of multipactor power input versus peak RF volts

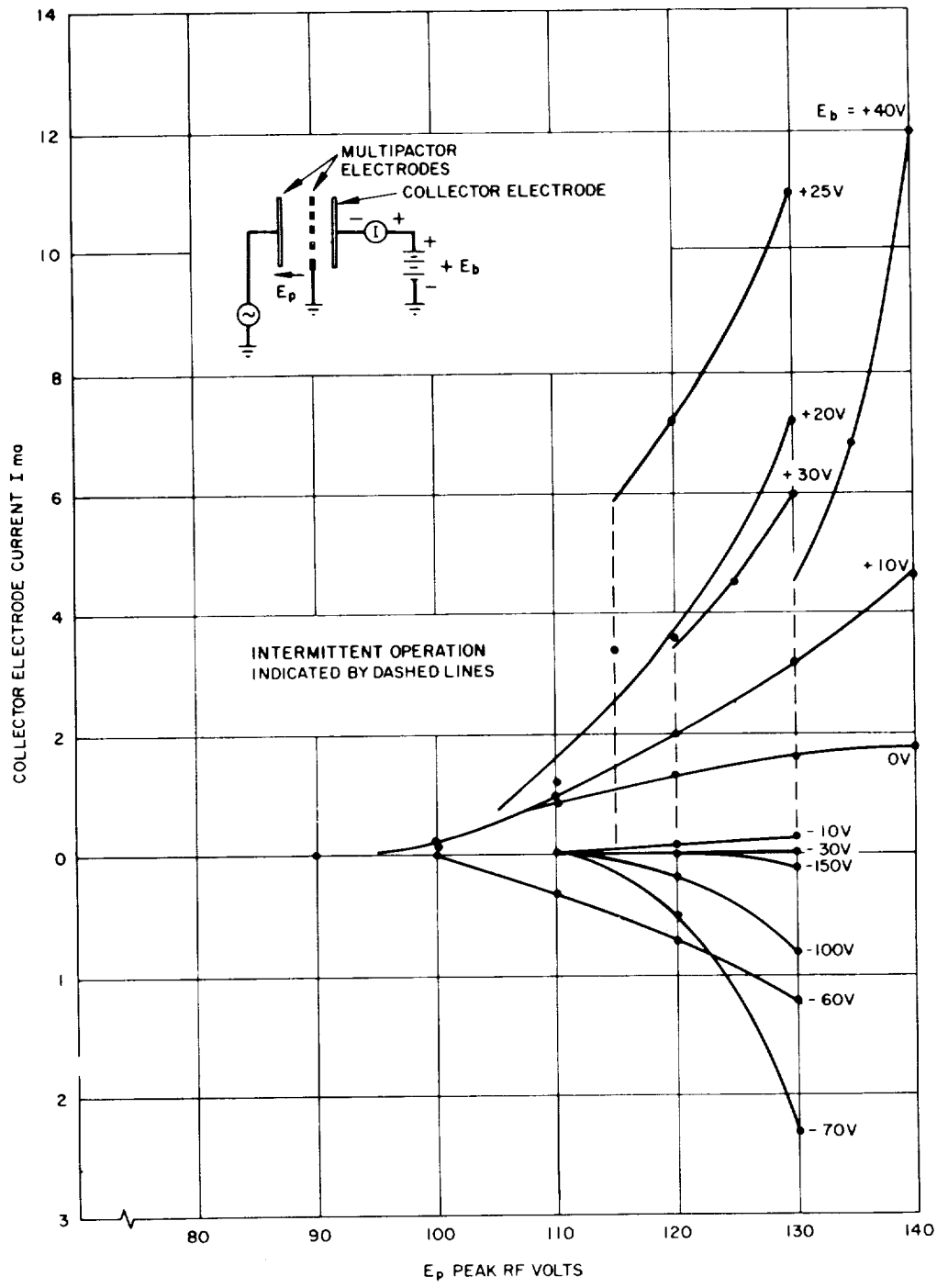

Figure 25. Collector current versus peak RF volts.

square for various bias levels. Multipactor power was determined by measuring the input power during the experiment and then later measuring the input power in atmospheric pressure for each peak RF voltage. The difference then is the multipactor power.

Data was also taken at a fixed value of peak RF voltage and readings were taken as the collector electrode bias voltage was varied. The curves shown in Figures 27 and 28 were prepared from this data. Figure 28 shows that a small amount of power can be extracted from the multipactor discharge when the bias lies between -30 volts and 0 volts. This is probably due to the collection of fast moving electrons with energy sufficient to overcome the retarding field of the collector.

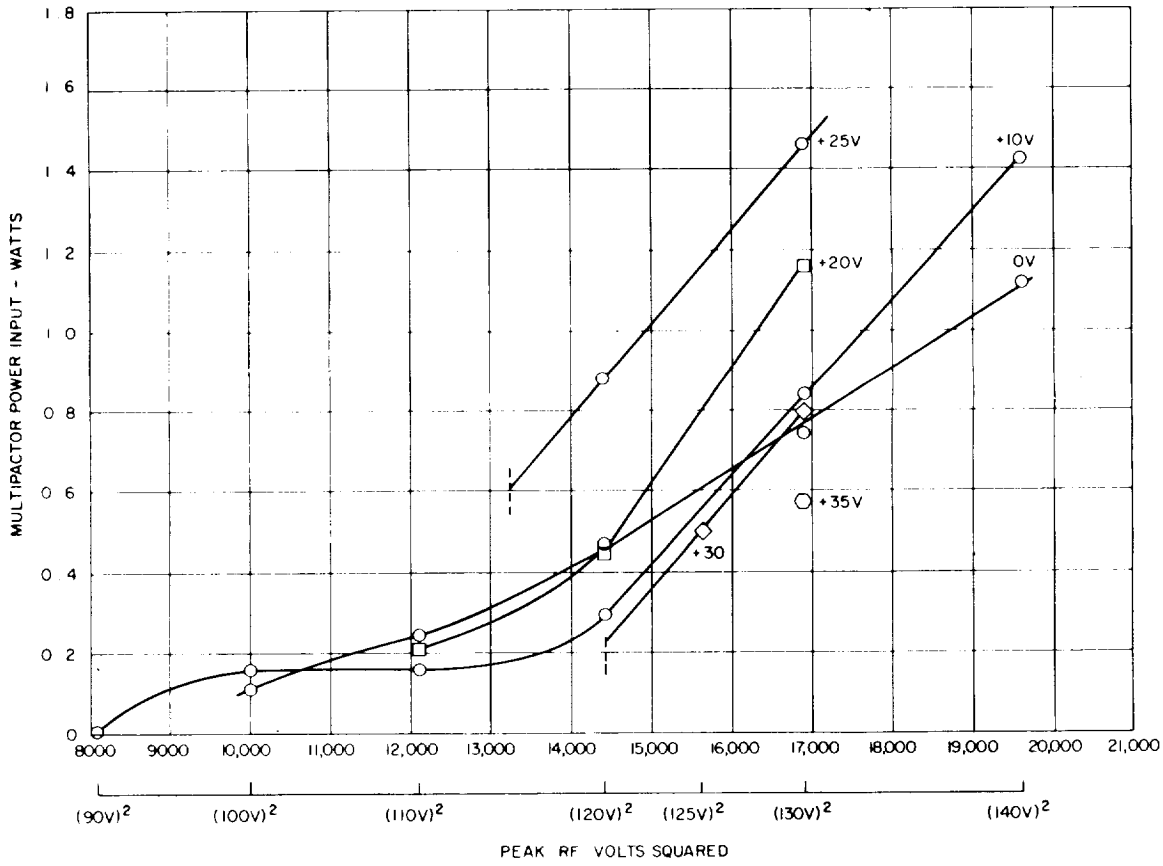

Figure 26. Multipactor power versus peak RF volts squared.

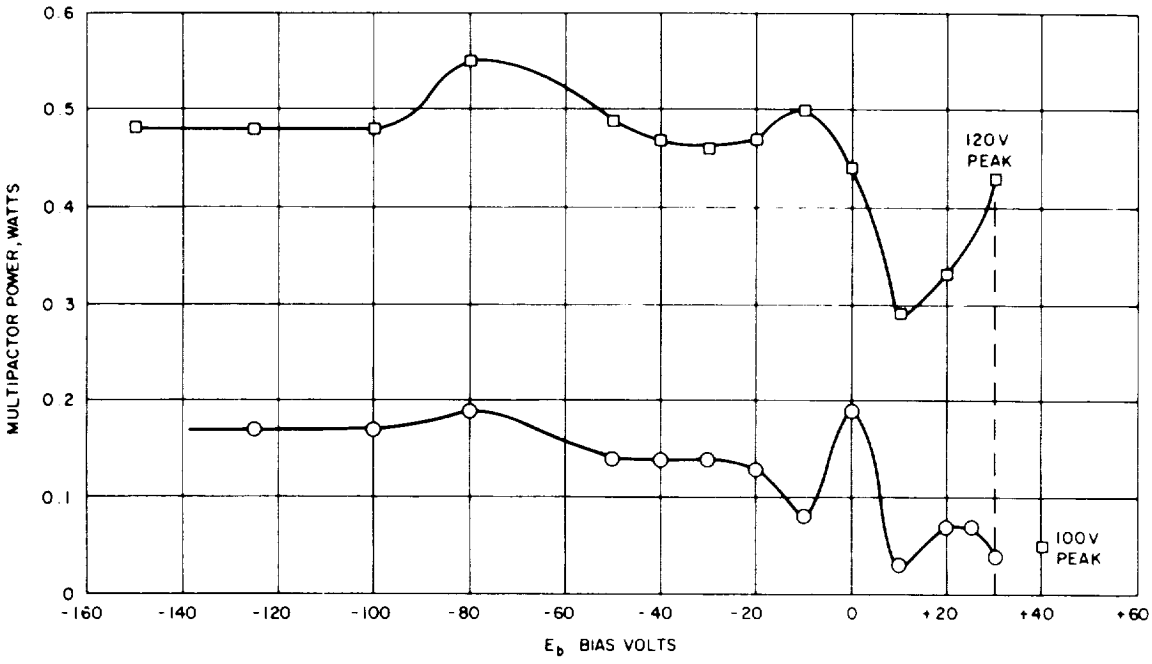

Figure 27. Multipactor power versus collector bias volts.

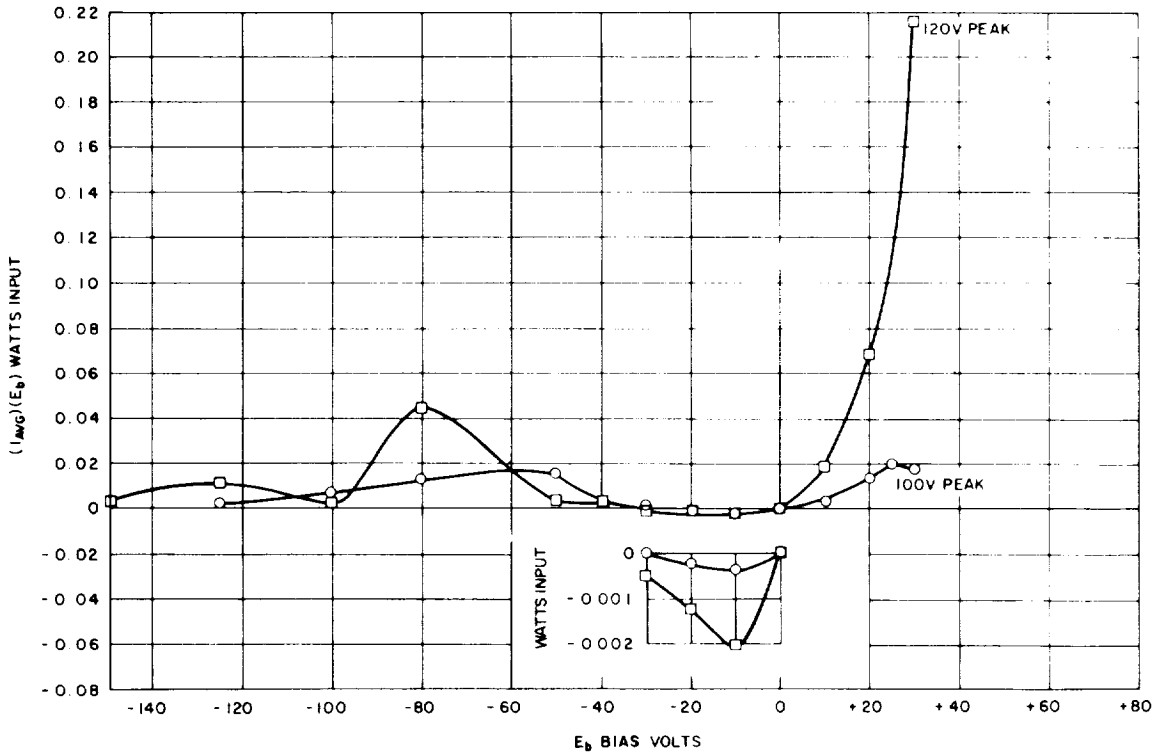

Figure 28. Collector power versus bias volts.

HARMONIC EFFECTS IN MULTIPACTOR DISCHARGE

Due to the non-uniform distribution of charge in the electron sheath, it has been anticipated that harmonic currents would be present. If so, a multipactor discharge on a spacecraft antenna, for example, might regenerate the harmonics which are usually filtered out by RFI suppression devices. For this reason, a laboratory investigation of the harmonic current was initiated.

The radio frequency setup was the same as that used for breakdown voltage tests. In addition, an isolated collector electrode was enclosed in a 4" square shielded box which also served as the grounded discharge electrode. The top (discharge) side of the box was pierced with 144 1/16" diameter holes to allow the passage of electrons; the holes had a combined area of only 2.5 percent of the total electrode area and hence did not disturb the discharge. As shown in Figure 29, bias voltage was applied to the collector through an isolating resistor, and it was capacity coupled to a 50-ohm attenuator which helped to isolate the circuit from the external connections. The attenuator output fed a coaxial cable which was connected to either a Hewlett-Packard 185 sampling oscilloscope or to harmonic measuring equipment. The equipment was operated and photographs of the collector waveform were used for Fourier analysis.

The 100-Mc, 30-watt, crystal-controlled transmitter was used to excite a multipactor discharge in an ambient pressure of about 10^{-5} mm Hg. One channel of the Hewlett-Packard 185A sampling oscilloscope was used to measure the waveform of the electron current collected by the isolated collector plate. The other channel was used to observe the signal from a small pickup plate placed between the electrodes to measure the phase of the applied field in relation to the collector current waveform. The surface of the grounded electrode was perforated so that the collected electron current was about 1/36 of the total electron current in the discharge.

A typical collector current waveform is shown in Figure 30. By graphical Fourier analysis, the following expression was found for the collector voltage:

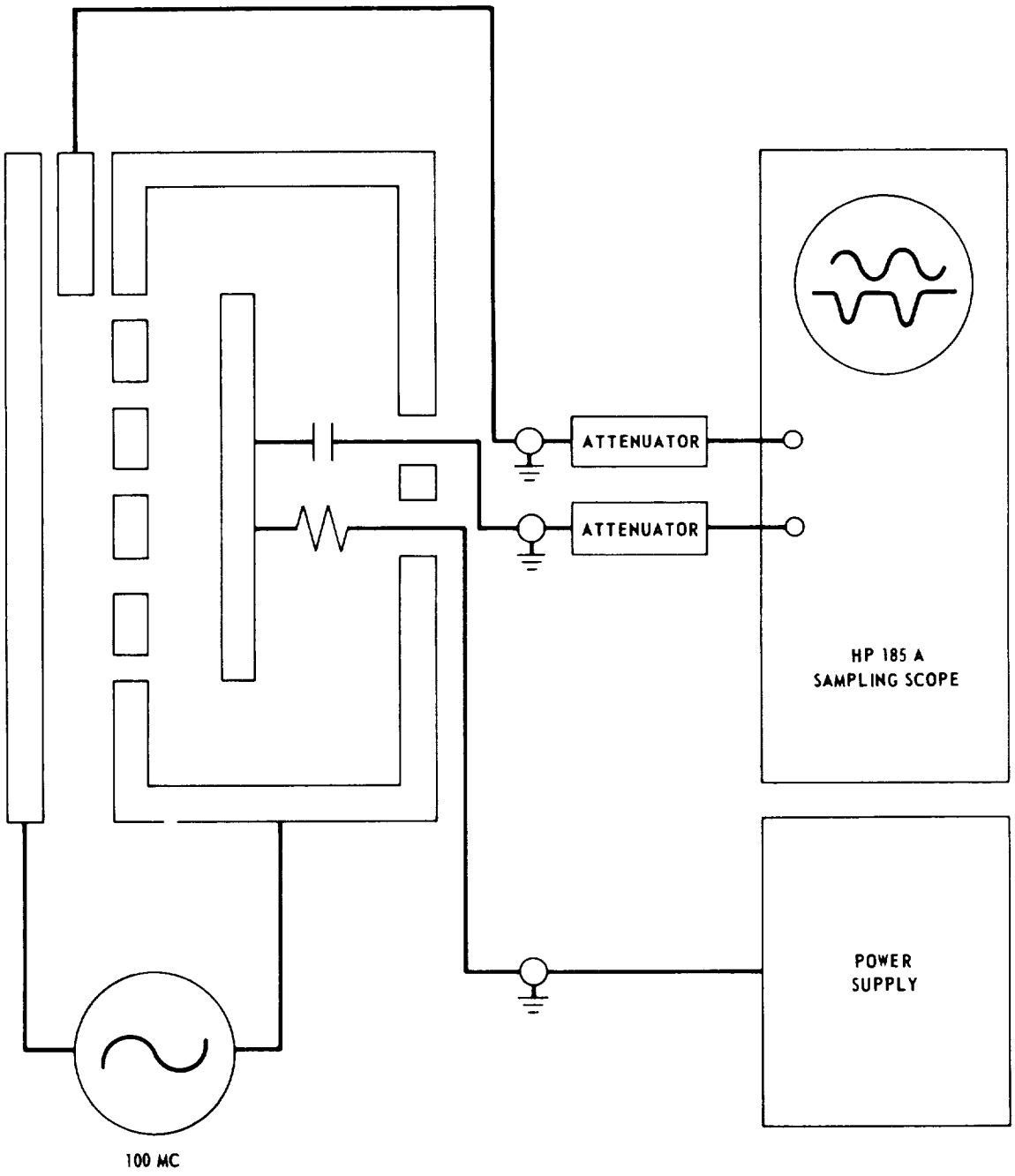

Figure 29. Schematic of harmonic measurement experiment.

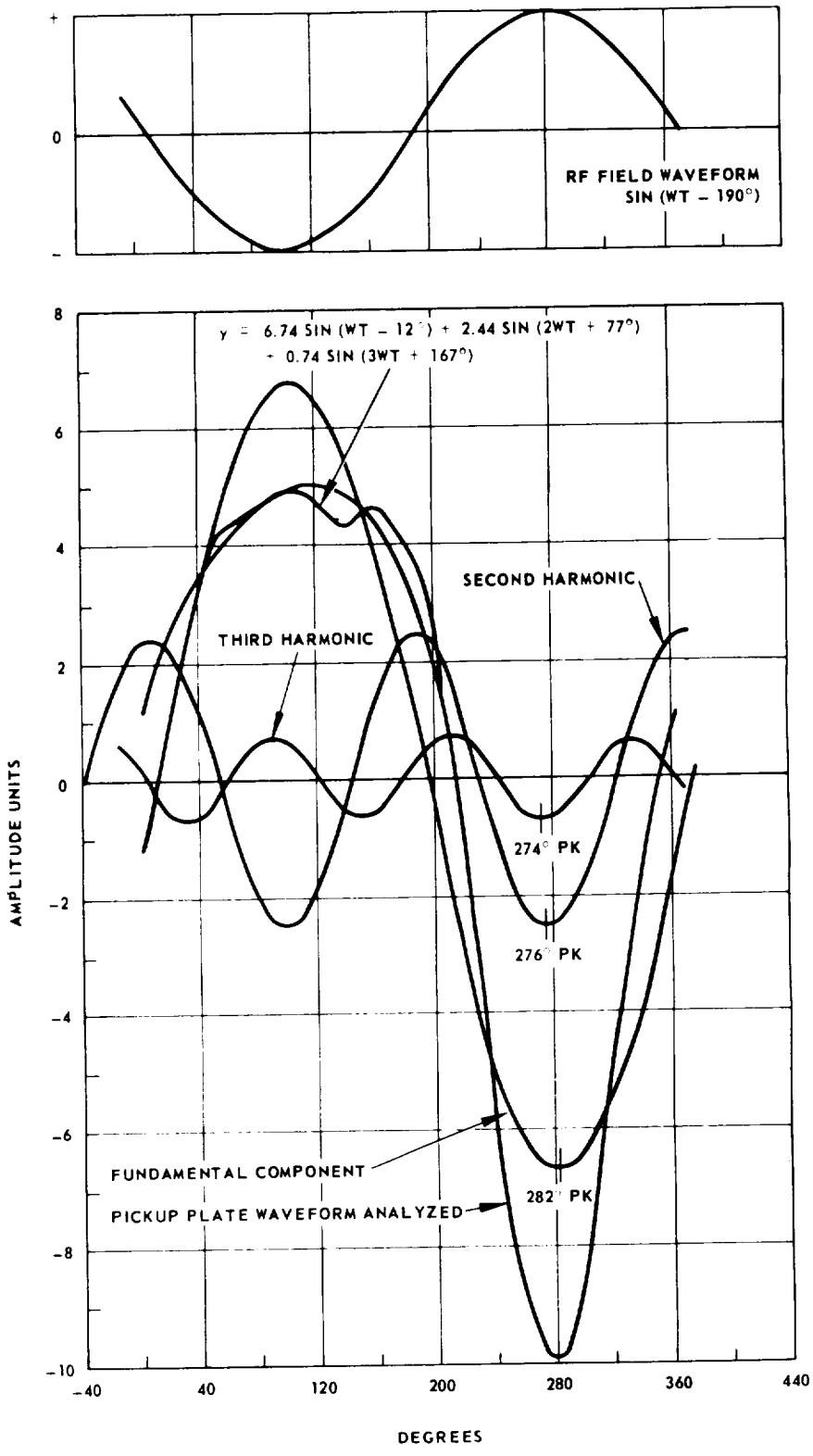

Figure 30. Fourier analysis of typical waveform.

$$E_{collector} = 666 \sin (wt - 12°) + 240 \sin (2\ wt + 77°) + 73 \sin (3\ wt + 167°) \text{ millivolts}$$

Higher order harmonic terms could not be determined with any certainty.

The analysis shows the negative peaks of the harmonics to be very closely aligned, as would be expected for the arrival of a thin sheet of electrons once each cycle of the applied RF field. Table VII gives the extrapolated total discharge current for the first three harmonics.

At the time these measurements were taken the voltage between the discharge plates was about 105 volts rms, and the power dissipation was about 3 watts. Since the total fundamental electron current was 0.34 ampere, the electron current must have been at a phase of about 85° with respect to the electrode voltage, and should have caused severe detuning of the RF structure, but this was not observed.

While measurement of the electron current simplified the tests by providing isolation from the fundamental RF field, in an actual operating circuit the net electrode current (difference between primary and secondary electron current) is of more interest. Therefore, the tests were extended to measurement and analysis of the current flowing in the low voltage (near ground) discharge electrode. A 3.3-ohm resistor was placed in series with this electrode. The current waveform signal

Harmonic	E Peak Volts at Collector	Collector Electrode (I) RMS MA $\frac{E}{50\sqrt{2}}$	Total Discharge Electrode Current RMS MA I(36.2)
Fundamental	0.666	9.43	341
Second	0.240	3.40	123
Third	0.073	1.03	37
Total	--	10.1	364

Table VII. Harmonic currents due to multipactor.

from this circuit as well as the voltage from a capacitively coupled pickup plate located near the high potential discharge electrode were each connected through attenuators to two channels of an HP-185A sampling oscilloscope (see Figure 31a). Measurements were first taken without the 100-Mc rejection filter but it was found that the fundamental current due to capacitance between the electrodes obscured multipactor effects.

The rejection filter was inserted to eliminate the 100-Mc components and current waveforms were obtained which showed prominent third harmonic components when multipactor was present. To obtain information on the fundamental component due to multipactoring, a parallel resonant tuned circuit was added to cancel the capacitive reactance at 100 Mc, as shown in Figure 31b. With the tuning capacitance adjusted for minimum fundamental amplitude the multipactor current waveform was about 10 times greater than the remaining stray signal amplitude, and contained second and third harmonic components. By means of a Fourier analysis the amplitudes of the components were determined. The results of these tests are summarized in Table VIII. For each measurement the electrodes were 5" diameter beryllium copper discs spaced 3/4" apart.

Electrode (volts)	Multipactor (watts)	Electrode Current		Notes
		Ipk amp	f MC	
100	0.50	1.1	100	Figure 31a. (without rejection filter)
110	0.90	1.2	100	
100	0.76	0.039	300	Figure 31a.
120	0.49	0.27	100	Figure 31b. (capacitance tuned out and Fourier analysis used)
120	0.49	0.030	200	
120	0.49	0.027	300	

Table VIII. Summary of electrode current harmonic measurements.

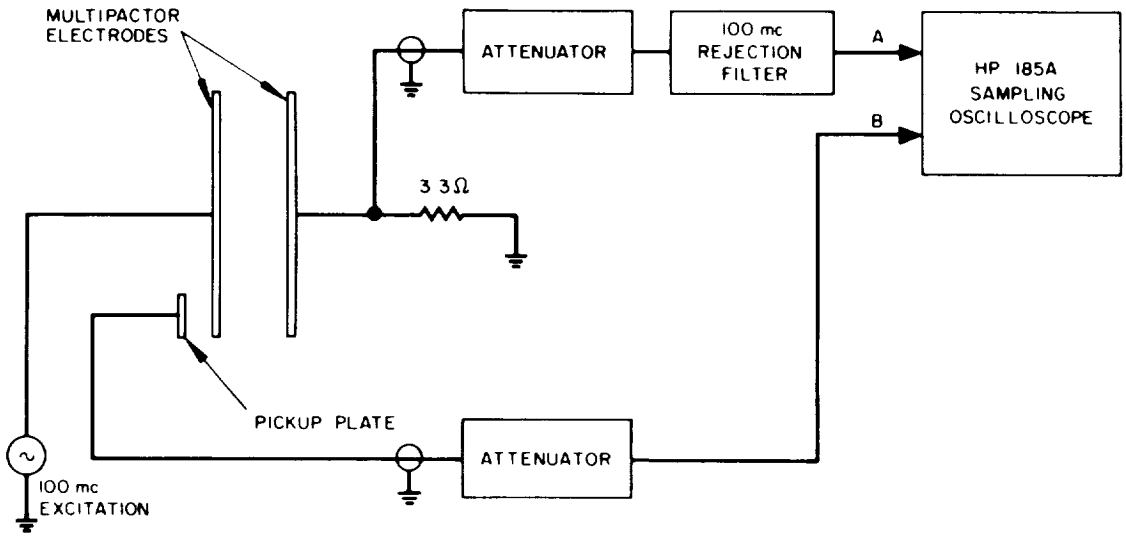

(a) Using filter

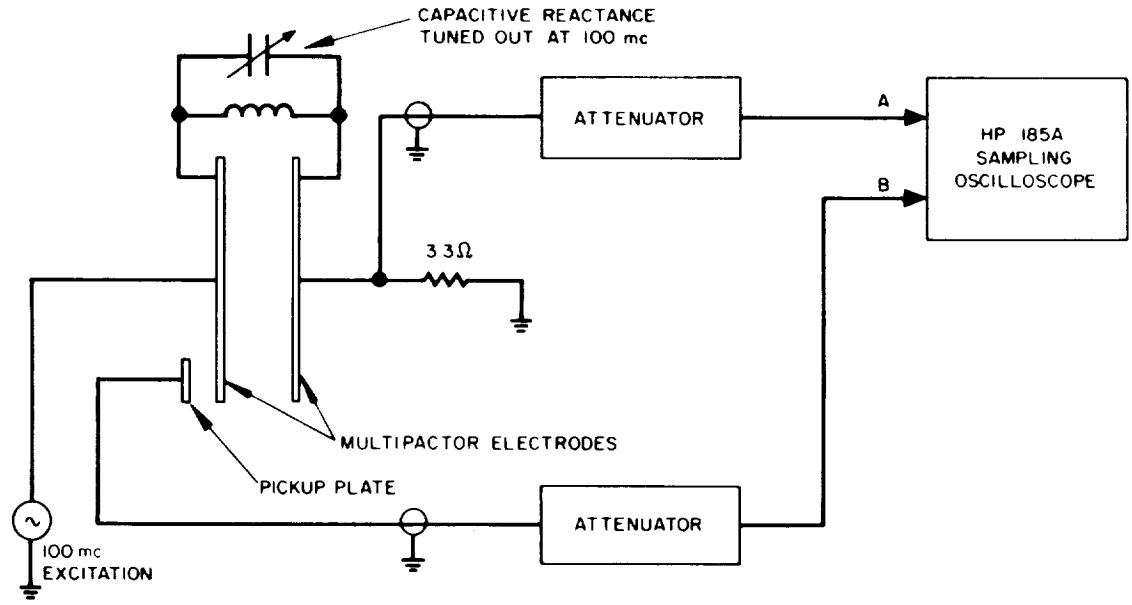

(b) With reactance tuning

Figure 31. Electrode current measurement.

One of the interesting results of the harmonic measurements is an evaluation of the second and third order non-linearity of the discharge current. It is possible to calculate the amplitude of cross-modulation products in a discharge from the observed magnitudes of these harmonic terms.

The following procedure can be used to evaluate the non-linearities of the discharge current/electrode voltage relation. If we assume the discharge (electron) current is related to the electrode voltage by a power series such as

$$I_d = K\left[a_1 V_e + a_2 V_e^2 + a_3 V_e^3 + \cdots\right]$$

and the electrode voltage is a sine wave of amplitude A volts and frequency ω_1, the harmonic content of I_d is, in terms of the power series coefficients,

$$I_d = KA\left[\left(a_1 + \frac{3}{4}a_3 A^2\right)\cos\omega_1 t + \frac{1}{2}A_2 \cos 2\omega_1 t + \frac{1}{4}a_3 A^2 \cos 3\omega_1 t + \cdots\right]$$

with any d. c. term neglected. From a Fourier analysis of the discharge current waveform the harmonic amplitudes can be determined, and the coefficients a_1, a_2, a_3, can be computed. If the main signal components of interest are the harmonics themselves the evaluation is complete at that point.

Since most transmitter-receiver systems would be designed to avoid receiving frequencies on or near harmonics of the transmitted frequencies, the direct harmonic terms probably would not cause significant interference. However, both cross-modulation (transfer of signal modulation from a large to a small signal) and intermodulation (generation of spurious signals) will also occur in a non-linear element, and either could cause trouble. Let us consider the case of a diplexer in which both transmitter and receiver might be coupled to a circuit in which a multipactor discharge would be initiated by the transmitter signal. Let the transmitter voltage at the discharge be A volts at

frequency f_1, and the small signal be B volts at frequency f_2. The resultant multipactor current will contain components of frequencies of f_1 and f_2 and all their harmonics, plus the sum and difference of all these frequencies. Interference to the receiver will probably be caused by difference frequencies near to the original signal frequencies. If f_1 and f_2 are nearly the same the most significant intermodulation component will be at a frequency of $2f_1 - f_2$. For example, if the spacecraft transmitter signal causing multipactor (f_1) is at 136 Mc a small signal at 149.1 Mc would produce a signal at 122.9 Mc.

Table IX shows the relative magnitudes of the three largest components of discharge current, computed from the measured harmonic coefficients. The magnitudes of the signal at frequencies f_1 and f_2 are given with respect to the value they would have if the discharge current had no non-linearities. The magnitude of the small signal current at f_2 is almost double the value it would have if the signal at f_1 were not present, indicating that there would be a strong transfer of amplitude modulation from signal A to signal B, or that signal A tends to suppress signal B. Note that in this example, the currents represent conversion of signal energy into multipactor electron energy, and an increase in the electron current increases the circuit loss. In order to calculate the actual percentage change in power

Frequency	Amplitude Equation	Relative Amplitude (Coefficients Substituted)
f_1	$A\left(1 + \frac{3}{4}\ a_3A^2\right)$	1.49 A
f_2	$B\left(1 + \frac{3}{2}\ a_3A^2\right)$	1.98 B
$2f_1 - f_2$	$B\left(\frac{3}{4}\ a_3A^2\right)$	0.49 B
$2f_2 - f_1$	$A\left(\frac{3}{4}\ a_3\frac{B^2}{A^2}\right)$	$0.49\left(\frac{B}{A}\right)^2$

Table IX. Important intermodulation components.

loss it would be necessary to know the exact coupling of signal power to the discharge electrodes. In addition to the signals at f_1 and f_2 there is a signal at $2f_1 - f_2$ which is comparable in magnitude to signal B and proportional to it.

SINGLE SURFACE MULTIPACTING

It has been shown in the literature, and also in the appendix to this report, that a combination of d.c. bias plus radio frequency voltages applied to parallel plates may, under appropriate conditions, produce a multipactor discharge. The conditions which make this possible include the following:

1. The magnitude of the RF voltage must exceed the d.c. bias by an amount sufficient to accelerate the electron away from the emitting surface.
2. The arrival energy of the electron must be sufficient to produce emission ratios greater than one.
3. The electron must not strike the second electrode.

As shown in the appendix to this report, the region of possible multipactor may be denoted as shown in Figure 32. The crosshatched area of this figure contains pairs of d.c. and a.c. voltages which are suitable.

The curved line A-B is a boundary which denotes RF voltage amplitudes for which the electron would strike the opposing electrode. The line B-C is determined by the minimum RF voltage which is required to carry the electron away from the plate for the duration of one RF cycle. The line A-C is a result of the minimum d.c. bias condition which is required to provide the necessary arrival energy for emission of a sufficiently rapid secondary electron.

It has been reported by Stanford Research Institute* that the lower RF threshold for one-side multipacting mode is generally lower than the lower threshold for the two-sided modes for a given bias. The one-sided mode has the effect of lowering the threshold of RF breakdown.

*One-Side Multipactor Discharge Modes, Technical Report 75, Stanford Research Institute, Menlo Park, California.

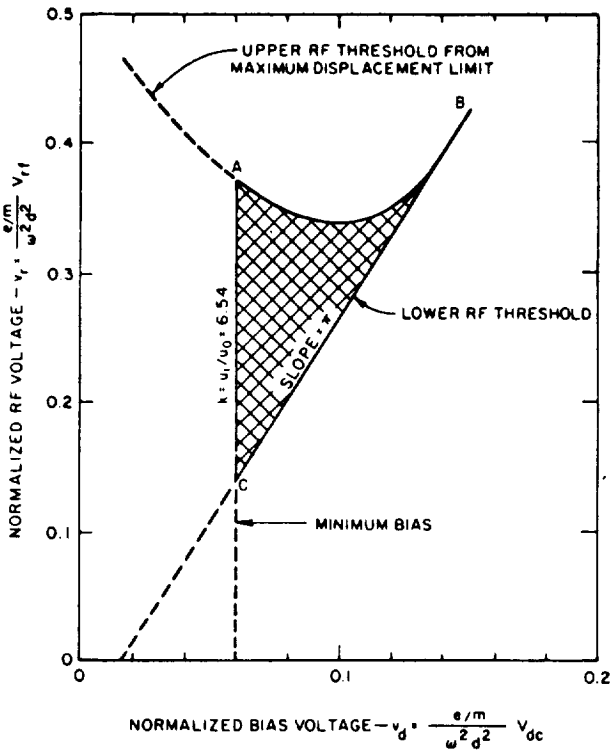

Figure 32. Voltage relationship for single surface multipactor.

An experiment was set up to compare the two surface multipactor mode with the single surface multipactor mode. The apparatus for the two surface mode has been previously described. The apparatus was modified for the single surface mode, by removing one of the beryllium copper electrodes and substituting for it a 1/4" mesh wire screen (see Figure 33). The wire screen was used to discourage multipacting. In addition, the screen was heavily coated with soot to reduce secondary emission. A d. c. potential was applied to the screen as well as the normal RF voltage.

To insure that two surface multipacting was absent, the RF voltage was slowly varied over the operating range with zero bias on the electrodes and the collector current observed to see there was no current flow. A fixed negative voltage was then applied to the screen. The RF voltage was varied over the operating range and the minimum and maximum multipacting voltage recorded. Figures 34 and 35 show single surface multipacting for spacings of 0.56", 0.625", and 1.325".

Spacing less than 0.56" would not multipactor reliably. It will be noted this spacing is just double that for two surface multipacting. The minimum voltage for this spacing is slightly higher than for the two surface mode. The two surface mode would multipactor with a voltage as low as 24 volts across the electrodes with a spacing of 0.282".

With a spacing of 0.625", minimum multipacting voltage was approximately the same as for the two surface mode.

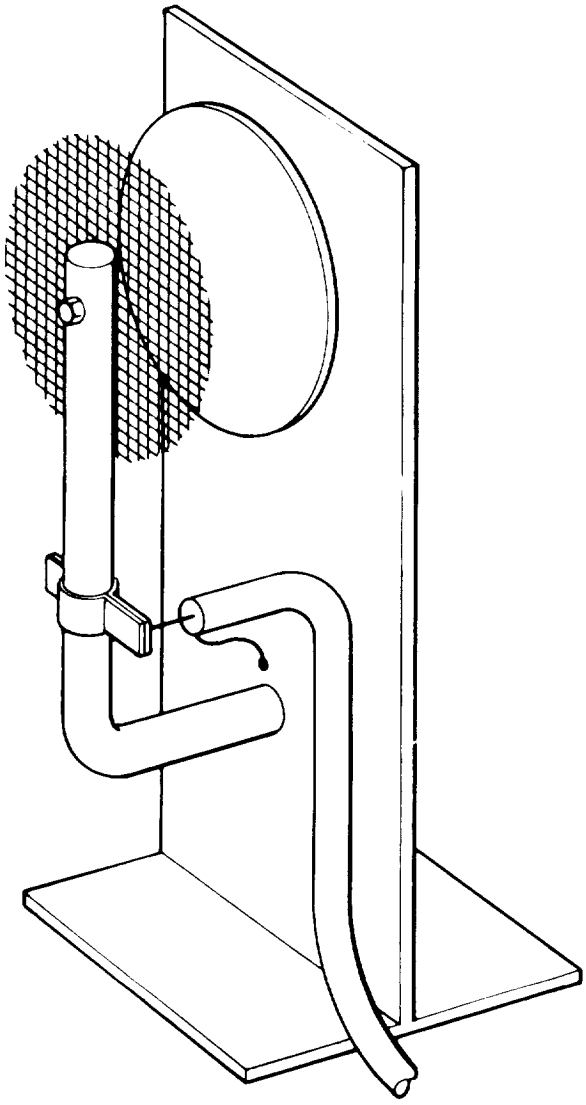

Figure 33. Single surface multipactor experiment details.

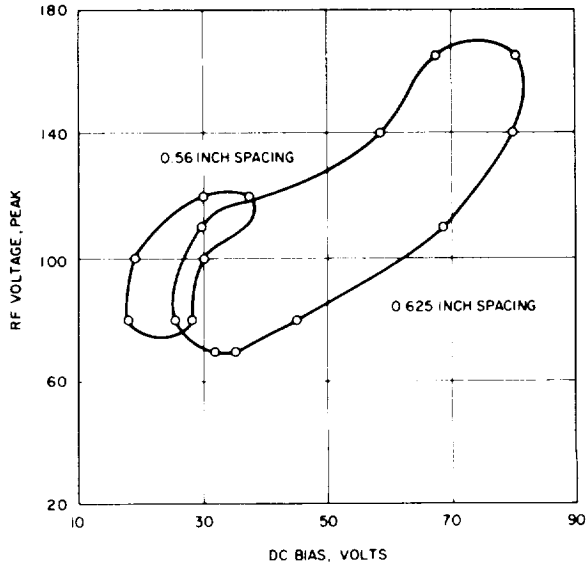

Figure 34. Single surface multipacting, 100 Mc.

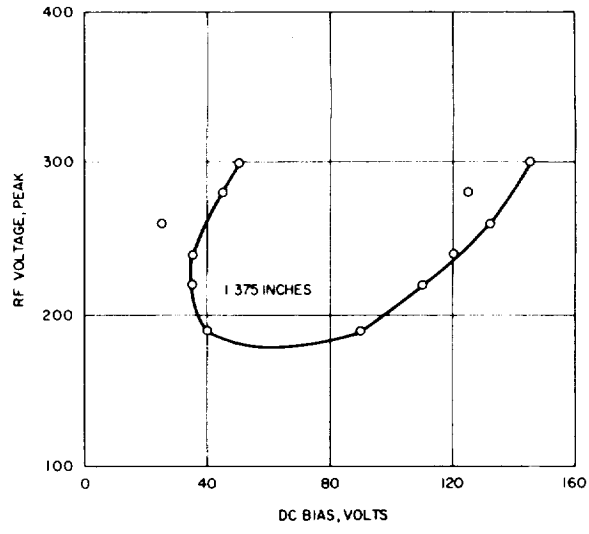

Figure 35. Single surface multipacting, 1.375" spacing, 100 Mc.

NOISE AND OTHER PARAMETERS IN A MULTIPACTOR DISCHARGE

This experiment was designed to measure noise generated in the discharge, and is shown schematically in Figure 36. The output signal was obtained from a small plate which was capacity coupled to the discharge electrodes. The output signal from this plate was passed through a rejection filter which provided over 90 db of rejection at the generator frequency of 100 Mc, but had less than 10 db of loss below 90 Mc and above 110 Mc. Initial measurements were made of the noise generated at 112 Mc, since this has the same spacing as a 136-Mc telemetering transmitter and a 148-Mc command receiver, thus representing a typical spacecraft system. A 100-Mc discharge was generated between a pair of 5-1/2" diameter electrodes spaced 3/4". The output signal was obtained from a brass pickup plate 3/4" x 1-3/4" located between the plates and 1/4" from the ground potential discharge electrode. The output was

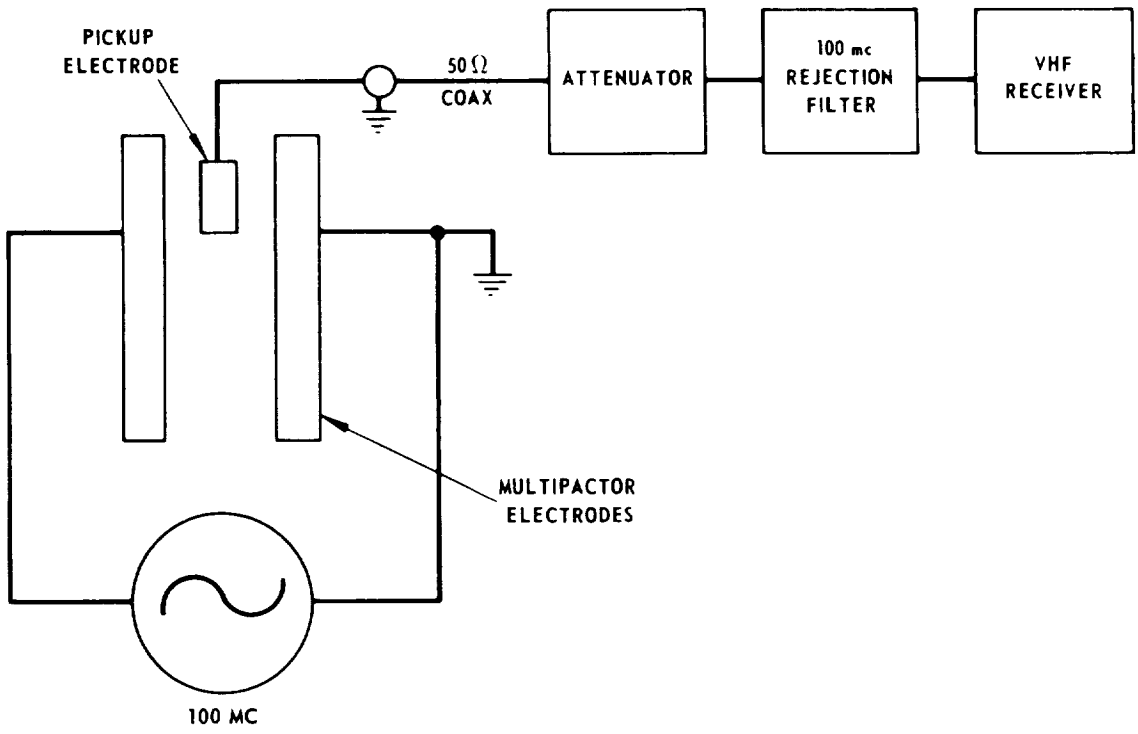

Figure 36. Schematic of noise generation experiment.

connected through a 50-ohm coax line to a 10-db attenuator, the 100-Mc band rejection filter, a resistive T mixer, and to a Nems-Clarke type 1306 receiver. After initial trials the receiver was set to the 300-kc IF bandwidth, 100-kc video bandwidth, automatic gain control, and amplitude modulation detector positions for all measurements. The high level video output of the receiver was connected to a Ballantine 643 a. c. voltmeter. A VHF signal generator was connected to the resistive T network so that receiver sensitivity could be measured with the transmitter turned on and off. There was no difference in sensitivity, showing that the receiver was not overloaded during the measurements.

Noise level calibration was obtained from a VHF noise source which uses a type TT-1 temperature limited diode with plate current variable over the range from 1 to 100 ma.

$$\text{Noise power} = qI_o b \frac{R}{2} + kTb \text{ watts}$$

where

$q = 1.6 \times 10^{-19}$ coulomb
$I_o = 10^{-3}$ to 10^{-1} amperes (adjustable)
$b = 1$ cps (for watts/cycle)
$R = 50$ ohms
$k = 1.37 \times 10^{-23}$ joule/°K
$T = 290$°K

This reduces to:

$$\text{Noise power} = 4 \times 10^{-19} I_o + 0.0397 \times 10^{-19} \text{ watts/cycle}$$

Calibration data was taken for each frequency monitored.

The experimental runs were performed at a pressure on the order of 2×10^{-5} mm Hg, the lowest pressure that could be maintained with the outgassing caused by the discharge. For each experiment the pickup plate noise power and discharge input power were measured as a function of the peak RF voltage between the electrodes while operating in vacuum and then the measurements were repeated at atmospheric pressure.

The true multipactor noise power and discharge input power were calculated by taking the difference between measurements in vacuum and the measurements at atmospheric pressure. It was found that the maximum discharge power and brightest glow between the electrodes occurred with about 160 volts peak RF between the electrodes. With voltages above this value the glow spread diffusely through the chamber and noise measurements varied unpredictably.

The noise on the direct pickup plate due to multipactor discharge was detected only at high input power levels, and the noise level was on the order of 10^{-19} watts/cycle or less. Next, a tuned coil was placed in the vacuum chamber with one end grounded and the other connected to the pickup plate. A tap on the coil near the ground end was connected to the 50-ohm coaxial line, as shown in Figure 37. The purpose was to increase the impedance of the pickup plate so that the noise intercepted from a high impedance discharge would increase. To determine the noise intercepted by the plate with the coil, it was necessary to measure the step-down ratio and Q of the tuned circuit by means of a signal generator. The noise intercepted by the plate is

$$N_p = \frac{k^2 N_o \, 50 \, W_o C}{Q_o} \text{ watts/cycle}$$

where

k = voltage step-up ratio of coil

N_o = measured noise level at output of coax (watts/cycle)

$W_o = 2\pi f_o$, where f_o is resonant frequency of pickup coil

C = capacitance of tuned circuit

Q_o = resonant Q of pickup coil

Measurements at 56.5, 118, 114, 112, and 110 Mc show a decrease in noise level as the separation of the 100-Mc discharge frequency and measurement frequency is increased. The tuned circuit was adjusted to be resonant at the measurement frequency for each run. The results are shown in Figure 38.

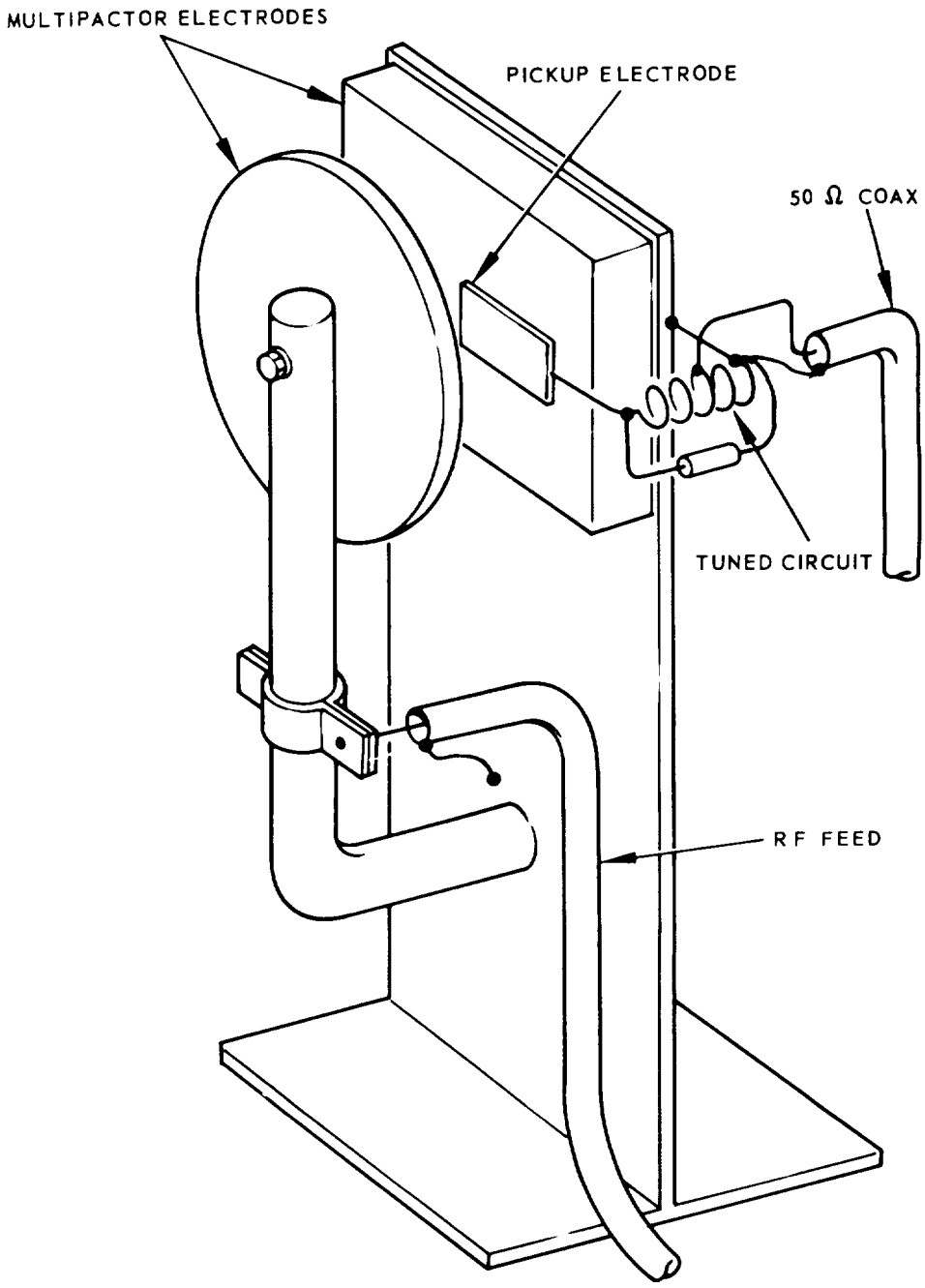

Figure 37. Noise generation experiment details.

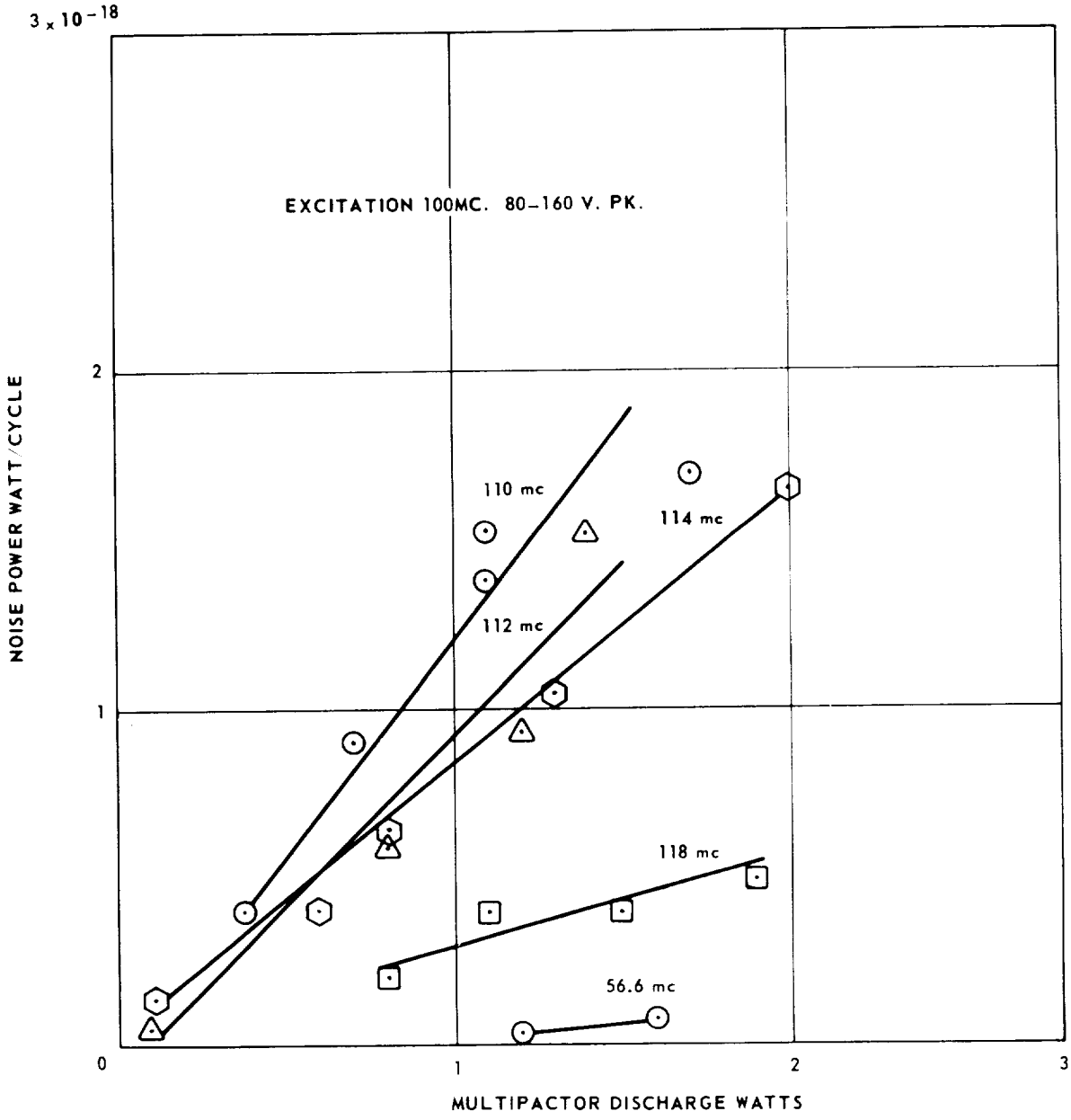

Figure 38. Multipactor noise-frequency measurements.

The graph of noise power versus multipactor discharge power shown in Figure 39 represents data taken during 5 hours of operation at the frequency of 112 Mc.

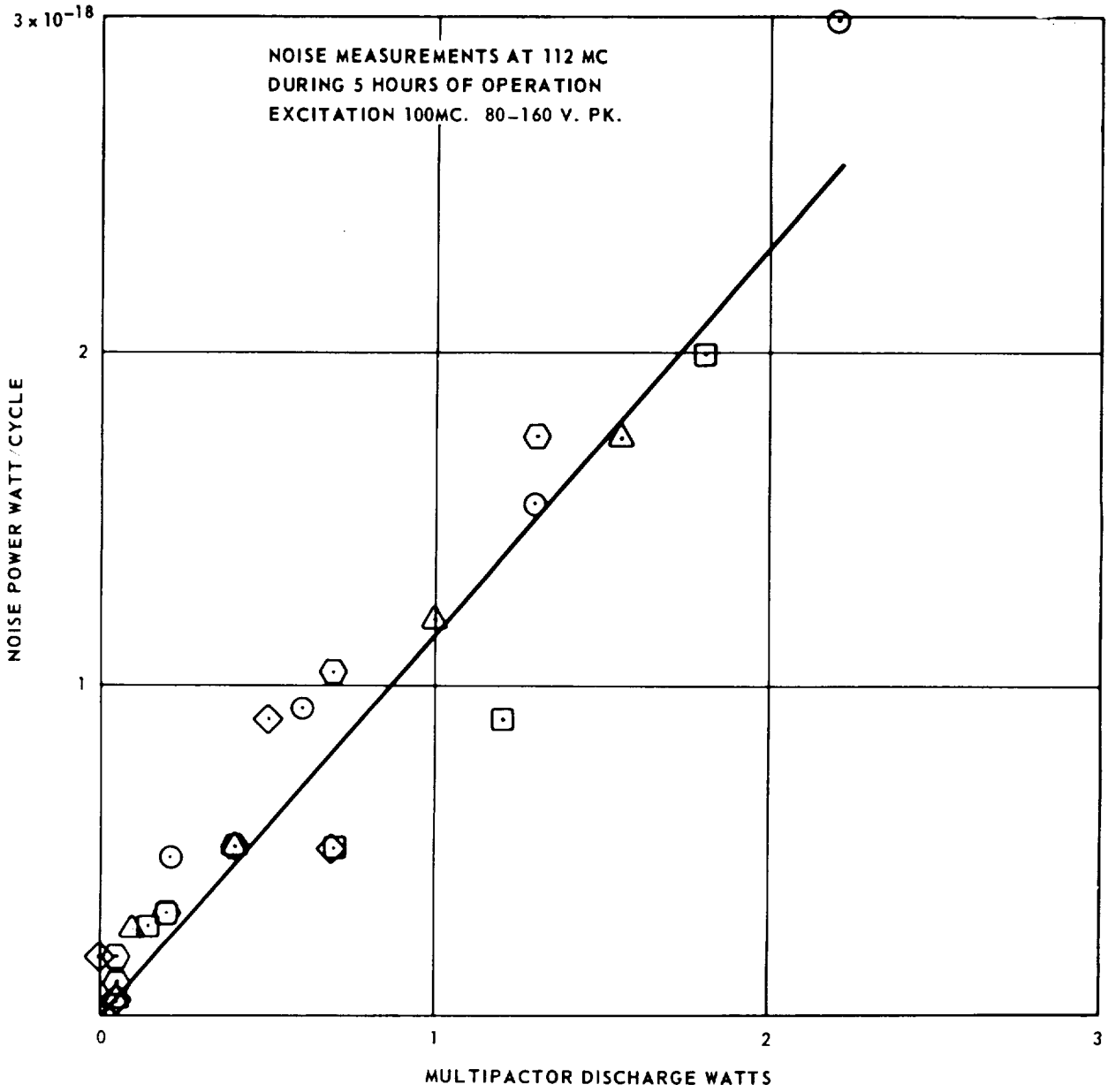

Figure 39. Multipactor noise at 112 Mc.

The setup shown in Figure 40 was used to measure the phase relation of the applied RF voltage and the metallic electrode current that flows. The parallel tuned circuit was adjusted to a null current

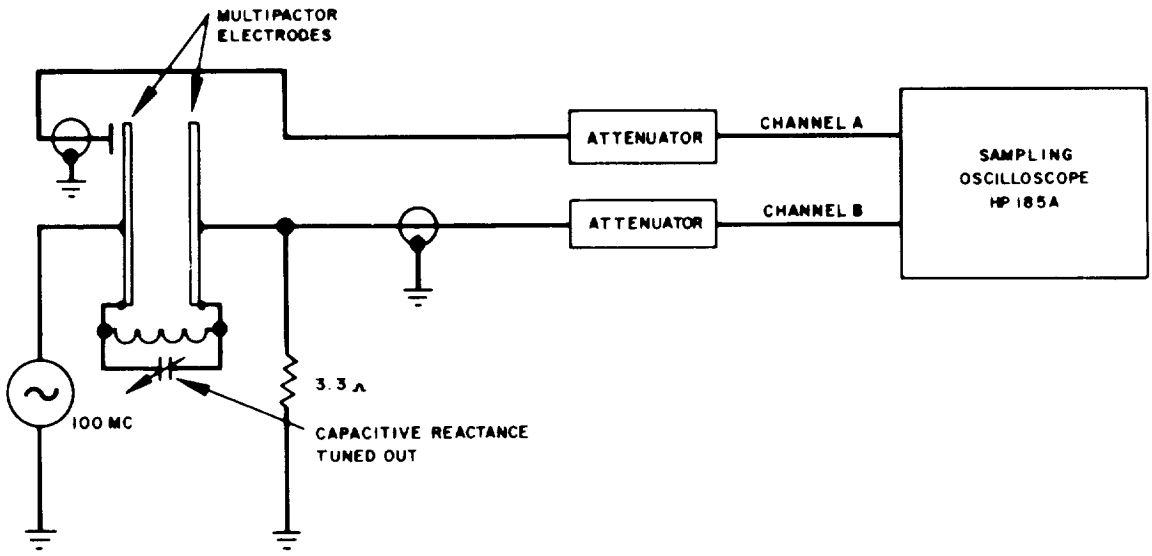

Figure 40. Multipacting current phase measurement.

output condition prior to evacuating the chamber and test fixture. Beryllium copper electrodes 5" in diameter spaced 1/2" were used. The current flow through the 3.3-ohm resistor due to multipacting was on the order of 10 times greater than extraneous pickup. The peak RF voltage was varied over the range of 60 to 78 volts with a corresponding multipactor power level of 0.24 to 0.88 watt. From photographs of the waveforms there was no measurable change in phase angle over the peak current range from 0.349 to 1.09 amperes. To measure the phase relation of the waveforms, atmospheric pressure was let into the setup and composition resistors of various values were connected across the multipactor electrodes. Values on the order of 1 or 2K were selected as giving least error. Photographs showed that an in-phase current waveform was positioned 132° leading the reference waveform on channel A of the oscilloscope. In the photograph of current, the waveform was measured as leading the reference by 204°. The phase of the current leads the voltage by approximately 85°. The accuracy of this method is limited. By calculation involving measured multipactor power, peak RF voltage and current, the phase angle can be calculated. This gives an angle of about 89° for this data.

DELETERIOUS EFFECTS OF MULTIPACTOR – TASK II

INTRODUCTION

The definition of Task II in our original technical proposal was:

(a) Antenna multipactor
Study conditions for existence, and electrical effects of discharge on antenna performance. Typical antennas may include dipoles, waveguide fed parabola, slots, planar arrays, etc.

(b) Transmitter radio frequency circuits and components
Study electrical and mechanical design of typical radio frequency circuits to determine conditions likely to cause multipactor and study its effect on circuit performance. Study voltage level and frequency conditions in typical components, such as connectors, coaxial line, capacitors, inductors to determine operating conditions which will cause multipactor.

(c) Study the long term effects of the discharge which may cause deterioration of components by erosion or deposit of material in films. Determine a quantitative measure of this deterioration, if possible, for use in estimation of reliability.

In addition to these experiments, the NASA Technical Representative provided a model of a typical transmitter similar to one used on the IMP Spacecraft to determine if it was susceptible to multipactor failure.

It should be noted that the study efforts described in the preceding section of this report have illuminated some of the goals of Task II. Among the deleterious effects of multipactor described in the material submitted relative to Task I are the following:

1. The discharge produces a local heating effect, which has been measured at a power density up to 20 mw per sq. cm. Although the direct physical damage or temperature deterioration due to this heating effect is probably negligible, outgassing of volatile matter may result. Since no vacuum environment has infinite

pumping rate, there is a possibility of gas ionization breakdown which can cause real physical damage. In tests performed prior to the beginning of this study in the Hughes laboratories we have observed direct sparks from 40 volt d.c. terminals to ground across 1/2" gaps when there was an intense gas ion cloud present.

2. Noise output has been found in the discharge.
3. Harmonic currents and nonlinear effects have been measured.
4. Power loss may occur due to loading or detuning caused by multipactor, although these effects would not be serious in low impedance circuits.

ANTENNA MULTIPACTOR

In order to perform meaningful tests on antenna elements at frequencies of 100 mhz and 430 mhz, it would have been necessary to establish a large RF absorptive vacuum chamber in order to accomplish multipactor tests under realistic conditions. Since this type of facility was not available, we have obtained data from another project at the Hughes Aircraft Company, which was performed, at no cost to this contract, in the Antenna Department of the Radar and Missile Electronic Laboratories. The work was performed at high microwave frequencies, with electromagnetic fields confined in waveguide.

This report describes an experimental study directed at investigating multipactor effects in certain waveguide devices. Attention was primarily directed to the study of waveguide slots. Other components tested include a section of tapered waveguide and a section of waveguide containing a capacitive iris.

When the electron transit time is equal to a half cycle, the breakdown is said to be in the first multipactor mode; the higher order modes are identified by the appropriate number of multiples of a half cycle of RF required for the transit time.

A plot of the different multipactor regions for a number of modes is shown in Figure 41. This chart was derived theoretically by Krebs and Meerbach assuming a parallel plate region. It can be seen that

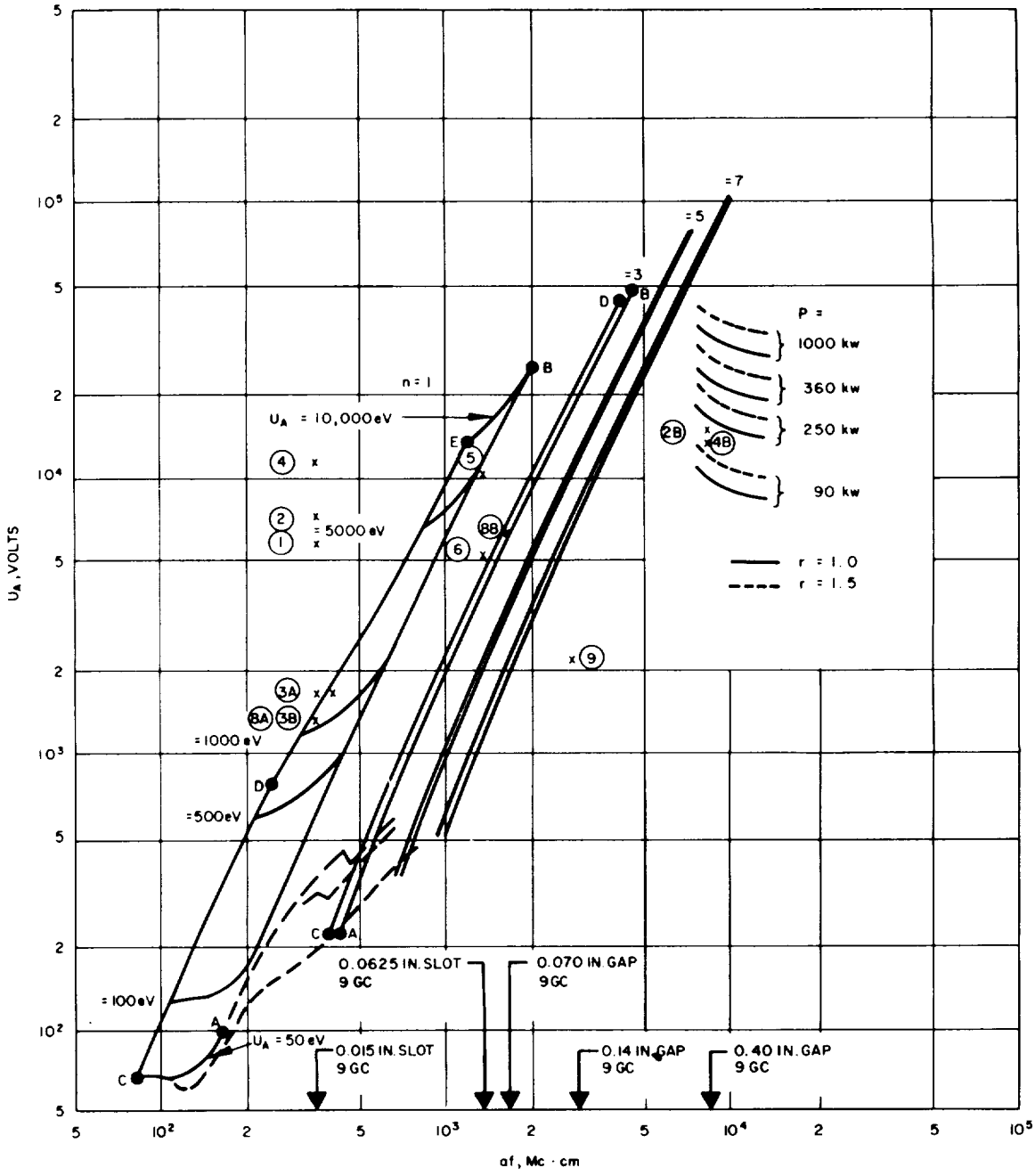

Figure 41. Existence regions for the multipactor effect. (from Zeitschrift für Physik, V. 175, 1963)

definite upper and lower field limits exist for a given fd product. In some instances however, when the upper limit of one mode is exceeded, multipacting in the next highest mode becomes possible. It should be recognized that in practice the boundaries of the existence regions plotted in Figure 41 tend to become indefinite and overlap. The antenna program reported herein however was primarily concerned with establishing whether multipactor breakdown would occur in an X-band slot array. Consequently, the structures studied were those which would typically be used in such an antenna. These structures include waveguide-coupling and radiating slots, and other equipment.

The experimental technique was to place the component under test in a vacuum chamber, the pressure was reduced to about 10^{-7} mm of mercury and power was applied. The power level was varied so that the exact voltage level at which breakdown occurred could be determined. The onset of multipacting was detected optically in some cases, and from RF transmission measurements through the component in others.

The equipment used is shown in Figure 42 which gives a view of the tee shaped vacuum chamber used, together with the RF power generator. A glass observation port was attached to one arm of the tee to permit optical monitoring of the test component. An ion pump was permanently connected to the chamber to maintain the vacuum over long test periods. The ion current was also useful as a check on the onset of multipacting since the multipactor discharge caused it to increase. A magnetron was used as the RF power generator. It was operated at a pulse repetition frequency of 2000 pulses per second with a 0.5 microsecond pulse width. A maximum peak power of 70,000 watts was available. The power level was adjusted during the tests by means of a power divider which shunted any desired fraction of the magnetron output into a fixed load.

Slot Measurements

The basic test fixture used in the investigation of multipacting in waveguide slots is sketched in Figure 43. It consists of two rectangular waveguides coupled by a resonant inclined slot centered in the walls of

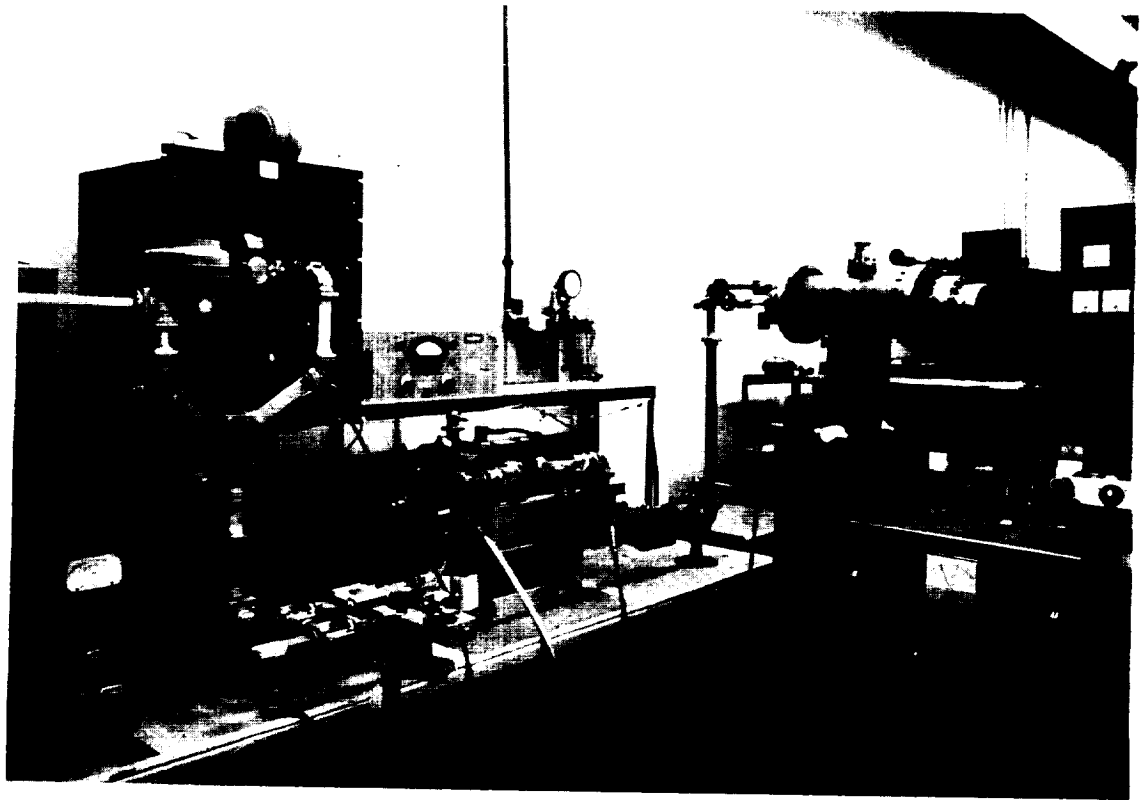

Figure 42. Antenna multipactor experiment setup.

both guides. If it is assumed that the slot field varies sinusoidally along the longitudinal axis of the slot, the peak amplitude of the slot field can be computed in terms of the input power. Since the form of the field distribution for a waveguide slot is independent of the position of the slot in the guide wall, and is the same for both radiating and coupling slots, it is sufficient to determine the breakdown potential for a single slot configuration. This result can then be used to determine the power handling capacity of any other type of slot (shunt, series, etc.) by simply calculating the slot voltage for that slot configuration.

In addition to the two different slot widths tested, several wall thicknesses were also used. This was done to determine the importance of the fringing fields outside the slot in setting the breakdown potential.

A total of seven fixtures were fabricated using coupling slots having widths of 0.015" and 0.0625". The narrow slot fixtures were specifically

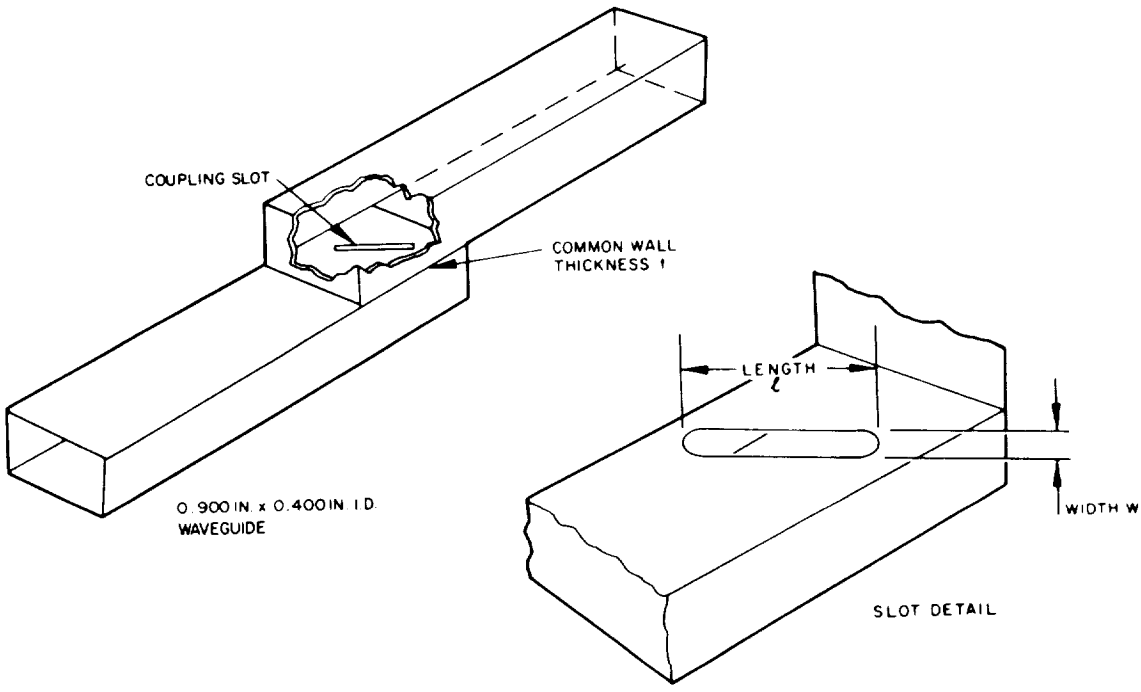

Figure 43. Coupling slot test fixture.

designed to multipact in the first multipactor mode, while the wide slots are of a width typically used in array design at X-band frequencies. These wide slots are subject to breakdown in the higher order multipactor modes. The breakdown slot voltages for the two different widths tested were computed on the basis of the parallel plate theory and are plotted on a graph of multipactor regions in Figure 44. Because of the sinusoidal field variations in the slot, an upper cutoff region on the breakdown voltage does not exist, since it is always possible to find a voltage less than the peak slot voltage simply by moving along the axis of the slot.

After finding considerable difficulty in photography or visual means of detection of the discharge, the experimental setup shown in Figure 45 was devised. A bridge was used with the test component in the vacuum chamber being inserted in one arm. The onset of the multipactor discharges is indicated by a change in the transmission

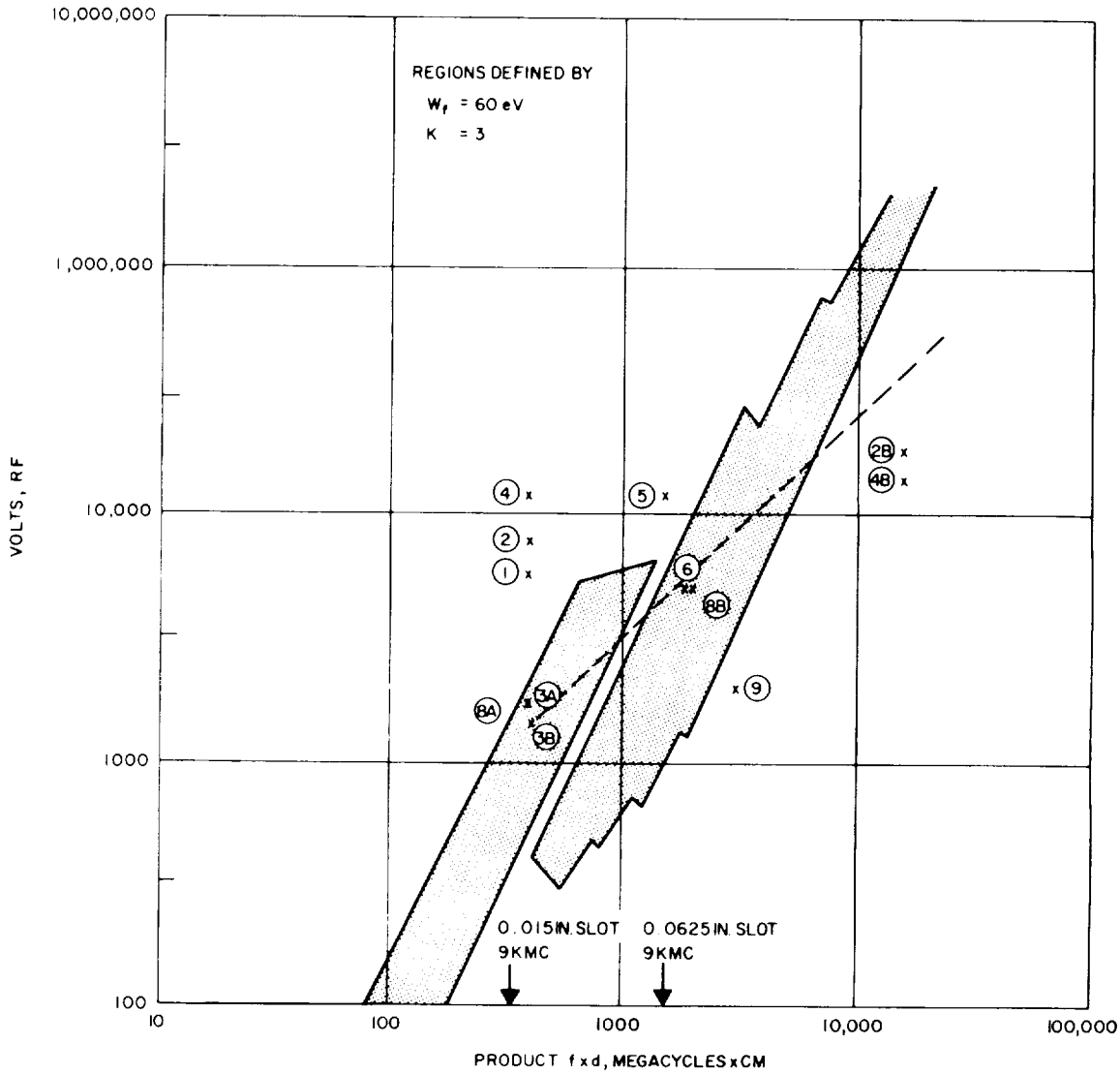

Figure 44. Multipactor breakdown parameters and test results.

through the slot. In practice it was soon discovered that the phase of the transmission was a very sensitive indicator. It was possible, using this arrangement, to measure both attenuation and phase shift through the slot while the multipactor discharge was present.

Results

The initial breakdown voltages for the different slot fixtures were computed on the basis of the parallel plate theory. These computed points are plotted together with this measured breakdown voltage in the

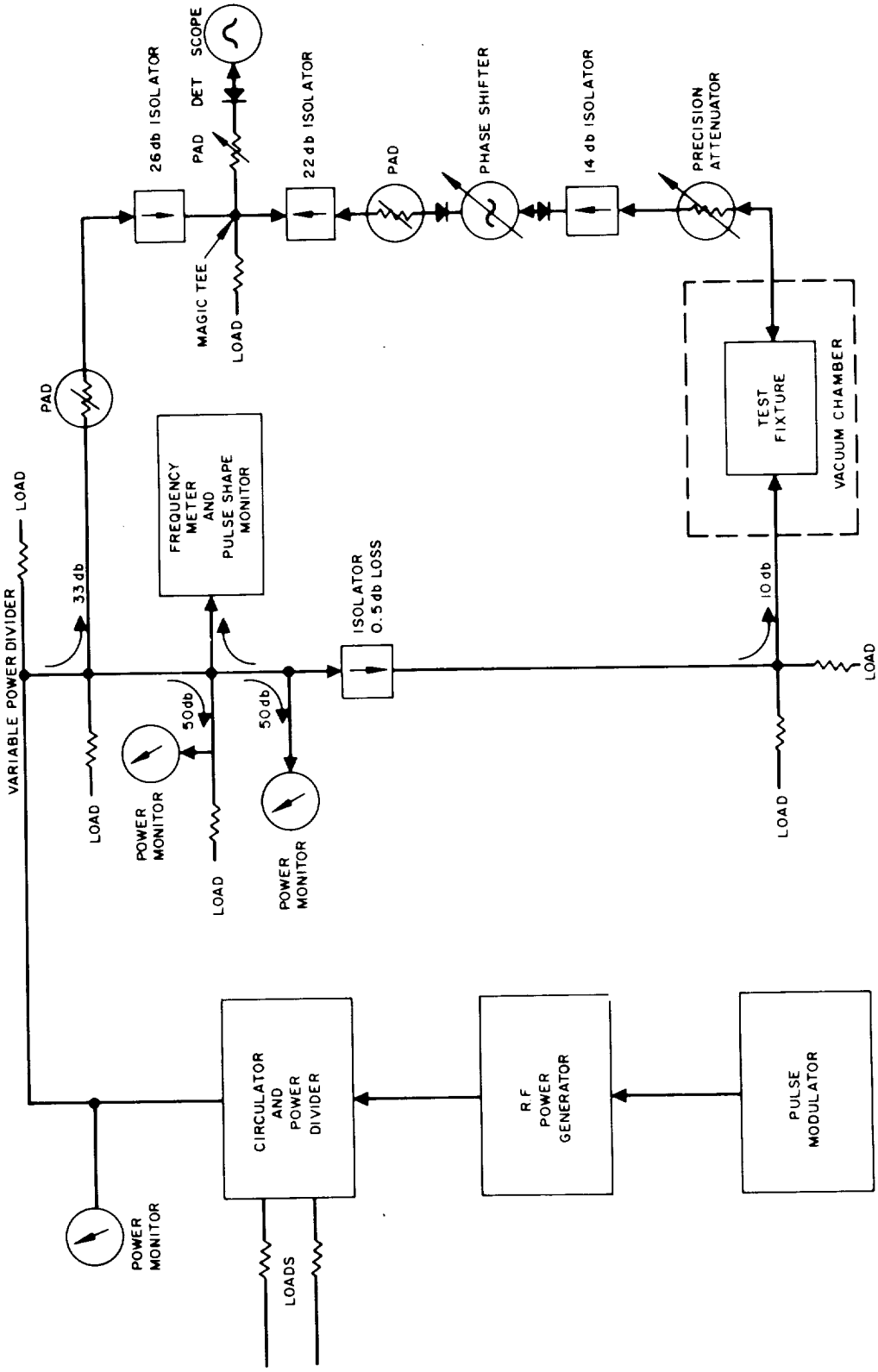

Figure 45. Multipactor detection test configuration.

multipactor breakdown chart given in Figure 44. The test results are also summarized in Table X, which identifies each slot fixture, the test procedure used, and the computed and measured breakdown voltages.

In Figure 44, data points No. 1 through No. 4 correspond to multipactor fixtures having slots of 0.015" widths.

Each fixture was tested while electrically matched. Slot No. 6 multipacted in the second mode (3/2 cycle electron transit time) region predicted by the simple theory. Slot No. 5, on the other hand, transmitted over four (4) times the corresponding peak power that Slot No. 6 handled before multipacting occurred. Breakdown did not occur in Slot No. 7, even though this slot was subjected to peak potentials up to ten (10) times greater than the level at which Slot No. 6 initially multipacted.

The graph in Figure 46 depicts the changes in voltage levels at which multipacting initially occurs as the slot wall thickness is varied. The numbering of the points corresponds to that of Figure 44.

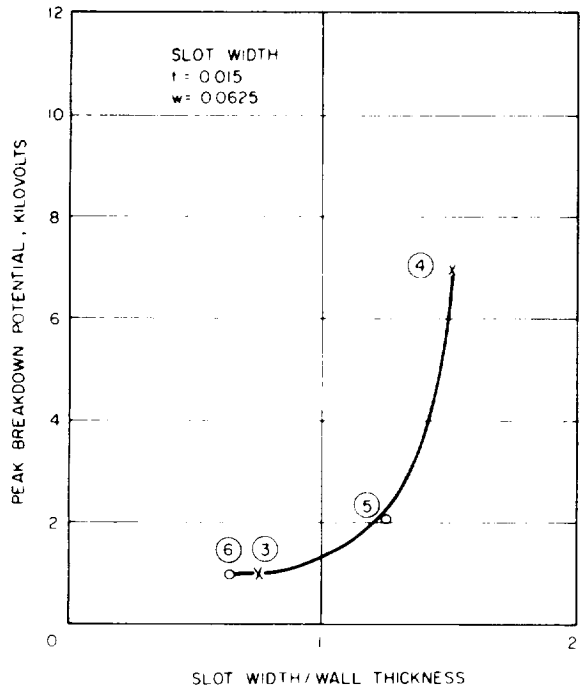

Figure 46. Slot breakdown potential as a function of slot width:wall thickness ratio (w/t).

The larger values of slot voltage necessary to induce multipacting for the thin wall slots is reasonable when one considers that from the viewpoint of the electron the slot gap only approximates a parallel plate region. When the slot width to slot wall thickness ratio, w/t, is small the electric fields within the slot are more uniform than they are for large values of w/t. As the slot thickness is decreased, fringing electric fields at the slot gap become more significant and more and more electrons tend to be accelerated along curved paths rather than along the straight-line path between the slot walls.

Slot No.	Slot Width (w)	Wall Thickness (t)	Minimum Breakdown Voltage (Peak)	Highest Test Voltage (Peak)	VSWR Under Test Condition	Pressure mm/Hg	f
1	0.015b	0.020	5,600	9,700	4.2	1.5×10^{-5}	8910
2	0.015a	0.020	6,000	10,400	3.9	4×10^{-4}	8910
3A	0.015a	0.020	1,500	8,900	3.5	3×10^{-7}	8910
3B	0.015a	0.020	1,300	5,100	1.17	1×10^{-7}	8910
4	0.015	0.010	10,660	30,000	1.09	1×10^{-7}	8910
5	0.0625	0.050	11,000	33,000	1.02	5×10^{-6}	9490
6	0.0625	0.100	5,200	41,000	1.01	5×10^{-7}	9125
7	0.0625	0.020	No breakdown	52,000	2.5	2×10^{-7}	9310

Table X. Test results.

The resonance condition for the gap is no longer valid since the longer effective path lengths shift the operating location to larger values of fd. Higher field gradients across the gap are thus necessary to effect the electron phase resonance for breakdown to occur as the chart of the multipactor region shows. Furthermore, many of the electrons are now likely to be accelerated completely away from the slot region into the waveguide where they are no longer available for the breakdown.

The physical effects of a typical breakdown were detected in several of the test fixtures. A photograph of the waveguide region about the input side of the coupling slot is shown in Figure 47. Fringing marks are present about the periphery of the narrow coupling slot. Indications of breakdown are also visible on the waveguide walls at periodic intervals down the guide. The breakdown occurred at 1/2 guide wavelength intervals at positions of maximum field strength. The presence of the waveguide breakdown marks on the input side of the coupling slot and their absence on the output side suggests that the slot was sufficiently shorted out to increase the input standing wave ratio to a value at which the corresponding waveguide electric fields were great enough to satisfy the electron resonance conditions for breakdown between the waveguide walls.

Ionization breakdown may have contributed in part to the severe breakdown burn visible in Figure 47. The high intensity of the breakdown caused the environmental pressure to rise to a maximum of 4×10^{-4} mm of Hg during this test which is somewhat higher than that maintained throughout the tests of the other fixtures. Although even at this pressure ionization breakdown would not be likely, (the mean free path of an electron is 79 cm at this pressure) it is quite possible that a much higher pressure did exist in

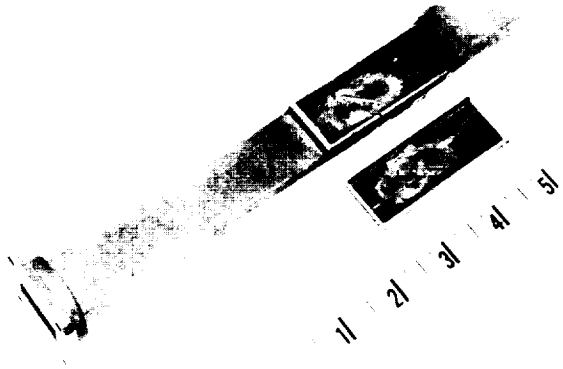

Figure 47. Input side test fixture No. 2.

the vicinity of the slot and within the input arm of the test fixture. This could be the result of relatively strong outgassing caused by the electron bombardment and heating.

Test of Other Fixtures

A section of X band waveguide that was tapered in height from 0.400" to 0.015" was also tested. The primary purpose of this fixture was to provide a large parallel plate region to check the application of the parallel plate theory to waveguide geometry.

The dashed line connecting points No. 8-a and No. 8-b in Figure 44 denotes the operating range over which this device was tested. Point No. 8-a locates the operating point where multipacting initially began. Breakdown occurred throughout the region where the height varied from 0.015" to 0.070". At the maximum input power used in the test the electric field across the 0.070" spacing is such that the breakdown occurred at the location denoted by point No. 8-b.

NOISE CURRENTS

In order to verify the conclusions concerning noise magnitude which are listed under Task I, a further test was performed. It had been difficult to obtain corroborative data by an independent experimental technique because of the necessity to separate out the noise inherent in the RF source from that caused by the discharge itself.

Attempts to measure noise by inserting a 3.3 r resistance value between the low potential electrode and ground were not successful because the noise coupled in directly from the transmitter obscured multipacting noise. The last experiment used a tuned circuit across the electrodes to tune out the capacitance coupling at the noise measurement frequency at 112 Mc, as shown in Figure 48 and Table XI. The accuracy of the measurement was unsatisfactory at levels such that the noise power produced by the test setup was comparable to that in the discharge. The data tabulated below is an indication of the problem. When the power in the discharge was small, the multipactor noise was undetectable, but when a strong glow discharge was established the

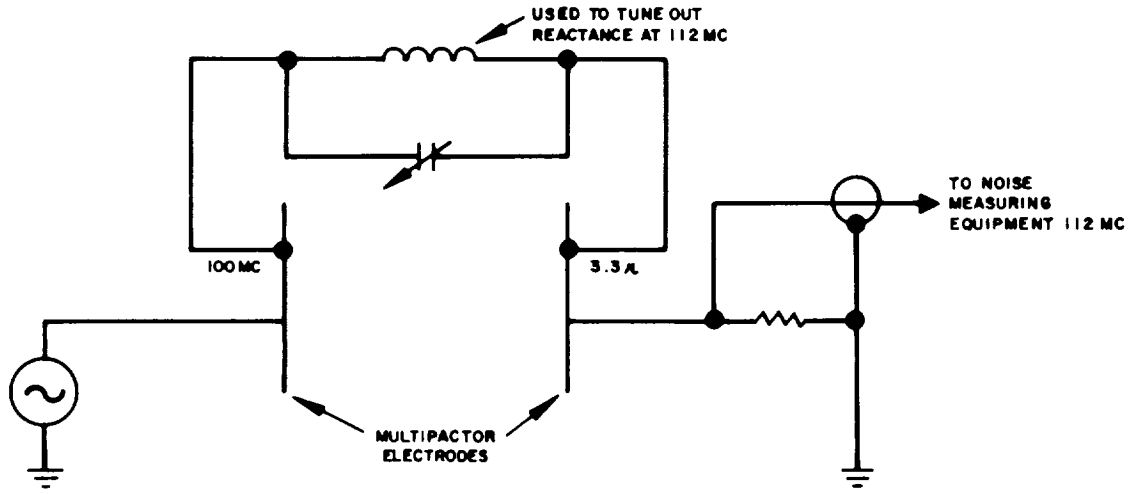

Figure 48. Noise test setup.

square of rms value of noise current was approximately 10^{-18} watts per cycle. Since Boltzmann's constant K = 1.37 x 10^{-23} joules per degrees Kelvin, the KTB noise at room temperature is approximately 4 x 10^{-21} watts per cycle. In brief, the noise from a strong multipactor discharge can be more than 30 db above thermal, at a frequency removed from the fundamental by the amount of the separation between typical NASA VHF transmitters and command receivers. Since some, but not all, command communication channels have adequate margin to withstand this type of noise, systems designers should be cognizant of the effect. In particular, one would avoid designs where commands are absolutely necessary to turn off the transmitter, since, in such an instance, the

Filter Network	E_p Peak RF Volts	P Multipactor Watts	i^2 Noise Amps^2 (with no multi-pacting)	i^2 Noise Amps^2 (with multi-pacting)
Parallel Tuned Circuit	100	0.25	1446 x 10^{-21}	1446 x 10^{-21}
	110	0.30	1446 x 10^{-21}	2050 x 10^{-21}
	118	0.60	1446 x 10^{-21}	2470 x 10^{-21}

Table XI. Summary of noise data.

multipactor noise might block the receiver and control would be forever lost.

The presence of harmonics in the currents of electrodes was measured, and reported under Task I, by Fourier analysis of voltage waveforms obtained with a series connected resistor, and by the use of a pickup electrode. The results showed currents at second or third harmonic frequencies of amplitudes greater than 10 percent of the fundamental. Since such effects are usually present in the power output stages of vacuum tube, transistor, or varactor devices, no added deleterious effects would result from multipactor. However, problems might be caused by a multipactor discharge on the antenna or in the transmission system. A frequently used RFI requirement is MIL-I-26600, which provides for harmonic suppression to levels 60 db below transmitted power. If, in fact, the spacecraft equipment would be affected adversely by harmonic power levels of -20 db, instead of -60 db, multipactor should be avoided.

PHASE ANGLE - DETUNING EFFECTS

The technique used to measure phase angle of currents has been described previously in this report. It appears that the electrode current as measured by a sampling resistor varies by almost 90° from the phase of the current observed without the discharge. The procedure which was used was to tune the electrode to parallel resonance by means of an L-C combination; in addition, a moderate resistive load was shunted across the tuned circuit to provide a reference current of sufficient magnitude for comparison on the oscilloscope.

A reference phase indication was obtained by use of a small collector plate in the chamber; by comparison with an external voltage it was shown that the phase of the pickup was not influenced by the presence of multipactor.

Photographs of the two voltages were obtained from a sampling oscilloscope, as shown in Figure 49. Channel A is a display of the reference phase. Channel B is the electrode current due to multipactor (i.e., with plate capacitance tuned out). As the multipactor discharge

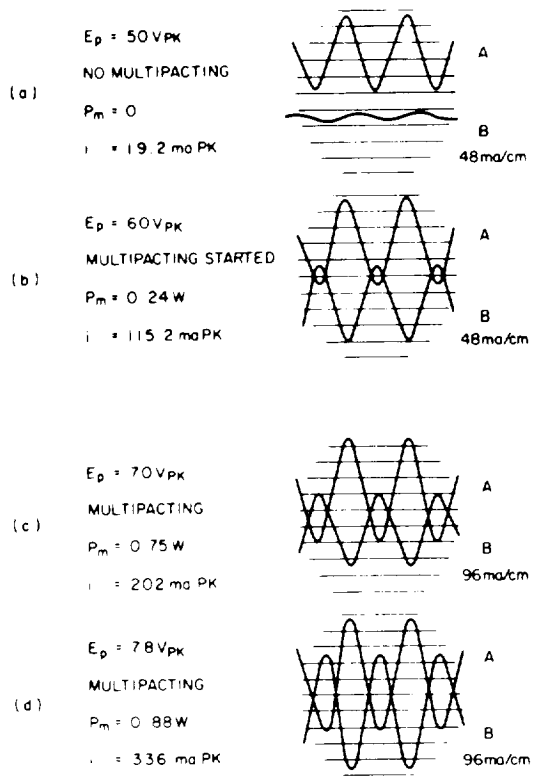

Figure 49. Phase angle data.

increases, the electrode current grows and appears at full amplitude shifted about 90° relative to the current drawn by the resistive shunt (visible in Channel B, Figure 49a). The measured power voltage and current data are also noted on the tracings of the photographs. The total volt amperes delivered for the strongest discharge was (0.707 x 78 x 0.707 x 0.336) approximately 13 VA. Since the measured power in the discharge was only 0.88 watts, Ohm's Law calculation for phase results in a value of phase angle slightly larger than 86°, with a reactance of 230 ohms. At lower levels of discharge, the reactance is still less than 1000 ohms.

Although the area of the multipacting plates used in this test was about 20 square inches we do not know that the impedance of the discharge could be increased under all circumstances by decreasing the area; in fact, very strong discharges have a tendency to spread out to fill the test volume.

In summary, it has been shown that the multipactor discharge has a reactive effect in addition to the power dissipation previously described. Whether or not a given circuit will be detuned by it is a function of the impedance level. High Q circuits will probably be affected. In the microwave antenna investigation previously cited it was observed that a multipactor breakdown in a slot could apparently reflect enough power to cause a standing wave amplitude that would initiate other discharges in the waveguide at points of maximum voltage.

It is to be hoped that some day it will be possible to perform more quantitative measurements of the electrical characteristics of a discharge.

While this would be more satisfying to engineers, it is not likely that all of the conditions can be controlled carefully enough (or that it is economically feasible to do so). In particular, the surface conditions and secondary emission ratio cannot be chosen, or maintained constant, and "accuracy" of a high degree cannot be expected.

PHYSICAL DAMAGE OF COMPONENTS

Although the early conclusions of this study program indicated that the only significant physical damage to components would not result directly from the multipactor discharge, but rather from the gas ionization breakdown accompanying it, we have tested a variety of typical spacecraft components. A photograph of a group of the parts which were damaged is included as Figure 50.

Type N Connector

A Tee type N connector was tested, after which it was cut apart. The insert and the empty barrel are shown adjacent to each other in the photograph. One of the test goals was to compare the effects observed on an unsealed connector (one end open) versus a sealed connector. We felt that the severe damage to type N connector experiment in the past on several space programs was due to a buildup of gas pressure. Our goal was to test this theory.

A biased collector plate was installed about an inch from the open end of the connector to detect the discharge. The strongest discharge, as indicated by collector plate current and brightness of the glow occurred with 125 volts peak applied to the plug. Vacuum chamber pressure was maintained below 4×10^{-5} mm of mercury for the 35 minute duration of the open-end connector test. As time passed, the collector current decreased from initial value of 10 microamperes to 2.2 microamperes, and the glow became less intense. When the connector was removed from the vacuum chamber, it was warm, but not hot, to the touch. Our conclusion was that a multipactor discharge had been present, had caused some outgassing, and that no physical damage had resulted. The nominal power level of this test corresponded to a flow of 150 watts into a matched load.

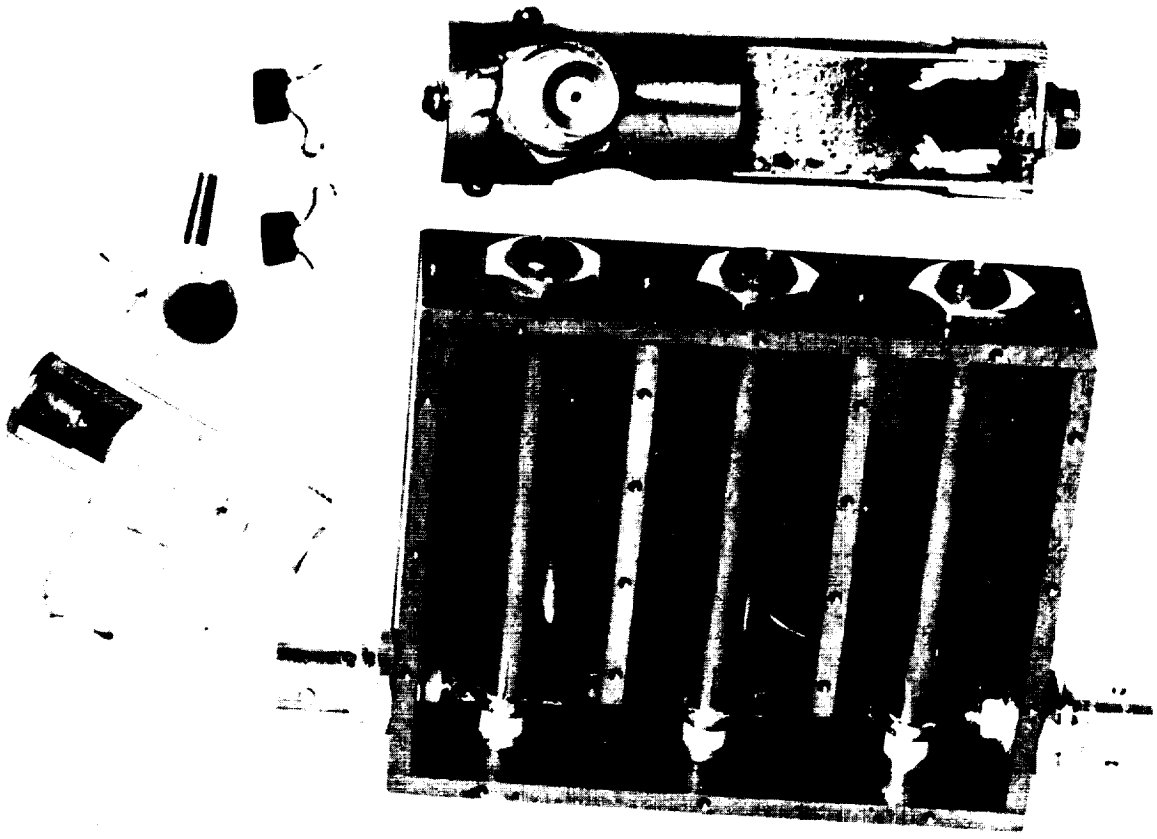

Figure 50. Physical damage of components.

Secondly, the plug was closed by means of a cap, which was devised with a mica viewing window. The diode which had been connected to the center rod at the end to measure RF voltage was shifted to center output pin of the "T". RF voltage was increased until multipacting was seen through the mica window. The voltage was adjusted for maximum glow brightness as before. The intensity of the blue glow now increased with time. The connection to the detector was soldered to the connector but melted in approximately five minutes. The color of the glow changed from blue to pink, indicating that a gas discharge was present. The connector was removed from the vacuum chamber. The connector temperature was above the melting point of solder. The blackened interior of the connector is shown in Figure 50. It will be noted that the teflon is eroded around the center rod. The other side of the connector did not multipactor since it was packed with insulation. There was no observable change in surface color of the silver plating during the previous test when the end of the connector was open.

The lesson of this test is clear. Multipactor discharges can occur inside of coax connectors, and when adequate power is available to liberate gas, physical damage may be done to a sealed connector.

Coaxial Resonator Test

A coaxial resonator similar to the design shown in Figure 51 was tested for physical damage by multipactor. The filter was filled with Emerson and Cummings FP type 12-2 low density foam. The purpose of the experiment was to verify if the foam could be used to suppress multipacting. The bandwidth and insertion loss of the resonator was 19.4 Mc and 0.4 db. After foaming the bandwidth increased to 21.7 Mc and the insertion loss increased to 0.65 db. The increased insertion loss could be tolerated for most applications.

The resonator was placed in the vacuum chamber. Two 1/2" diameter holes were used for foaming the resonator and to observe any light generated inside from ultipacting or gas breakdown. Low density foam will transmit light for a distance of an inch or two from one cell wall to the next. The resonator was placed in the vacuum chamber at a

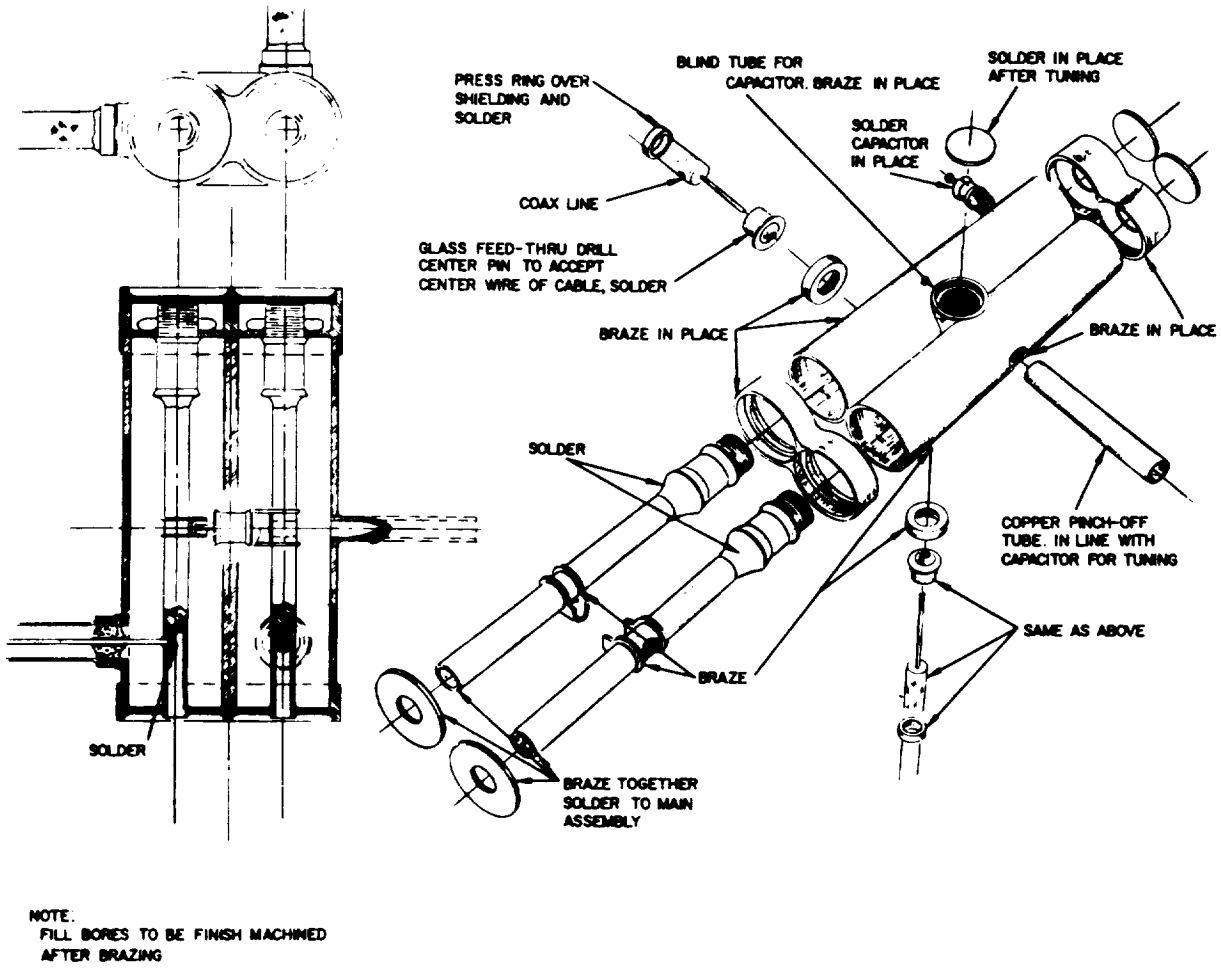

Figure 51. Suggested design for pressurized filter.

pressure of 2×10^{-5} mmHg. Twenty watts were passed through the resonator at 430 Mc. Outgassing increased with time as the resonator heated from RF losses, pressure inside the chamber increased above 10^{-4} mm. After approximately 10 minutes, a blue-pink glow appeared from the foam. There was severe enough outgassing of the foam at this time to "trip" the ionization gauge for the vacuum chamber.

After 15 minutes the resonator was removed from the vacuum chamber. The resonator was quite hot to the touch from the gas

ionization discharge taking place inside. Figure 50 shows the burnt area due to the gas ionization discharge. Since this area of the resonator has the highest RF voltage, the local heating of the foam would be the greatest and, therefore, the most likely area to break down. The foam had initially stopped any multipacting as expected. The experiment points out that local heating, with resulting outgassing, may cause physical damage of a serious nature, particularly at a high voltage junction.

430 mHz Diplexer Test

A three section diplexer was constructed, using drawings and a design provided by the Space Technology Laboratories of Thompson Ramo Wooldridge Inc. This company has designed an 11-cavity diplexer to be used with a 25-watt, 400-mHz transmitter in the IRLS data collection system. Since representative results could be obtained with fewer sections, the model was built as shown in Figure 52. All of the internal critical dimensions and components were in accordance with the NASA design.

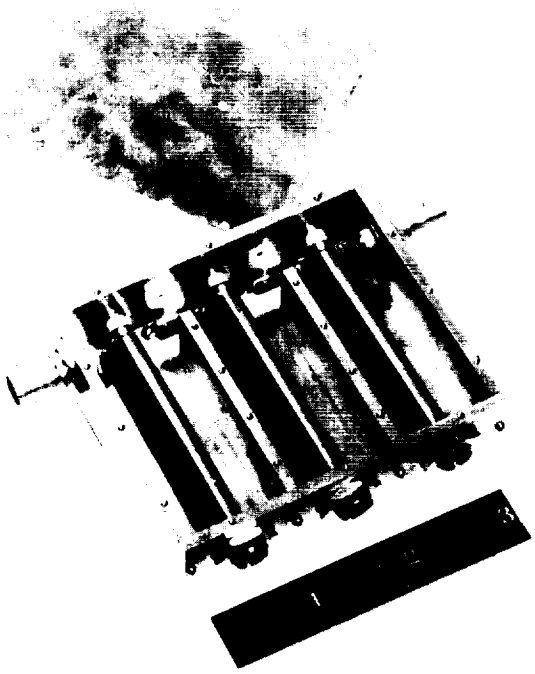

Figure 52. 400-mHz diplexer.

The diplexer was tuned to pass the transmitter drive frequency of 430 Mc after initial testing. The electrical test setup is shown in Figure 53. The brass cover was replaced by a brass screen which allowed observation of elements when the diplexer was placed in the vacuum chamber. The power input level was increased. Multipacting of the first section occurred with 47 watts input. By varying the frequency and increasing power input to 55 watts input, all three

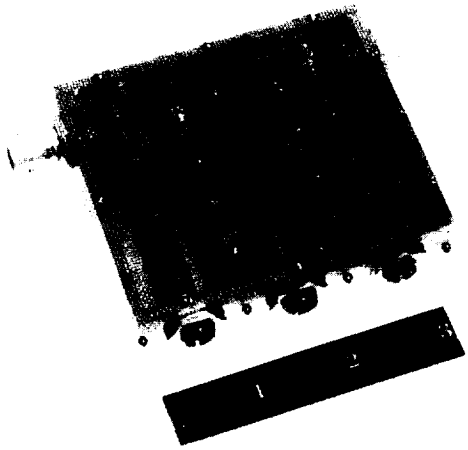

Figure 53. Duplexer with cover screen.

sections multipacted. The glow occurred between the glass capacitors and the brass shields. It spread to cover the RF line from input to output. The test was terminated by a blue flash at both coaxial connectors. Upon examination of the filter it was found that the input and output dipped mica capacitors were discolored with one lossy and the other with reduced capacitance.

A photograph of these capacitors is included in Figure 50 and in Figure 54, which also shows two undamaged units for comparison.

Our conclusion is that the IRLS diplexer may have an interior multipactor discharge, and that, even if the dipped mica capacitors are not used, there is a marginal possibility of a failure in the coax plug connectors.

TEST OF THE IMP-NASA TRANSMITTER

The IMP transmitter S-74 IT7 furnished to Hughes by NASA was tested for multipacting during this reporting period. The RF components in each compartment of the transmitter were examined for probability of multipactor, using the values of spacing and RF voltage existing at the components.

At least one area in each compartment of the transmitter was selected for the installation of a collector plate that would attract electrons if multipacting should occur. A piece of insulating tape was attached to the inner wall of the compartment. A strip of aluminum tape about 3/4" square was attached to the insulating tape to act as the collector plate. In the final transmitter stage and the varactor multiplier

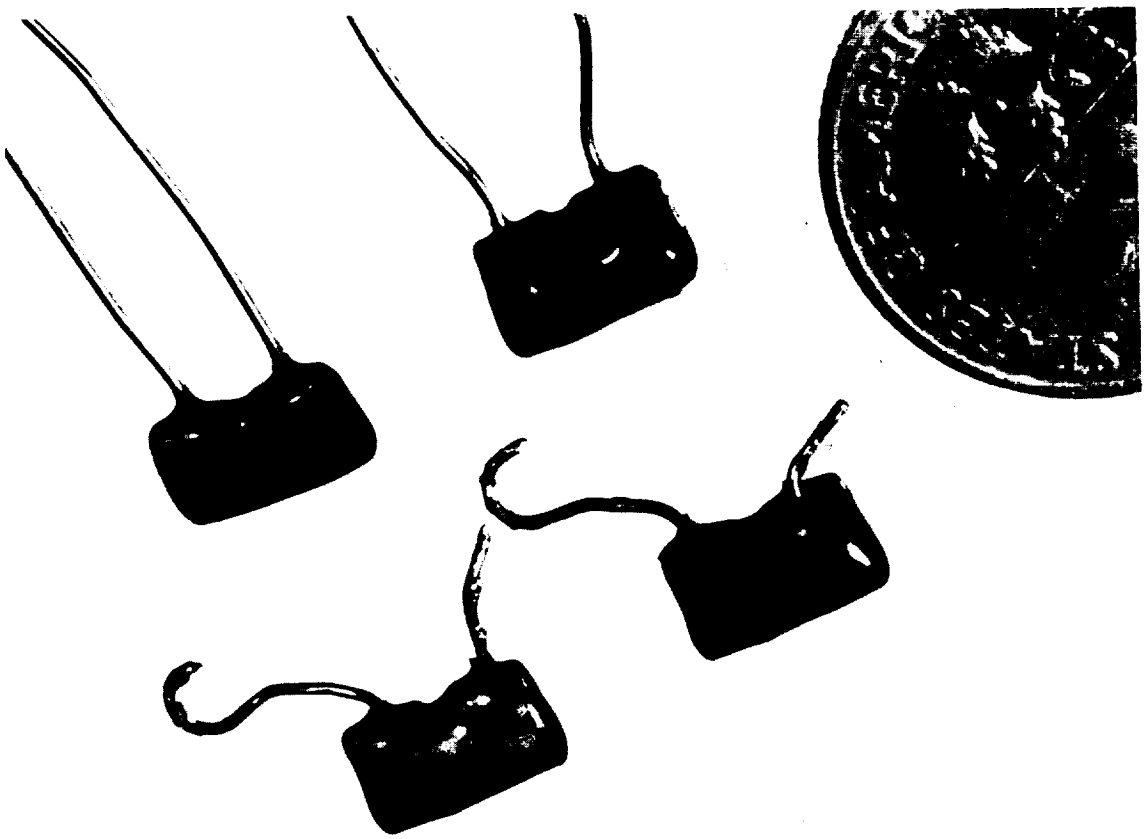

Figure 54. Capacitors damaged by multipactor. Undamaged units for comparison.

stage, three collector plates were installed. All collector plates were wired together in parallel and attached to a potential of +300 volts through a microampere meter. Fluorescent phosphor powder was lightly dusted on all RF components in each compartment. In addition, a strip of fluorescent tape was installed by each collector plate.

Output power from the varactor multiplier measured 3.0 watts showing the transmitter was operating satisfactorily. Both covers for the transmitter and multiplier were removed in order to observe any multipacting.

The transmitter was operated 30 minutes at a pressure of 2×10^{-5} mm of Hg. There was no fluorescence of the tape or powder and no indication of multipacting due to current flow from the collector plates.

A second test was conducted to see if the transmitter would operate at higher pressures where gas ionization might occur. The transmitter was turned on. Then the vacuum pump was started. The transmitter was observed in a darkened room for any sign of gas ionization. None occurred from ambient pressure to a pressure of 10^{-3} mm of Hg. Next the air was slowly permitted to enter the vacuum chamber. Again no gas ionization was observed (ionization at this pressure range manifests itself by a bright pink glow). The output power was next observed using the above procedure. No charge was noted in the output power.

It is clear that the power and voltage levels in existence in the IMP transmitter are low enough so that there is no danger of difficulty from the multipactor effect.

METHODS OF ELIMINATING MULTIPACTOR – TASK III

INTRODUCTION

At the beginning of this study, the scope proposed for Task III was the list shown below:

a. Study electrical design techniques, including use of d.c. bias, magnetic fields, low impedance, low voltage designs, and use of best components.

b. Study material and packaging techniques to eliminate multipactor including surface treatments, use of solid dielectric, methods and reliability of pressurizing, use of coating or potting compounds.

c. Study antenna design techniques, including design for low voltage and use of most suitable materials. Study designs of pressurized "radome" containers, or seals, for large antennas, including space craft installation and reliability aspects.

Items a. and b. above have been thoroughly studied and reported in the foregoing material, as well as in the remainder of the report. Item c. is treated in the antenna material included in this report which is included in Task II and in the discussion given below.

Although all of these items are treated to the extent originally proposed, it is regrettable that no experimental facilities have been available to us which permit the operation of UHF antennas in a suitable vacuum environment. To the best of our knowledge, no such facilities are available anywhere. In view of the increasing emphasis on long range wideband communications for spacecraft, it seems inevitable that higher power transmitters will soon be needed. The Nimbus spacecraft is scheduled to carry a 25-watt 400-mHz transmitter within two years as part of the on-board Interrogation Ranging Location System. The Ranger spacecraft has already been flown using a 60-watt 960-mHz transmitter, whose power output lines have been troubled by multipactor induced breakdown. It seems to be very important for NASA to consider seriously

the possibility that space electronics is approaching the time of use of these new transmitters without an adequate test facility.

The methods of eliminating multipactor proposed in the definition of Task III have all proved to be useful to some extent; more or less convenient solutions have been found for all the equipment design problems inside the transmitter, itself. As noted above, there is less certainty about the magnitude of the problem or the feasibility of solutions with regard to antennas.

A report of individual studies performed as Task III is given below.

FOAMING

It is clear that foam with voids smaller than the mean free path of electrons can eliminate multipactor discharge if no other adverse problems are created by the foam itself. To study this technique, a parallel plate multipactor setup was employed. Tests were run using samples of Emerson and Cuming type 12-4 foam, as suggested by the project engineer. Sample foam discs were molded in 1/8" and 3/16" thickness. With a piece of 1/8" thick foam between the plates the RF voltage was varied slowly from zero to 500 volts and back to zero, but no evidence of discharge was observed. Upon examination of the foam after the test several brown spots were found where the foam had apparently overheated and a breakdown had occurred. Since experiments on foam materials used in the Surveyor and Syncom programs had showed that considerable trapping of air within the cells of foam was possible, another experiment was performed with one of the 3/16" foam discs, whose surface had been sanded to remove the crust formed by the molding process. With this disc between the plates it was not possible to obtain any sign of discharge, and examination of the foam following the experiment shows no change.

In the next experiment the foam was placed so as to cover one half of the electrodes, and normal multipactor discharge was observed over the uncovered portion of the plates, with some ionization at the surface of the foam. After about four minutes a strong blue glow was noticed along the edge of the foam next to the discharge, indicating that the foam

was breaking down and outgassing. The chamber was returned to room pressure and the entire RF structure was found to be very hot; most of the foam had disintegrated. The experiment was repeated with similar results. As long as the foam covered all of the plates the discharge was completely suppressed, but when the plates were uncovered a discharge occurred which soon resulted in destruction of the foam. From these experiments it appears that foam materials of this type should serve as an effective multipactor suppressor, provided that they completely surrounded all of the metal surfaces involved. However, there is still a potential problem with trapped air, since it might escape sufficiently slowly to permit pressures to exist at which ionization breakdown could occur.

The apparatus shown in Figure 55 was constructed in order to get a better idea of the rate at which trapped air would escape through the foam. The foam sample (see Figure 56) was sealed in a glass cylinder which was connected to a vacuum pump and two vacuum gauges, while the other side of the sample was connected to another vacuum gauge and a mercury manometer. Experimental data was obtained by starting the vacuum pump and measuring the pressure on each side of the foam as a function of time. Two samples of foam were tested; one had the original surface crust removed with sandpaper and the other was left with the surface undisturbed. Results of the two tests are plotted in Figure 56, and showed clearly that removing the surface crust resulted in a much higher flow rate. Similar measurements on the CPR type 23-8 heat cured polyurethane foam used in Surveyor showed a very much smaller flow rate under the same test conditions, indicating that the Emerson and Cuming foam was far superior, at least as far as the release of trapped gases is concerned.

From the appearance of the data in Figure 57 it was assumed that the flow of gas through these foam samples followed the same type of exponential law which could be expected when a reservoir was evacuated through a porous plug.

In order to verify these conclusions, the Components and Materials Laboratory was asked to evaluate the foam and to measure its conductance.

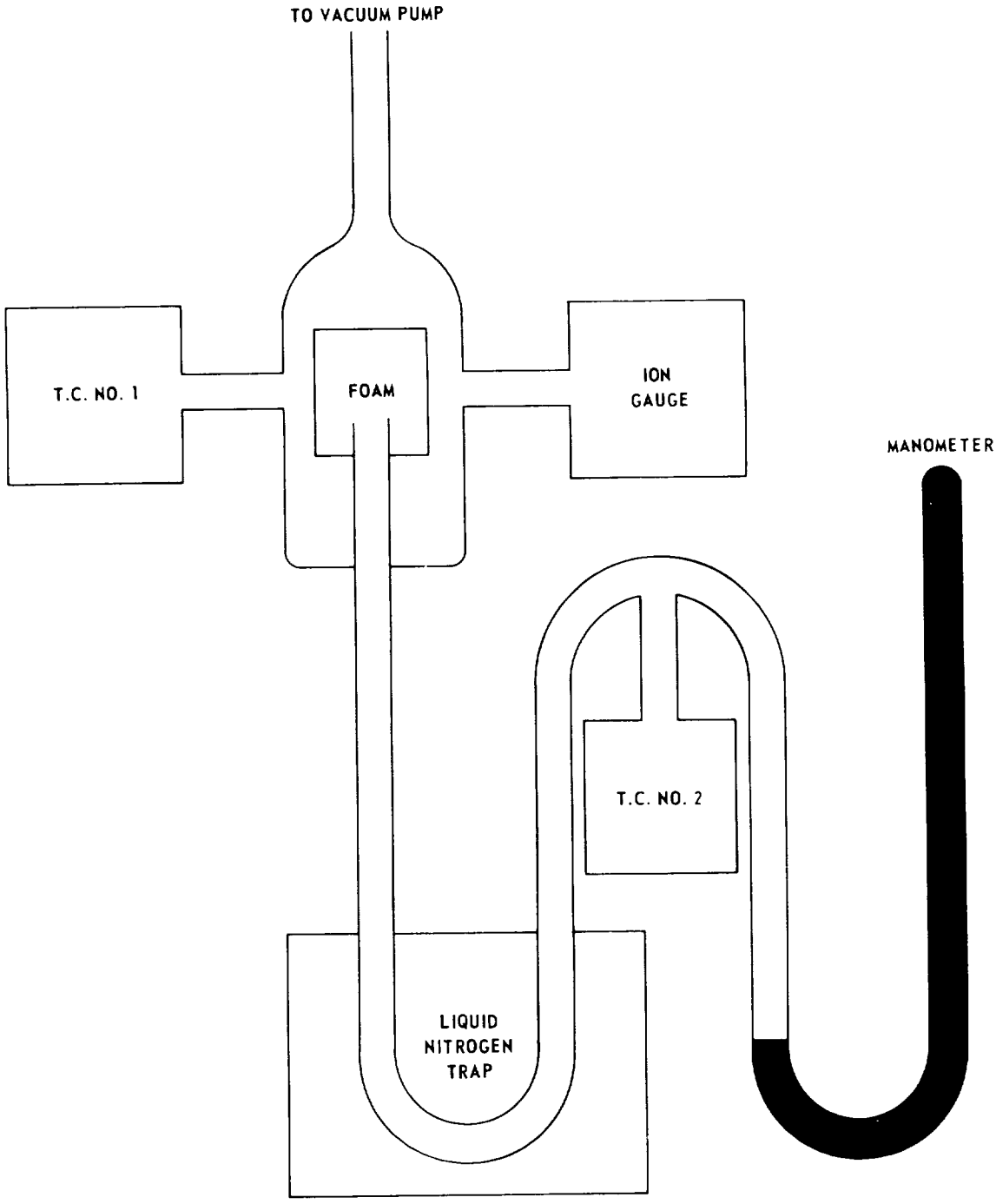

Figure 55. Foam pressure measurement experiment.

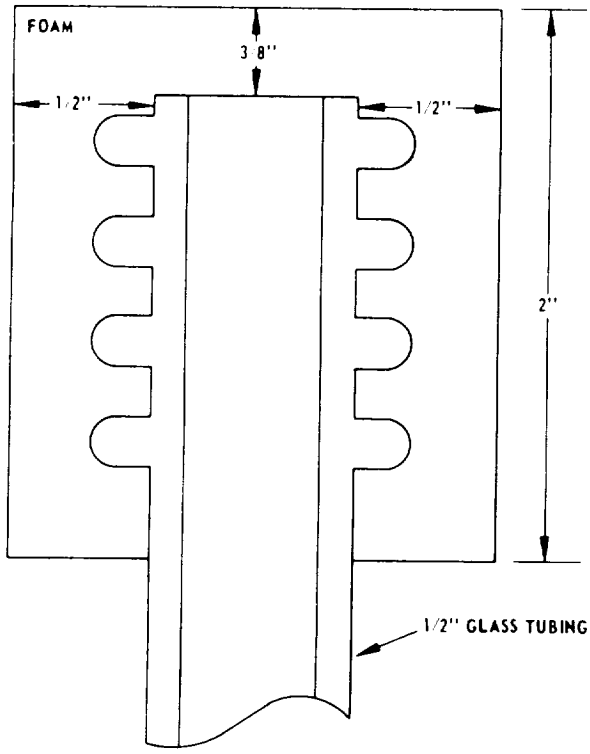

Figure 56. Details of foam sample.

The test setup is shown in Figure 58. Basically it consists of a restricted portion of the 3/4"O. D. copper tubing and a means of measuring the pressure differential across the restriction. The outer ion gauge tube (IG-2) served as a gas load for the test. The assembly was attached to the Laboratory bell jar system with a valved adapter and a 3/4" quick coupling. The sample was cut from a 2-3/4" thick sheet of the foam using a cork borer. The 1-1/2 cm diameter plug was forced into the assembly before the outer ion gauge tube (IG-2) was attached. The two end surfaces of the plug were left as it was supplied, with the smooth mold finish. The fit between the plug and the copper tubing was quite tight, and the plug did not move visibly during pump down or venting to air. Pump down was quite slow, but after an overnight pumping (system speed about 400 liters/second), it was possible to operate both ion gauge tubes.

Over a three day period, periodic pressure measurements were made. By outgassing the grid of IG-2, the gas load was increased. The results are given in Table XII, as well as the intermediate values of the calculation. From the pumping speed and the pressure as measured by IG-1, a thru-put (Q) is determined. From this thru-put and the measured pressure differential (IG-2 less IG-1), a conductance is found. The values range from 5.2 to 8.9 liters/second. There is a possible trend of decreased conductance with increasing pressure, although the limited data makes this conclusion difficult to support. Perhaps the best conclusion is that the conductance is constant over the pressure range measured, which is predicted in the molecular flow region for a normal

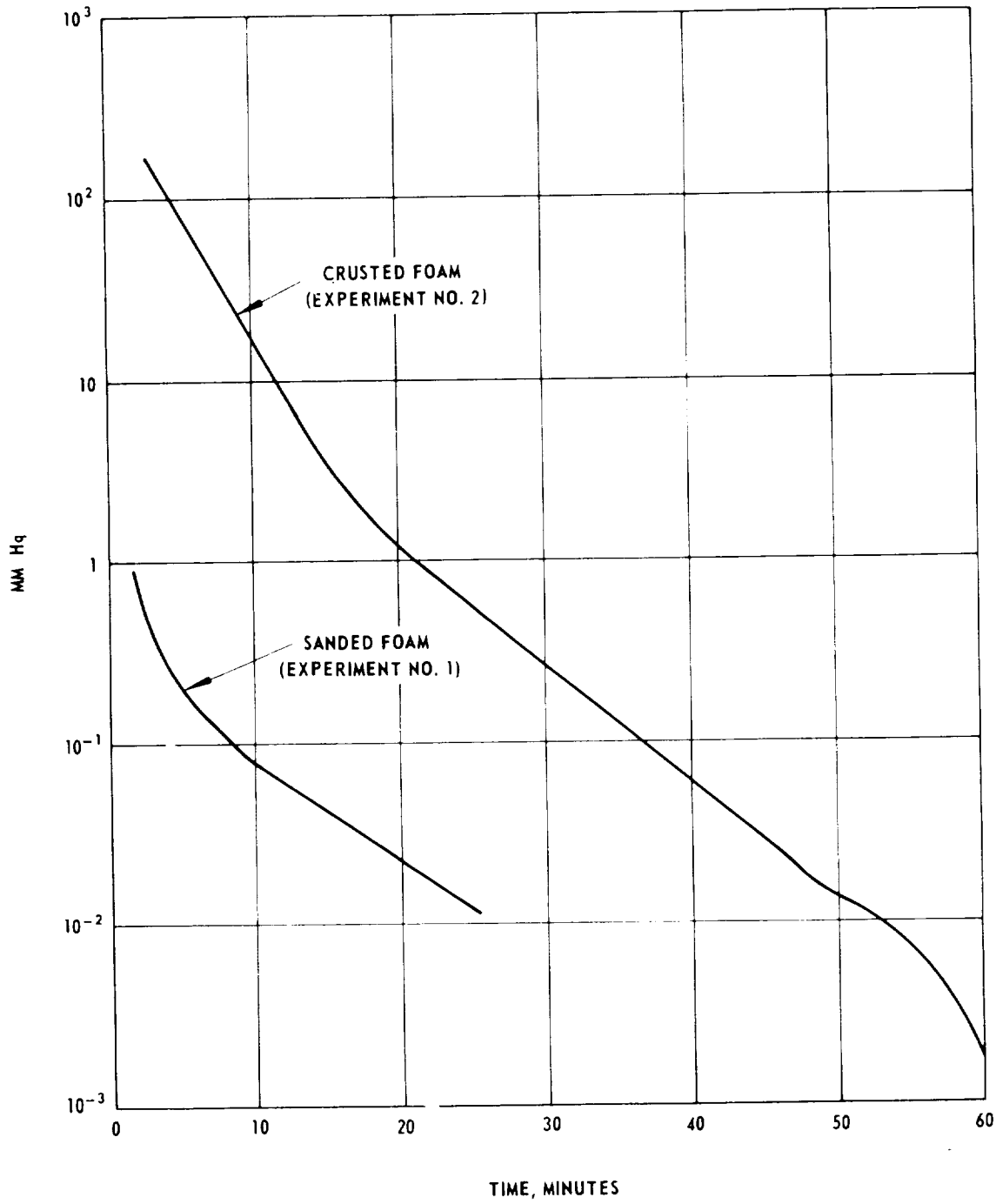

Figure 57. Pressure versus time for two foam samples.

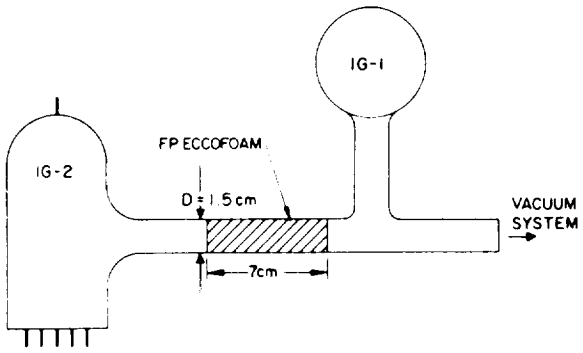

Figure 58. FP Eccofoam test fixture.

capillary type leak. The data gave an average value of 6.5 liters/second.

After this series of measurements was completed, the test assembly was removed from the bell jar, and the porous plug removed. In the removing of the plug, small pieces of the foam were scattered throughout the assembly. These were washed out with several rinses of Freon TF. When the assembly without the porous plug was returned to the bell jar, the pressure readings were again compared. At equilibrium, IG-2 read 1.1×10^{-6} T, while IG-1 read 1.3×10^{-6} torr. Ideally, the two gauges would have read the same. No correction has been made for this effect, since it is within the pressure measurement accuracy at this pressure level.

A limited number of mass spectrometer sweeps were made during this test. Comparing the empty test manifold to the system with the manifold valved off from the bell jar, the main change was an increased water and carbon monoxide content from the operating ion gauges. The water was about twice the carbon monoxide level. Sweeps with the foam plug showed a higher water and carbon monoxide level, and a slight response at mass 36, 39, and a significant amount of carbon dioxide. The quantitative result with the foam plug was: water 61 percent, carbon monoxide 20 percent, carbon dioxide 17 percent, and mass 36, 39 at about 2 percent. The mass spectrometer had a mass range of 2-80, so many materials did not show parent peaks. However, most complex molecules fractionate and show peaks within the range of the instrument. The mass 36 and 39 peaks observed are probably hydrocarbon fragments of this type.

In summary, the conductance of a porous plug of FP Eccofoam 1-1/2 cm diameter and 7 cm long was measured in the 10^{-4} torr pressure

IG-2 10^{-4} mm	IG-1 10^{-4} mm	ΔP 10^{-4} mm	Pumping Rate Liters/Sec	Conductance Liters/Sec Per Torr
7	0.1	6.9	385	5.6
5.2	0.093	5.11	385	7.0
4.2	0.072	3.93	380	7.1
3.5	0.062	3.44	380	8.9
4.4	0.076	4.32	380	6.75
1.1	0.014	1.086	375	5.2
0.53	0.012	0.518	375	8.5

Table XII. FP Eccofoam conductance.

range. The value measured was 6.5 liters per second, with a probable error of about ± 30 percent. No serious outgassing of contaminants was detected at room temperature.

The conclusion to be drawn from this test is that the foam tested will not support a significant pressure difference, i.e., it has a good "conductance." However, the multipactor tests show that a multipactor breakdown can cause outgassing and if the foam material is not designed so as to allow almost unimpeded venting of accumulated gas to the vacuum outside, an ionization breakdown may occur.

SURFACE TREATMENT

Several experiments were run to determine the extent to which multipactor could be suppressed by placing dielectric material between the parallel plate discharge electrodes. Plates made from 1/16" sheet teflon and large enough to extend about 1/2" beyond the edge of the electrodes were found to eliminate the discharge completely, but when they were moved so as to uncover part of the electrodes the discharge started again and covered all of the electrodes, including the teflon. It would appear from this experiment that, where it is possible to completely enclose any possible discharge electrode, teflon may serve as an effective suppressor, although application of the teflon could be quite difficult.

Additional data is shown in the curves for breakdown voltage of common materials in an early part of this report indicate that for certain close spacings the discharge could be suppressed with surface treatments of epoxy, glass laminate, teflon, and Dow Corning 200 fluid. However, even these materials could be made to multipactor at higher voltages and wider spacings. A simple surface treatment of the types mentioned is evidently very helpful in all cases since it increased the minimum breakdown voltage by a factor of two, approximately, and in certain circumstances, it eliminated the discharge entirely. The designer can determine the applicability of these techniques by careful reference to the Tables III and IV of this report, entitled, "Spacing and Voltage to Multipactor."

BIAS

A definitive treatment and experimental verification of the use of bias voltage to suppress multipactor is given by Nanevicz* in the literature. Since this material and the theory discussed in the Appendix to this final report appeared to be complete, we have not devoted efforts to this problem. The data indicates that a direct voltage substantially larger than the peak radio frequency voltage was able to suppress multipactor in a wide variety of coaxial cylinder configurations. For further information, it is necessary to utilize the theory developed for single surface multipactor. Sperry** Gyroscope Co. determined that parallel plate multipactor should be suppressed by bias voltages shown in Table XIII below.

Mode	Bias Voltage
1/2 Cycle	$0.34\ V_1$
3/2 Cycle	$0.12\ V_1$
5/2 Cycle	$0.07\ V_1$

Table XIII. Bias to suppress multipactor. $V_1 = \frac{1}{\pi}\left(\frac{\omega d}{e/m}\right)^2$

*J. Nanevicz, "Study of Radiation and Reception of Electromagnetic Energy from Aircraft and Guided Missiles", Progress Letters 8, 9, 10, Contract AF 19(628)-325, Stanford Research Institute.

**"Final Report on Multipactor Study Program", Contract NR-217(01) Report 5270-6144; October 1953.

PRESSURIZATION

There is little to be said about pressurization as a cure for multipactor. It is completely effective since it reduces the mean free-path to negligible values.

This technique has been used successfully by Hughes on the OAO transmitter filter and, apparently, by RCA on the Ranger television transmitter. The engineer who uses this technique must make an early decision because it influences many of the mechanical features of design. Great care must be exercised to prevent leaks, even in components such as hermetic sealed glass headers which have proved to be fragile in our experience. The procedure of pressurizing must be done carefully to insure the presence of traceable quantities of helium within the device. We do not know of any long time life test data in an actual spacecraft. However, experience with the OAO transmitters has shown that standard helium leak test apparatus has produced data which has proven to be a reliable predictor of good performance during the shelf life and qualification testing period; in this particular case, no difficulties have been observed in any delivered equipment over a period in excess of a year.

ELECTRICAL AND MECHANICAL DESIGN

The choice of voltage and dimensions which cause or prevent multipactor has been the subject of a great deal of the test and theoretical work on this program. The electron resonance equation [equation (1)] has been verified thoroughly, and is a necessary condition for existence of a discharge. The fact that it is not sufficient is due to the other conditions, such as surface emission; the surface condition is largely responsible for the variations in measurements of breakdown voltage.

Of course, it is not always possible to choose a physical configuration which at no single location will have a potential multipactor resonance. Wherever voltages are greater than 50, and the product of f x d (frequency x distance in mHz x cm) is a number greater than 30-40, a multipactor breakdown is unlikely. Figure 12 of this report also indicates another critical matter; the arrival energy of electrons which caused multipactor from many materials is seen to be in the range from 15-30 electron volts.

We have seen many engineering calculations based on higher threshold values of arrival energy. Our experiments prove that lower arrival energies must be considered.

In some instances, the ultimate voltage which should be achieved by a component is high enough to prevent multipactor. However, if the impedance of the discharge is enough of a load to prevent the use of voltage, the circuit may never operate normally. This effect has been observed in klystron gaps, for example. There is no certain simple cure for such a problem. Sometimes it is effective to provide for a very rapid use of voltage through the multipactor region so that the discharge does not "have a chance" to establish itself. Klystron designers who face such problems do not have any successful method of attack which they will recommend, except for complete redesign and a lot of patience.